Innovative Autonomously-Driven Offshore Wind Turbines: a pre-feasibility analysis

DTU Electrical Engineering

Department of Electrical Engineering

Xavier Martínez Beseler

Kongens Lyngby, August 2019

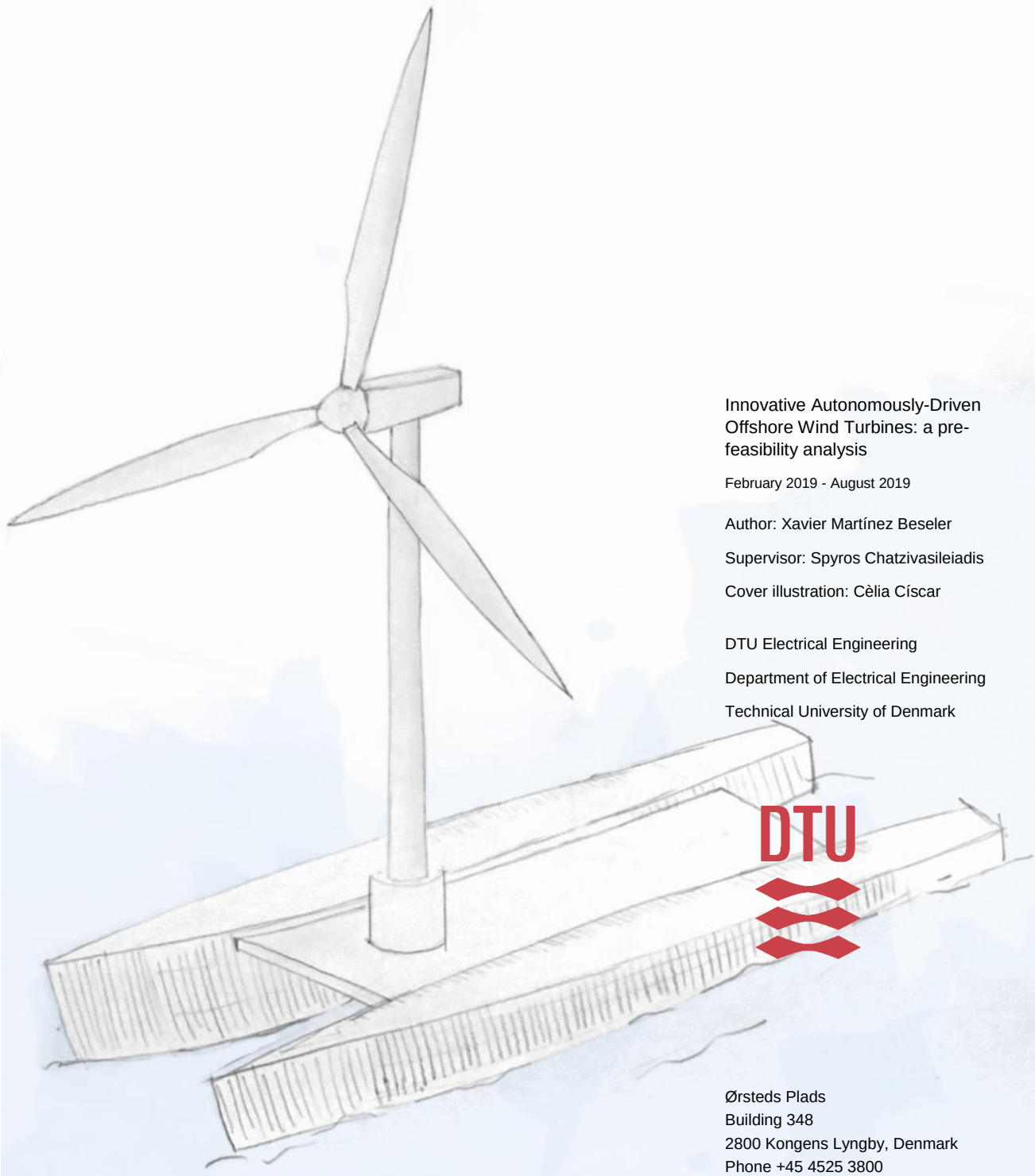

Innovative Autonomously-Driven Offshore Wind Turbines: a pre-feasibility analysis

February 2019 - August 2019

Author: Xavier Martínez Beseler

Supervisor: Spyros Chatzivasileiadis

Cover illustration: Cèlia Císcar

DTU Electrical Engineering

Department of Electrical Engineering

Technical University of Denmark

Ørsteds Plads
Building 348
2800 Kongens Lyngby, Denmark
Phone +45 4525 3800
elektro@elektro.dtu.dk
www.elektro.dtu.dk

Abstract

This M Sc Thesis describes a disruptive technology inexistent up to date envisioned by the author of this M Sc Thesis called "Autonomously-Driven Offshore Wind Turbines" (ADO-WTs). Two integrated models independent from each other plus a costs analysis pave the way for future research. The two models presented are the Wind Energy Yield Assessment model and the Power Losses model.

The Wind Energy Yield Assessment model constitutes three models used to quantify potential benefits from moving wind turbines (WTs) on the North Sea: the first model is the reference to assess the extra energy from the other two. The second model sets an upper bound for the proposed technology and the third represents a more realistic implementation. Neither of these models account for the energy losses required to move the WTs nor model the energy system storage. Results for a simulation ran in the Southern North Sea for the whole 2018 historical data shown 45.19% of extra AEP for Upper-Bound model, and 20.98% for Reachable Area model, both compared with the energy production based on the Conventional model, which was verified based on results from other research.

A review of the current State of Art of Energy Storage System (ESS) is shown and three ESS technologies were found suitable for being installed aboard moving wind turbines: Li-ion batteries, Hydrogen and Zinc-Air batteries.

The Power Losses model accounts for power required to move ADO-WTs on the sea. A simple catamaran hull to ensure buoyancy was designed for each technology. Results show Hydrogen to be the lightest technology providing the least power losses profile followed by Zinc-Air batteries. Moreover, because of moving the whole system, the wind turbine can work for a wider range of free wind speeds, able to produce at rated power for free wind speeds up to 31m/s for LH2 ADO-WTs, without increasing loads on the blades or rotor. Moreover, optimal boat speeds are shown for each free wind speed and technology.

A cost analysis was carried out with huge limitations regarding data availability. Five cases were analysed: a conventional wind farm with an offshore substation ($LCOE = \$88.34/MWh$), ADO-WTs wind farm with an offshore terminal for both ADO-WTs with hydrogen as ESS ($LCOE = \$104.81/MWh$) and Li-ion batteries ($LCOE = \$3,774/MWh$) and ADO-WTs wind farm with an onshore terminal for hydrogen ($LCOE = \$99.37/MWh$) and Li-ion batteries ($LCOE = \$3,767/MWh$).

Acknowledgements

First of all, I want to thank **Spyros Chatzivasileiadis** to believe in my idea from day one when I went to his office and he immediately said he wanted to supervise my work. I am immensely grateful to him for giving me freedom and respecting my decisions on what to research, for giving me advice when I needed it and opening me the door to his network, for instance, to the first meeting of the North Sea Energy Hub Steering Committee where my idea was pitched and I could get feedback from industry.

I could not have carried out my works on Naval Architecture without the priceless help of **Harry Bingham**, who carries with the best attributes a professor cut have. Spending a Friday evening at DTU enlightening me about the world of Archimedes and Froude, for providing me with literature and precise advice as well as for looking after my calculations and foremost, for sharing such positive energy! I also want to thank my friend Andreu Micó for giving me clearly explanations and introducing me to the romantic and archaic jargon of Maritime Engineers. In addition, I give thanks to Manuel Ventura for sharing his estimations for calculating ship costs.

People from DTU Wind helped me in several steps of my work. I want to thank **Bjarke Tobias Olsen** for recommending me the dataset I used to prove my idea. **Martin Otto** helped me formulating the Power Loss model to which I am truly thankful. **Henrik Bredmose** was the first who told me about the people from Central Nantes to whom I exchanged ideas. Thanks in particular to **Roshamida Abd Jamil** and **Aurelien Babarit** to share their literature and key findings and for their inspiring work: I give my best wishes to your future findings!

I want to thank **Fitim Kryezi**, Project Manager at Energinet, his inputs and feedback helped me improving my concept and his tireless enthusiast gave me extra energy to bring my idea one step forward. He also connected me with **Martin Hartvig** Senior Engineer at Energinet who provided me specific knowledge of Power to Gas applications, dreamed with me and gave me invaluable inputs for my ESS analysis both in costs and technology. In general, I have the feeling that people working at Energinet share a huge enthusiasm and willingness to find new solutions and bet on R&D: thanks for that, keep that spirit!

Thanks to **David Johnsen**, Senior Director of COP, who provided me detailed and customized information of how cable arrays are designed in offshore wind farms. I also want to thank to **Magdalena Zajonc** Business Developer at Peak Wind, who shown a special interest on my idea and contribute with her knowledge to my costs approach providing me some literature and interesting discussions.

Thanks to **Morten Nielsen** from Ørsted who listened to my idea, gave me positive feedback, completely new inputs and cheered on me to keep exploring this idea. In addition, I give thanks to **Lucas Marion**, R&D Roadmap Manager at Ørsted, who thought over my idea with criticism and shared with me the weak points he saw on my concept. It was really important to me that the uncertainties I foresaw on my concept were shared by those working in R&D at the world's leading company for offshore wind development.

Also, thanks to **Bruno Kotovich**, Project Manager from Vestas, who always expresses interest on what I am working on and shows a willing to share his knowledge with me.

I want to thank in general workers from industry to spend some time thinking out of the box and giving constructive feedback to my idea. I have no doubt that the involvement of such renown companies provides my work with a more complete analysis. Please keep giving feedback to future students!

The cover illustration was created by my old friend **Cèlia Císcar**. **Núria Martínez** and **Dani Catalán** also contributed in the process. I am immensely thankful to all of them, for allocating part of their time to translate my drafts into such a beautiful piece of art!

Finally, thanks to my colleague and good friend **Jorge Izquierdo** who saved me a lot of time with the LaTeX template and, in general, to all my class mates and friends who throughout informal conversations helped me maturing the idea: let's never stop dreaming together!

Contents

List of Figures

List of Tables

Nomenclature

ADO-WT	Autonomously-Driven Offshore Wind Turbine
AEP	Annual Energy Production
BFOWT	Bottom-Fixed Offshore Wind Turbine
BoP	Balance of Plant
CAPEX	Capital Expenditures
DC	Direct Current
ESS	Energy Storage System
FCR	Fixed Charge Rate
FOWT	Floating Offshore Wind Turbines
IEA	International Energy Agency
LCOE	Levelized Cost of Energy
LH2	Liquefied hydrogen
P2G	Power to Gas
PtG	Power to Gas
OPEX	Operational Expenditures
O&M	Operation & Maintenance
OWEC	Offshore Wind Energy Converters
WEYA	Wind Energy Yield Assessment (model)
WT	Wind Turbine
WTG	Wind Turbine Generator

CHAPTER 1

Introduction

Nowadays, humanity faces a huge challenge to fight climate change. In order to mitigate its adverse effects, all the energy sectors must be decarbonised. According to the International Energy Agency (IEA), the largest source of emissions in 2016 was the electricity and heat generation sector, representing 42% of the total emissions of the whole world whereas transport accounted for 25% of total global emissions in 2016 [1]. Even though the solution must come from an integrated project involving every country and every sector –not only power & heat but also and specially transportation and industry–, switching the electricity generation from fossil fuel based power plants to sustainable energies as well as finding new processes to obtain sustainable fuels to power the transport sector are two key points in the sustainable transition the society must take. Renewable energies must grow both in capacity installed –while shutting down polluting power plants– and in maturity, finding integrated solution to compensate fluctuations of the natural sources renewable energies are fed from, such as wind and sun.

This M Sc Thesis proposes a disruptive concept emerged from an already established technology: wind power. More precisely, this research proposes a concept called "Autonomously-Driven Offshore Wind Turbines" (ADO-WTs), which are WTs envisioned to freely move on the sea to yield more wind power and minimize overall costs. It is the believe of the author that with the intent of clarifying uncertainties related with the new technology proposed, current issues the wind power sector faces might be re-considered, as well as new solutions and perspectives may be discovered along the way.

This report shows methods and first results obtained in a first approach to this new concept carried out by the author who constantly consulted experts from both industry and academy with the intent of providing an integrated solution. This M Sc Thesis pretends to answer whether researching this new concept further is worth it.

1.0.1 Need of Innovation

Aidan Cronin [1] introduced the 2018 report for the Strategic Research & Innovation Agenda (SRIA) with these words: "the wind energy sector has been one of the champions of applied technology Research & Innovation in Europe. This has made wind

[1] Chair of the ETIPWind Steering Committee (Advisory Specialist, Siemens Gamesa Renewable Energy)

power competitive with traditional fossil power generation. Onshore wind is now the cheapest form of new installed power capacity" [2].

Every sector is fed by energy: transportation, industry & commerce and residential. By electrifying these sectors and replacing coal and gas power plants by green energy sources, integrated with other sustainable solutions such as biofuels, carbon emission levels would aim at fulfilling the target set in the Paris Agreement.

The Global Wind Energy Council (GWEC) has set up a task force to accelerate the development of offshore wind across the world, Henrik Stiesdal [2], as GWEC's global offshore wind ambassador, stated that ´´Offshore wind has huge potential in many regions as the world looks for competitive, zero-carbon energy sources that can be deployed at scale and in relatively fast time frames. However, the industry needs to find the most appropriate technologies for deploying offshore wind in different conditions – for example, floating offshore wind in regions with deep water levels, and creating efficient supply chains across the globe."[3].

According to WindEurope, Europe needs to support R&D to sustain the current cost reduction trend, both in onshore and offshore wind, while at the same time ramping up the transition towards a flexible energy system with variable renewables at its core. In fact, one of the recommendations stated in the SRIA report [2] is to facilitate market-uptake of floating offshore wind concepts through regulatory improvements. Along the report, 5 Research & Innovation priorities are outlined:

- Grid & system integration
- Operation & maintenance
- Next generation technologies
- Offshore balance of plant
- Floating wind

In addition, the report supports the need of a fundamental research into radical and/or disruptive innovations. All these trends go along with the research presented in this report. As a matter of facts, the solution proposed in this text includes potential improvements –although also uncertainties– within the fifth pillars and it is, in fact, a disruptive concept.

Moreover, the European Network of Transmission System Operators (ENTSO-E) sees the rapidly rising transmission congestions (and distribution congestions to follow) due to concentrated Renewable Energy Sources development as one of the main

[2]Henrik Stiesdal's contribution to Wind Industry goes from the three-blade rotor which replaced the previously preferred two-blade back from 1980s version to the IntegralBlade, a 75m blade cast in a single piece or the TetraSpar, a flooting platform that can be towed out to sea with the turbine already mounted `https://www.epo.org/learning-events/european-inventor/finalists/2018/stiesdal.html`.

[3]Found online at `https://www.windpoweroffshore.com/article/1494035/gwec-sets-offshore-wind-task-force`.

challenges and key findings the System Operators will face in the coming future, as published in the Advocacy Paper in May 2019 [**entsoe2018RD**]. Finding innovative solutions for Grid & System integration is therefore a shared goal by different parties involved.

Regarding operation & maintenance, the report presenting results from the Floating Wind Joint Industry Project (2018) [3] states that there is currently a considerable interest in disconnecting floating wind turbines and tow them to port (so-called *tow-to-shore*) for maintenance, to avoid high costs of expensive heavy lift vessels.

This push for innovation from both market regulators and players is the best foreword to introduce the concept proposed in this report.

1.1 Introduction to the concept

The idea proposed in this report, the so-called Autonomously Driven Offshore Wind Turbines (ADO-WTs), consists on floating wind turbines that can individually move around the sea in order to track best wind spots. ADO-WT would carry a large energy storage system aboard to store the wind energy yielded and an algorithm, coordinating every ADO-WT, would send the next location set-point where the ADO-WTs would go in order to harvest more wind power. This algorithm would receive *real-time* power output and location of each ADO-WT so that forecasts models would be improved and ADO-WTs would perform increasingly better; also current wake and lay-out configurations models could be improved by playing with the ADO-WTs location with exclusively R&D purposes. The propelling system is the responsible to bring them to each spot –which would be found to maximize revenues from selling wind power– but also to shore to be checked for scheduled maintenance operations, to decrease O&M costs. A discharging-substation or terminal, similar to the current substation, would have a floating pier system where ADO-WTs would berth and discharge the energy yield and stored aboard, which would be transferred to the grid through transmission lines –if energy is stored as electricity– or pipelines –if energy is stored as hydrogen–. In some cases this substation or terminal could be sited onshore, reducing enormously construction and decommissioning costs as well as Health and Safety at work. In addition, ADO-WTs are envisioned to produce energy at the same time they travel as similar studies do (see 2.3). Finally, ADO-WTs would discharge the energy whenever the prices are higher and wherever it is required, as long as the terminal is prepared to such purpose facilitating the grid and system integration.

Figure 1.1 shows the main components of the envisioned ADO-WTs, these are:

- Wind Turbine: A WT similar to the ones currently used in offshore wind farms would be placed on top of the hydrodynamic floating platform (hull).

- Energy Storage System (ESS): the energy yielded would be saved aboard in the ESS.

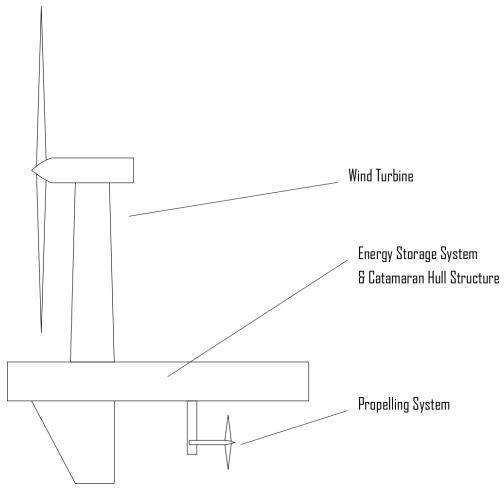

Figure 1.1: ADO-WT - scheme of the whole system.

- Hull & Propelling System: the hull is in charge of ensuring buoyancy and well hydrodynamic performances whereas the propellying system is the responsible for moving ADO-WTs to the sent location.

In this research, the WT is modelled as the NREL offshore 5-MW baseline wind turbine [4]. That is, 3 blades horizontal axis WT, the hub height is 90m and the rotor diameter 128m. However, future research should explore greater WT sizes. Chapter 3 shows method and results of the implemented model, namely Wind Energy Yield Assessment. Figure 1.2 presents a 3D perspective of the ADO-WTs.

A research on different technologies is presented in Chapter 4. Conclusions from the whole research aim at a hydrogen ESS as the most cost-effective technology.

A simple catamaran hull structure is designed in order to account for power required to move the whole system –including WT, ESS, and the proper hull & propelling system–. Chapter 5 shows method and results of the so-called Power Losses model.

Notice that the ESS and the hull & propelling system are shown together in Figure 1.1. This is because no study was carried out studying where to install the ESS. It is believe that it could be placed within the hull structure inside the side-arms and/or as a keel, to low the centre of mass of the whole system, providing more stability. However, a proper stability research should be carried out to define this.

Besides the components than can be seen in Figure 1.1, the ADO-WTs system would also have:

- Optimization algorithm, which would coordinate the whole fleet of ADO-WTs in order to maximize revenues from selling the energy –either electricity or hydrogen–. ADO-WTs would monitor weather variables and power production

associated to their current location and send these data to a remote computer which sends back the optimal position to each of the ADO-WT to maximize profits.

- Discharging substation –for electricity– or terminal –for hydrogen–. It could either be installed offshore or onshore. ADO-WTs would berth at floating piers, be automatically plugged and discharge their energy. If offshore, the energy would be transported through transmission lines or a pipeline to an onshore terminal; if onshore, the whole transmission line or pipeline and offshore substation would be suppressed.

Reachable Area implemented model is a first approach of the optimization algorithm (see 3.1.4 for method and 3.3.3 for results).

The keel –not studied in this research– and the water depth, could force the substation/terminal to be installed offshore. However, this would allow ADO-WTs to yield further which could foster higher energy yields.

From ADO-WTs huge challenges associated to each uncertainty are derived. However, it also brings a huge potential. 1.2 describes the approach taken throughout this report to tackle them.

The disruptive idea presented in this report means a change in the way wind farms are currently installed and operated. It aims at a future scenario where the new technologies they relay on will be mature, cheaper and more efficient. In fact, it is an attempt to pave the path for a whole new R&D area. In a few words, a future scenario where WTs have a storage system aboard, are autonomously driven over the sea to maximize wind yielded and discharge the energy to terminals connected to the main system is envisioned.

Offshore WTs would no longer be fixed to the seafloor but move around the sea and discharge energy in a pan European Power Grid and ultimately in a Global Power Grid. Because the idea is such disruptive, it brings along new perspectives of several

Figure 1.2: ADO-WT - 3D model. Credits: Núria Martínez and Dani Catalán.

fields involving offshore wind farms and other technologies such as floating PV or tidal energy which might be feasible by themselves.

Thus, this MSc Thesis proposes an initial approach to such scenario, considering from an energy production perspective, how much extra energy one could harvest by moving WTs. The whole idea depends on whether the extra energy that one could harvest compensates the extra cost associated to such new technology yet to be explored.

1.2 Approach

Because the project was proposed by the student, it had intrinsic associated risks. Therefore, before the project even started, a simple risk analysis was carried out, which outlined four risks for which mitigation tactics were planned.

First risk: it could have happened that data was not found on time; the mitigation tactic was to start with one of the extra analysis defined if there was enough certainty that the right data was going to be found on time; if not, the whole thesis topic should be changed.

Second risk: data which was going to constitute an input of the first model implemented was going to be the outcome of models based on observations. It couuld have happened that what was meant to be checked: geographical compensation of wind speeds within relatively close areas, could not be observed due to the way models are built. It was decided to allocate all necessary resources to clarify this as soon as possible. The mitigation tactic was to find a new topic.

Third risk: it could have taken more time to develop the project. The contingency plan was to develop an extra analysis less.

Fourth risk: results could have shown that the extra energy from moving ADO-WTs was not worth it to move them. The mitigation tactic was to quantify the limits that would make it worth it: how big the area should be, how much energy was required to move them, etc.

Luckily non of the mitigation tactics had to be followed. Both first and second risks were avoided within the first week, which let the project start.

The approach followed in this investigation is very simple. From day 1, the concept was broken down into different uncertainties which were prioritized by applying a concept from Project Management which states that the sooner an error from a project is found, the less costly it will be to fix it. Moreover, a spiral of improvement was applied, in order to have results as soon as possible, being aware of the limitation of the models, and iteratively keep researching either that or new uncertainties.

First of all, it is was identified the main goal of ADO-WTs, the reason why they were envisioned by the author: to yield more wind energy [4] which constituted the main driver to decide which new uncertainty had to be clarified.

[4] Throughout the research, other potential benefits from ADO-WTs were found, such as a potential decrease of installation, decommissioning and O&M costs were discovered as well.

To illustrate with an example, the idea has associated a huge concern regarding maritime routes and permits –which Babarit solve by referring to a sea desert [5]–, which is definitely a question to investigate further; however, it would make no sense to check this uncertainty before knowing that one can in fact get more energy by moving WTs. Or by *reductio ad absurdum*, if at the end WTs would not yield enough extra energy thanks to moving them, all the previous job would be lost.

Because the goal was to obtain more energy, it would not make sense to move wind turbines if less energy was yielded by doing so. Thus, it was firstly checked the extra energy one could get by moving ADO-WTs. The North Sea was defined as the field where quantifying it. Since an artificial island –or several– is planned to be built in the North Sea with the goal of connecting several European power system grids and promote more wind power penetration, it was decided to study ADO-WTs moving around the North Sea.

Three models were carried out to assess the extra energy yielded from moving WTs (see Chapter 3): the Conventional model, modelling BFOWT and used as a reference, the Upper-Bound model to quantify which is the maximum limit that one could get by moving WTs and the Reachable Area model, in an attempt to quantify more realistically what was studied through the Upper-Bound model.

Results from these models were positive and therefore it was decided to explore the idea further. Two big questions were found interesting at that point: what to do with such huge amount of energy and how much energy would be required to move the whole system. The solution to both answers came in an integrated solution.

The state of art of current Energy Storage Systems (ESS) was reviewed to find every technology able to store energy aboard ADO-WTs (see Chapter 4); each technology had a different energy density, fostering a different total weight to be carried. A Power Loss model was implemented to estimate how much power would be required to move the whole system –as defined in Figure 1.1, except from the keel– (see Chapter 5). The three pre-selected technologies from the literature review (Li-ion batteries, Zn-air batteries and hydrogen produced through electrolysis) were included in the model to quantify the losses and results were surprisingly better than expected.

Finally, a cost analysis was carried out with the attempt to have an initial idea of how costly this technology would in a future scenario where the technology itself would be already mature (see Chapter 6). No final decisions are expected to be taken from this analysis since the lack of data forced the author to make a lot of assumptions; however, results for hydrogen based ADO-WTs shown very promising results which perhaps could inspire future research.

In general, during the 5 months this research was carried out, plenty of new uncertainties, ideas, concepts –or in one word: questions– were found along the way. The method used to canalize all these new inputs was as simply as writing them down as soon as they were arising –to immediately forget about them and keep working– and every few days, it was checked that the project scope was clear and the inputs were reviewed and either allocated within the coming/future tasks, held on or directly rejected. To do so, the answers that each of those questions could give were envisioned

and the most significant for the scope were selected always foreseen the time it would take to clarify them.

Other uncertainties, as well as deeper study of the ones clarified in this research should be analysed in future research. Section 7.2 lists all the future works proposed along the report.

1.3 Structure of the report

The following lists summarizes what is written in each chapter:

- Chapter 1 is the introduction to the report and the concept itself.
- Chapter 2 was though to be a general state of art of what is not included in the other three. Most likely it was meant to present similar studies. I am thinking to delete it and spread it through the other four chapters (Energy Wind Assessment, Energy Storage, Power Losses and Costs). So please do not loose time on it.
- Chapter 3 shows explains the Wind Energy Yield Assessment model implemented to quantify the extra energy that ADO-WTs may get from moving over the North Sea and presents results from a few simulations.
- Chapters 4 shows the literature review of the Energy Storage Systems and the three pre-selected ESS technologies.
- Chapters 5 explains the Power Losses models, which quantifies the power required to move ADO-WTs for different values of wind speed and boat speeds, as well as presents its results.
- Chapter 6 explains method and results of five cases studied to compare wind farms made of the current technology (BFOWT) with wind farms made of ADO-WTs with either the discharging substation onshore or offshore. Moreover, each ADO-WTs case is in turn completed with Li-ion batteries and hydrogen to clarify which technology is more cost-effective.
- Chapter 7 concludes the report and proposes a roadmap to continue this new R&D branch.
- Appendices complement information shown throughout the whole report.

CHAPTER 2

Review of the current Offshore Wind Power

The total installed capacity of wind energy (both onshore and offshore) was 178.8 GW at the end of last year (2018). Wind energy remains the second largest form of power generation capacity in the EU-28 and is likely to become the first source overtaking natural gas installations in 2019 [6]. Figure 2 shows the evolution of several forms of power generation capacity in the European Union from 2008 to 2018 showing how wind energy represents the bigger increase. In fact, Wind power installed more capacity than any other form of power generation in the EU in 2018, accounting for 48% of total power capacity installations [6].

Regarding offshore wind power, by February 2019, it accounted for 10% of the accumulated wind power installed capacity in Europe (19GW) [6] and according to a Bloomberg research, the global offshore wind market will grow 16% annually from

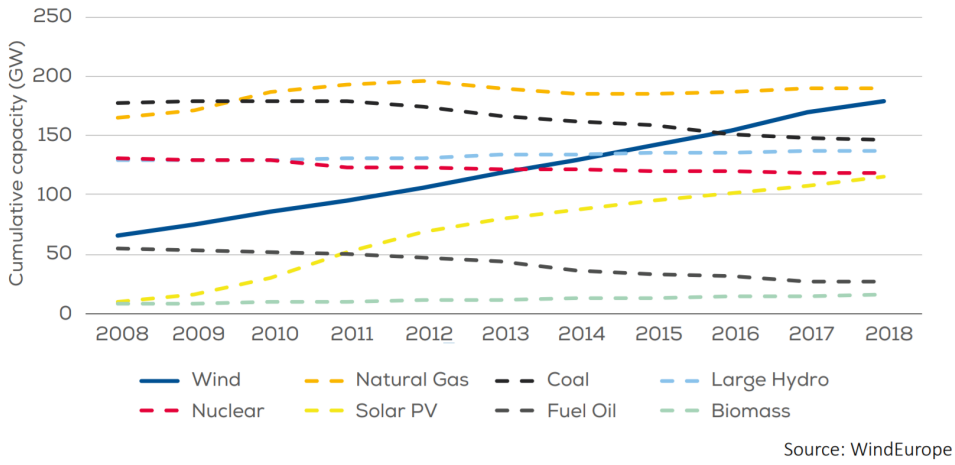

Figure 2.1: Total power generation capacity in the European Union 2008-2018 [6].

2017 to 2030, reaching 115GW of cumulative capacity [1].[2] is more optimistic and states wind energy capacity in the EU could double by 2030 to 323 GW, meeting close to 30% of the EU's power demand.

In just four years the strike prices for onshore wind auctions have dropped from over 100 €/MWh in 2013 to around and even below the 40 €/MWh mark in 2017. And costs in offshore wind are falling rapidly too. In 2014 bids were coming in at over 150 €/MWh, whereas in 2017 prices dropped to 65 €/ MWh and even lower [2].

This chapter first explores the current state of art of Offshore Wind Power focusing on both BFOW and FOW. Secondly, it presents studies which share certain similarities with the proposed technology: ADO-WTs, introduced in 1.1.

2.1 Bottom-Fixed Offshore Wind (BFOW) - Current numbers and trends

By the end of 2018, there were 18.5 GW of installed offshore wind capacity in Europe, with a total of 4,543 turbines connected to the grid across 11 countries. 98% of this capacity is concentrated in just five countries: the UK (44%), Germany (34%), Denmark(7%), Belgium (6.4%) and the Netherlands (6%) [7].

Regarding the location of these wind farms, the North Sea accounts for 70% of all offshore wind capacity in Europe, followed by the Irish Sea (16%), the Baltic Sea (12%) and the Atlantic Ocean (2%) [7].

Figure 2.1 shows both the annual wind installations –by country– and the accumulated capacity. Despite the 15.8 % of less new capacity installed in 2018 compared with 2017 –which was a record year–, a total of 2.66 GW new capacity was installed in 2018.

Since 2014 the average rated capacity of newly installed wind turbines has grown at an annual rate of 16%. In less than 20 years, the size of Wind Turbines has almost multiplied by 4, from 2MW average in 2000s to almost 7MW average in 2018 [7]. In fact, GE recently finished the nacelle of the largest offshore wind turbine –12MW– in last July 2019 [2], its tower is made up of four segments; a prototype is planned to be ready by late summer 2019 [3].

Likewise, wind farms have increased in size. The average offshore wind farm has increased from 79.6 MW in 2007 to 561 MW in 2018. To date, the largest offshore wind farm planned –currently under construction– is Hornsea One Project, in UK of more than 1.2GW [7].

[1] From the Bloomberg New Energy Finance: `https://about.bnef.com/blog/global-offshore-wind-market-set-to-grow-sixfold-by-2030/`

[2] Found online at: `https://www.greentechmedia.com/articles/read/ge-finishes-first-nacelle-for-12mw-haliade-x-offshore-wind-turbine#gs.sbsotr`.

[3] Found online at: `https://www.rechargenews.com/wind/1804846/ges-world-record-wind-turbine-takes-shape-as-tower-ships`.

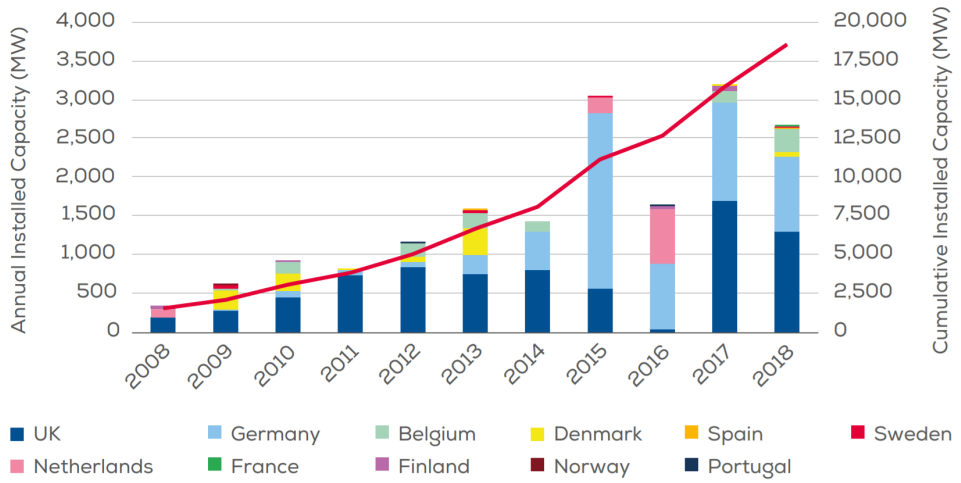

Figure 2.2: Annual offshore wind installations and cumulative capacity [7].

Currently, Bottom-Fixed Offshore Wind Turbines (BFOWTs) represent almost the whole accumulated installed capacity in 2018 worldwide (the only commercial floating offshore wind farm installed nowadays is Hywind Scotland which started producing electricity in October 2017 [4]). 25% of the EU's electricity demand could, in theory, be met by BFOWT wind energy at an average of €54/MWh in the most favourable locations [8]. However, BFOWTs also have some limitations which can be complemented with Floating Offshore Wind Turbines (FOWT). The biggest limitation of current BFOWT is mainly water depth.

There are mainly two BFOW foundations which are consolidated: monopiles – for shallow waters and jackets up to 50m approximately [9]. In 2018, monopiles remained the most popular type of all installed foundations (74.5%) whereas jackets installations represented 24.5% of all foundations installed the last year [7]. Regarding accumulative values, Monopiles represents 81.5% of all installed substructures in Europe followed by jacket foundations (8%); other types are tripile (1.6%), tripod (2.5%) and suction-bucket jackets; refer to the whole report for more information [7].

The average water depth of offshore wind farms under construction in 2018 was 27.1 m –very similar to the previous year's– and the average distance to shore of those projects was 33 km, a decrease on the previous year (41 km). Hornsea One in the UK and EnBW Hohe See in Germany both currently under construction are the projects located farthest from the shore, 120 km and 103 km, respectively. Deutsche Bucht, also in Germany, follows at 93 km from the shore [7].

[4]Found in Equinor's website, which developed the project, `https://www.equinor.com/en/what-we-do/hywind-where-the-wind-takes-us.html#why-hywind`.

As already mentioned, Hornsea One in UK will be the largest offshore wind farm in the world with a capacity greater than 1.2 GW [5]. Two teams will be responsible for operating and maintaining the wind farm, 24 hours a day, seven days a week, throughout its 25-year life-span [6]. To date, 172 out of 174 monopile foundations have been installed at the site, and turbine installation is expected to continue until late summer 2019. The electricity generated by the turbines will pass via undersea cables through one of three massive offshore substations, and the world's first offshore reactive compensation station, all fully installed, before reaching shore at Horseshoe Point, Lincolnshire. The electricity is then transported via underground cables to the onshore substation in North Killingholme, where it connects to the UK National Grid, in order to reach well over one million homes in the UK [7].

Moreover, the overall quality of offshore wind sites until 2030 is expected to be at the same level as the current offshore wind sites regarding distance to shore, water depth, wind speed, etc. After 2030, the best wind sites are expected to be utilized. Hence, slightly worse wind sites will be used resulting in an increased cost per kWh relative to an average pre 2030 wind site. The main drivers for this increase will be distance to shore and water depth since the post 2030 wind sites are expected to be located in the Northern Sea [10]; where Wind Energy Yield Assessment model has ben tested (see 3.1.1.2).

2.2 Floating Offshore Wind (FOW)

Bottom-Fixed Offshore Wind (BFOW) is only applicable in selected locations. Bottom-fixed foundation concepts consist of a jacket, utilised at intermediate depths (30-50 m of water), and a monopile suitable for shallower water, whereas floating systems become available in waters from 30 to 40 m and deeper [9]. [9] also found that LCOE of FOWTs applied in depths of 50-150 m was comparable to BFOWTs which generally experience increased LCOE at higher rates than FOWT. There are currently four substructure designs for floating offshore wind: barge, semi-submersible, spar buoy and tension leg platform (see Figure 2.2). The first three are loosely moored to the seabed, allowing for easier installation, while the tension leg platform is more firmly connected to the seabed. Through the Floating Wind Joint Industry Project, Carbon Trust published a report [3] in which four dominant types of floating wind foundations are identified:

- Barge: it is the foundation with the most shallow draft which constitutes both its bigger advantage and drawback: it is easier to install beside shallow quays,

[5] Found in Ørsted home web page `https://orsted.com/en/Our-business/Offshore-wind/Our-offshore-wind-farms`.

[6] Found online at `https://www.offshorewind.biz/2019/06/03/orsted-kicks-off-hornsea-one-operations/`.

[7] Found at Ørsted home page: `https://orsted.com/en/Media/Newsroom/News/2019/02/The-worlds-biggest-offshore-wind-farm-Hornsea-one-generates-first-power`.

however, it may need extra reinforce from the mooring systems. Some of the Barge include a moon-pool to suppress wave-inducted loading [8].

- Semi-submersible: free-surface buoyancy-stabilised structure with relatively shallow draft. Its advantages is its versatility to different site conditions. Its drawbacks are mostly its manufacturing complexity and its relatively high required mass of steel.
- Spar: it consists of a ballast-stabilized structure with relatively large draft. Its bigger advantage is its design based on an already proven concept providing huge stability. Its major drawback is the huge draft with also makes it more difficult to assembly and transport.
- Tension-Leg platform (TLP): tension-stabilised structure with relatively shallow draft and limit motions during operations. Its bigger advantages are its lower material costs, whereas its disadvantages are the risk in case of mooring failure and its performance highly dependant on the soil conditions.

Moreover, Henrik Stiesdal proposes a fifth concept called TetraSpar with an attempt to industrialize the manufacturing process and minimize costs [11]. For more information about wind floating foundations refer to [12] and [3].

[8] Find more information at `https://www.ideol-offshore.com/en/floatgen-demonstrator`.

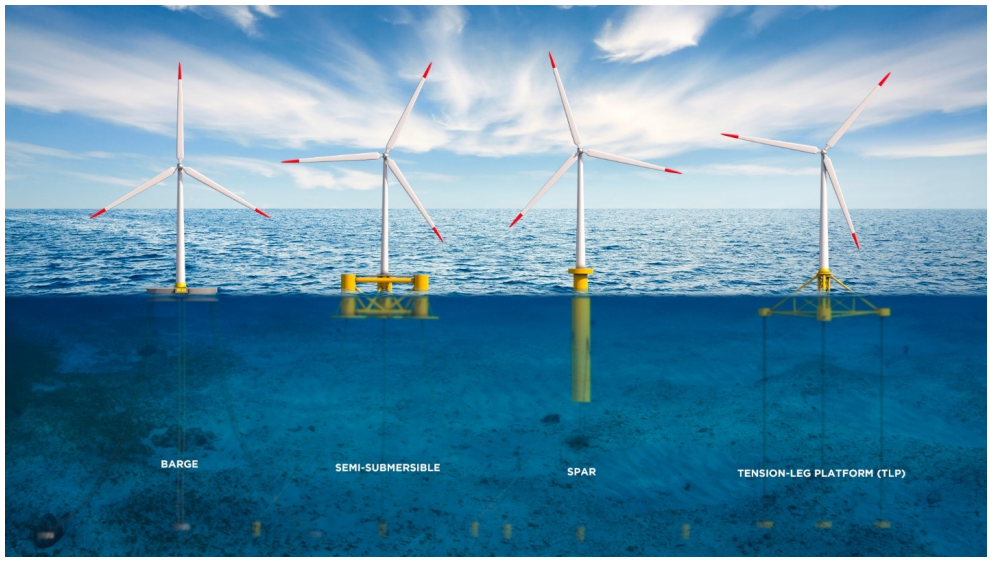

Figure 2.3: Floating wind typologies [3] obtained from Wind Europe.

The technology readiness level (TRL) related to semisubmersible and spar buoy –used in Hywind Scottland wind farm– has entered a phase (>8) in which the technology is deemed appropriate for launch and operations. The barge and the tension leg platform (TLP) concepts are projected to reach this stage in the coming years [13]. One floating barge was commissioned for the Floatgen project and 2 floating semi-sub structures were commissioned respectively for the Eolink Prototype and the Kincardine project [7].

A report from BVG Associates Limited [8] shown offshore wind power projections for 2030. Among other analysis, the report presents the economically attractive resource potential by foundation type (monopile, jacket (or gravity base) and floating foundations in general) for two scenarios. In the baseline scenario, FOWs produce 14% of the economically attractive resource potential and in the upside scenario FOWs produce over 70% of the additional economically attractive potential (the rest is BFOWT).

FOW (Floating Offshore Wind) complements the BFOW industry by adding more capacity to the supply chain and by introducing new technology and developers which will improve not only the existing conditions of the industry, but will also speed up technological development, as more overlapping research will be carried out on turbines, cabling, electrical interconnections and operation and maintenance (O&M) [13]. In the same way that BFOW followed the progress from onshore wind and allowed an increase in wind power capacity in Europe, FOW has the potential to further increase offshore wind power capacity [13]. Statoil ensures that Hywind Scotland project had a capacity factor of 65% during its first winter [9]. Indeed, deeper offshore areas represents 60-80% of the offshore wind potential in Europe [13]. FOW can also be an alternative solution to BFOW, as it can be more easily installed in areas with poor seabed conditions and would also allow for the potential recycling of currently abandoned sites initially studied for bottom-fixed [13].

To date, Hywind Scottland is the biggest floating wind farm in the world, with 30MW power installed, five 6MW Siemens Wind Turbines, model SWT-6.0-154, are sited 25m far from shore, with 108m water depth, using Spar floating technology [10]. The rest of floating wind farms are pilot projects of 2MW [11].

In the future, larger floating wind farms are to be constructed: Kincardine (in the UK) is due to be fully operational in 2020 and could be the world's largest floating offshore wind farm [12], consisting on one 2MW wind turbine and six 8.4 MW [14] with an average water depth twice as deep as all the bottom-fixed offshore wind farms, with 77 m [7]. Windfloat Atlantic in Portugal, 25MW floating offshore

[9] Found online in `https://www.4coffshore.com/windfarms/project-dates-for-hywind-scotland-pilot-park-uk76.html`

[10] Found online at `https://cleantechnica.com/2018/02/16/hywind-scotland-worlds-first-floating-wind-farm-performing-better-expected/`.

[11] Found through the interactive offshore map application found at Wind Europe website `https://windeurope.org/about-wind/interactive-offshore-maps/`.

[12] Found online at `https://www.windpoweroffshore.com/article/1497569/first-power-kincardine-floating-project`

wind farm will come into operation this year [13] using Principle Power technology, semi-submersible foundations [14]. Other FOW farms are planned: 200MW at South Korea which may start constructions in 2020 due to be commissioning by 2022 [15] and 200MW in Canarias Island (Spain) which could start operations in 2024 [16]; both of which are to be developed by Equinor.

2.3 Similar Studies

ADO-WTs were initially envisioned to capture more power by changing to spots with more wind whenever there is poor wind resources at the site where BFOWTs would be sited and staying still during up to 30 years a wind farm will last [15]. The author discovered that the concept of having a WT on a vehicle was, nonetheless, not new.

Back in 1969, Andrew B. Bauer [16] wrote "Faster than the wind" in which he presented performance charts for water and land vehicles which by use of wind energy alone could accelerate in the wind direction from zero speed to a speed larger than the wind. Moreover, he described the land vehicle he built himself claiming he operated at speeds faster than the wind. Two years later, Bauer published another paper [17] aiming at finding which type of ship, if windmill-driven or sail-driven ships, was more efficient. However, no clear answer was given stating that they may each do equally well in elapsed time from point A to B.

Fourteen years after Bauer's first publication, in 1983, Jean-Pierre Vidal patented a system for propulsion of boats by means of wind and streams and for recovery of energy [18]. He claimed his floating station –neither moored nor anchored– moved forward by using energy from the wind and water streams and was able to recover energy aboard. He said that navigating facing the wind was perfectly possible and if sailing before the wind speeds higher than that of the wind were achievable. Both the airscrew and the water propeller could be set to variable pitch during operation capable of functioning as energy collecting turbine or propeller alternatively. Figure 2.3 shows a sketch of the invention with a 4 blades wind turbine mounted on a catamaran hull structure. Just one year after Vidal's patent, H.M. Barkla proposed a vertical axis wind turbine/propeller for ship propulsion [19].

50 years after Bauers first paper, Mac Gaunaa, Senior Scientist for DTU Wind Energy, wrote ´´Theory and design of flow driven vehicles using rotors for energy conversion" [20], in 2009. For five consecutive years, Mac Gaunaa and Robert Mikkelsen with a group of students from DTU enter the Racing Aeolus Den Helder, an international competition for wind-powered cars moving against the wind stream. Last

[13]Found online at `https://www.repsol.com/en/sustainability/climate-change/new-energy-solutions/windfloat/index.cshtml`

[14]Found online at `https://www.youtube.com/watch?v=IO7GXLR4YUo`.

[15]Found online at `https://www.rechargenews.com/wind/1822306/equinor-ties-up-with-korean-groups-for-200mw-floating-play`.

[16]Found online at `https://www.rechargenews.com/wind/1798896/spain-grants-equinor-ok-for-worlds-biggest-floating-wind-farm`.

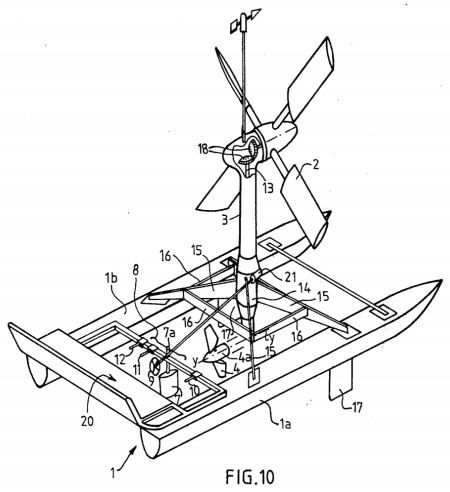

Figure 2.4: System for propulsion of boats by means of wind and streams and for recovery of energy US patent from 1983 [18].

year they achieved a top speed of 113.1% of the incoming free wind speed whereas the wining team achieved 113.9% [17].

In 2017, Guilloteaux and Babarit presented their work on a wind driven vessel dedicated to hydrogen production. Flettner rotors propel the ship and, while moving forward, a hydro-generator –water turbine– converts the vessel's kinetic energy into electricity which is converted to hydrogen and stored aboard [21]. They assumed the ship to be a catamaran. Two different cases were analysed: one with 1 Flettnor rotor and another with 4 Flettner rotors. First case could produce 100kW of net power while the second could produce 500kW.

One year later, Babarit *et al.* published a techno-economic feasibility study of ships producing hydrogen by means of wind energy in the far offshore claiming that they could produce hydrogen at a competitive price of 3.5 to 5.7 €/kg in the long term [5]. The study compares four options of producing, transporting and distributing hydrogen generated by fleets of far offshore wind energy converters. Two options consider hydrogen transported as liquid whereas the two other as gas. Also, two options consider the fleet moving to shore to offload the hydrogen and in the other two they only yield at the far wind and offload the hydrogen in an offshore terminal from which ship carriers transport it to shore. Finally, even though in [5] it is not clear how the ship would move nor how the energy would be obtained, there are clearly signs to think they propose water turbines to capture energy and Flettner rotors to propel the

[17] Found in DTU home page: `https://www.dtu.dk/english/news/2018/09/dtus-wind-powered-cars-perform-well-racing-against-the-wind?id=5eaf5266-bfe4-4e40-aefc-dc7660b690ef` for more information about the race, please visit: `https://www.racingaeolus.online/`

ship, as they did in previous and later works [21] and [22], respectively; however, their costs estimations are based in FOW and onshore wind costs evolutions. The main difference between [5] and ADO-WTs is the way of obtaining energy. Whereas [5] proposes a water turbine, this research proposes a wind turbine as the commercially available nowadays.

The team working in Central Nantes on this topic is continuously researching and presenting results in several conferences. To highlight one, Roshamida Abd Jamil presented her works on energy ships in the far-offshore, where she compared the capacity factor of BOFWTs and vessels with optimal routing system [23].

2.4 Challenges for Offshore Wind: potential of ADO-WTs

Despite the fact that offshore wind as known nowadays has still room for development and creating new business opportunities, it faces a few challenges which are niche for new solutions such as far fleets as described in [5] or the one proposed in this research, the so-called ADO-WTs.

Construction costs of offshore wind farms are 1.5–2 times greater than that of onshore wind farms because offshore wind farms require expensive foundations, installation, and grid connections (e.g., underwater cabling and offshore transformer stations) [24]. Moreover, LCOE values for offshore wind are strongly dependent on depth and distance from shore, due to mooring costs and export cable length, respectively [9]. Especially, the cost for a foundation of an offshore wind increases depending upon water depth: the cost for foundations at the water depth of 40–50 m is 1.9 times higher than the cost for the water depth of 10–20 m [24] and costs of grid-connection increase linearly with the distance to shore [5].

ADO-WTs dependency on water depths and distance to shore is almost non-existent as they would be built onshore and sail autonomously. Moreover, ADO-WTs would reduce the grid connection. For instance, if carrying hydrogen, transportation would be cheaper; transporting gas is 20 times cheaper than transporting electricity [10] and with much less losses [25]; also, independently from the type of energy carrier, the connection to the main grid, as well as the substation or the terminal could be lower than the total *capacity installed*, if ADO-WTs were scheduled to discharge/offload at different times.

Offshore wind operation and maintenance costs are a major part (20-30%) of the Levelised Cost of Energy (LCOE) [26]. A major contributor to high O&M costs is downtime caused by accessibility restrictions, as severe weather conditions offshore restrict times for technician transfer to the wind turbine platforms or completion of maintenance tasks [26].

Autonomously-Driven Offshore wind turbines would have no crew, they would be governed by an optimization software targeting best locations and workers would

check and fix them onshore, guaranteeing workers health and safety at work all the time without costs detrimental.

Moreover, a research from Bloomberg shows that ships are very expensive and scarce, there are approximately only 12 vessels around the glove able to carry new WTs, and as they get bigger in size the ship industry would need to re-design specific ships for installing wind turbines offshore. There is also a issue with logistics, which may lead to cost overruns due to the unavailability of such ships, which represents itself an uncertainty which may be disadvantageous to future projects [18]. Also, Transport and installation of wind turbines are two of the highest capital expenditures which may increase in the far shore [2]. The same report [2] proposes that research should focus on supporting the development of a supply chain with installation and hoisting systems suited to floating wind systems. Despite that fact that ADO-WTs would need tailored designs in a first stage of R&D, its construction would be more simple because their size would be smaller, they would relay on mature technologies used by shipping industry nowadays and, finally, they would transport themselves autonomously over the sea, which presents much less restrictions than land transportation, and with no operators, reducing enormously costs and simplifying logistics for the installation, decommission and the whole operation during the lifespan of the *wind farm*.

Moreover, wind turbines are nowadays sited in the location presenting the highest wind energy density over 20-30 years, extrapolating approximately 5 years-historical data acquired from an observation point (mast) and building an observed general climate atlas using models which include topography and roughness of the terrain. Nonetheless, this does not necessarily mean that such location is the best one at every moment within its lifespan. ADO-WTs would simply move to sites where wind blew if it was not blowing where they were.

In addition, [2] suggests that increased research on robotics, automation and the development of autonomous underwater vessels (AUVs) will facilitate the installation and monitoring of anchors and moorings. This could facilitate the berth of ADO-WTs as they arrived at the terminal to discharge the energy yielded. Finally, [2] states that direct power-to-x application combined with floating wind concepts should be assessed and, in fact, ADO-WTs are studied in this report to store energy as electricity and as hydrogen; showing that the latter presents greater advantages regarding both energy density, which relates with lower losses while travelling, and overall costs which leads to a competitive LCOE. Along the report more advantages as well as the drawbacks from ADO-WTs are explained.

[18] Found online at `https://www.bloomberg.com/news/features/2019-05-13/offshore-wind-will-need-bigger-boats-much-bigger-boats`.

CHAPTER 3

Wind Energy Yield Assessment model. Methodology & Results

Firstly, Autonomously-Driven Offshore Wind Turbines (ADO-WTs) were envisioned to move in order to harvest more wind power. Instead of staying at one site during the 20-30 years of their lifespan, they would be allowed to move whenever there is no wind towards better locations. Therefore, first thing to check is how much extra energy one can get by moving Wind Turbines (WTs). The approach followed consisted in building three different models with the aim to compare the extra energy that a moving WT –within the North Sea– could extract in comparison to a fixed WT. Thus, first model constitutes the reference model whereas the following two model the proposed technology. These three models are called:

- Conventional model
- Upper-Bound model
- Reachable Area model

And all of them constitute what is called Wind Energy Yield Assessment model (WEYA). Figure 3 places qualitatively each model in a realistic/unrealistic scale. The Conventional model is not perfectly realistic, since WTs are not sited as done in this model [1]. The Conventional model is the reference, the energy harvested according to the other two models will be compared with the conventional model output. Upper-Bound model does not account for either the time it takes to travel from one point to another or travelling losses to do so. It is an unrealistic upper bond, *the best one could do in an ideal world*, also called "teleportation model", since it takes no time to move to one spot to the other regardless of how far these were. Finally, Reachable

[1] Wind Farms are located according to a probabilistic function called Weibull distribution, based on data collected from masts and more sophisticated models accounting for wake effects between wind turbines, costs, etc. For example, the one developed by Researcher from DTU: WAsP

Area model, which does not account for the energy lost by travelling, it does account for the time it takes to travel and therefore, only moves to *reachable* spots. Moreover, inefficiencies of the generator, power train, etc. are not included *per se* in any of the models. In general, the focus was put on the particular differences between the current conventional offshore wind turbines (either BFOWT or FOWT) and ADO-WTs in order to quantify the improvement from the last (i.e., electrical losses within the WTG would affect equally both models unless a new generator was particularly designed for ADO-WTs which is out of the scope of this research at this stage).

This chapter describes the methodology used to build each model in 3.1, presents results from calibrating the WEYA model in 3.2 and, finally, presents final results from a simulation run for the Southern North Sea during the whole 2018 in 3.3. The code implemented can be found in the Appendices A.

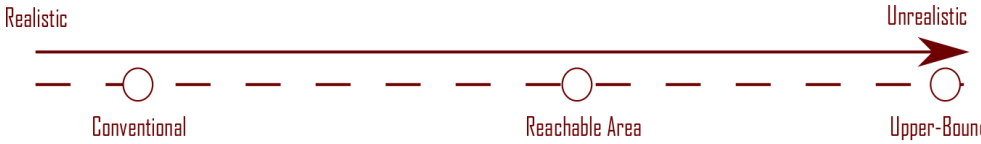

Figure 3.1: 3 Scheme Wind Energy Yiel Models.

3.1 Wind Energy Yield Assessment model. Method

This section explains the methodology used for implementing each model. Firstly, most relevant pre-treatment data used by all three models as well as the main indicator used to assess the wind energy yield is presented in 3.1.1. Last three sections explain each of the models: Conventional model 3.1.2, Upper-Bound model 3.1.3 and Reachable Area model 3.1.4).

3.1.1 Pre-treatment data functions for all three models

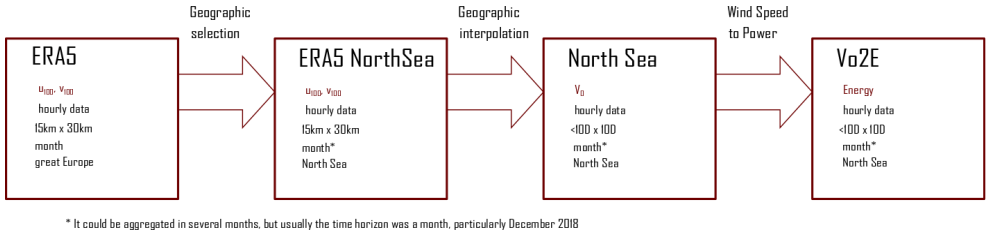

Figure 3.2: Data flow scheme.

This sections presents pre-treatment data functions used by all three models: data set 3.1.1.1, geographic and time frame 3.1.1.2, interpolation 3.1.1.3 and wind speed transformation into wind energy 3.1.1.4. Figure 3.1.1 shows the data flow used in Conventional and Upper-Bound models from the raw data until transforming it into Wind Energy. However, Reachable Area model has a previous step to *Vo2E* function.

Moreover, last section 3.1.1.5 defines how the extra energy was computed in order to assess how good the proposed technology is –compared with the reference model–.

3.1.1.1 Data Set: ERA5 Copernicus

Different Data Sets were considered to be used as input for the Energy Yield Assessment models. Roshamida Abd. Jamil PhD student from Central Nantes who is currently studying a similar concept –vertical-axis wind turbines harvesting far-offshore wind power and route calculation to maximize the capacity factor [23]– used ERA-Interim dataset by European Centre for Medium-Range Weather Forecasts (ECMWF) reanalysis for the results she presented in the EERA DeepWind 2019 conference celebrated from 15^th to 17^th January this year in Trondheim. The author discussed with researchers from the DTU Wind department which data set was the most appropriate. Particularly, through interviews with Bjarke Tobias Olsen [2] the information presented in this section was gathered. Mainly these were the two dataset considered:

- ERA5 data from Copernicus. This is a better version than ERA-Interim. Resolution is 15 km x 30 km approximately. Wind Speed can be interpolated between locations in order to have more points. Wind Speed can be obtained at 10m or 100m of height in two perpendicular direction –so that both module and angle could be computed–, data can be obtained hourly from 1979 to 2018. A month of data –which is given for the whole world– weights around 3GB.
- NEWA data set. This is the newest data set released. It is more precise –and heavy– than ERA5. It is specially interesting for studying convective weather phenomenon, whose duration is usually lower than 1h.

For the purpose of this research, ERA5 was chosen as the best option, accurate enough, specially having the possibility to linearly interpolate wind speed between points in order to have a finer mesh. ERA5 and NEWA would provide quite similar data at 100 m offshore and because ADO-WTs would not move fast enough to benefit from NEWA extra accuracy (such as high-resolution, short wave-length and fast-moving phenomena) it was decided to use ERA5 dataset.

Next topic discussed in Risøwas the wake effect. It was concluded that if WTs were not allowed to be closer than 10 times its rotor diameter (i.e., a distance of 1130m approximately) wake effect could be considered vanished; for lower distances, wind speed between points is not equal to the linear interpolation, because it is reduced by the WT sited upstream –towards the free wind coming flow–. This was

[2] Through interviews with Bjarke Tobias Olsen, Postdoc researcher at DTU Wind Energy.

confirmed through conversations with David Johnsen from COP, who stated that wind developers leave approximately a distance of 8 times the diameter between WTs.

Thus, data input is the Wind Speed from ERA-5 (Copernicus data base) –either for December 2018 or the whole year (for final results)–. Specifically, hourly u and v wind speed perpendiculars components at 100m height where used. Temporal resolution is an hour whereas geographical resolution is approximately 15km x 30km –it is given in 0.5x0.5º degrees which makes the distance vary slightly–. However, linear interpolation can be executed. The interpolation is required in order to let single WTs to freely choose the best spot. Figures 3.1.1.3 and 3.1.1.3 show the data before and after linearly interpolating for the North Sea pre-selected data. However, interpolation increases the size of variables and computational time.

Moreover, it was decided not to transfer from 100m height to hub's height in this study (which is 90m for NREL offshore 5-MW baseline wind turbine [4]). It is believed that in order to compare ADO-WTs with BFOWT this would not add big differences –specially in the sea where roughness of the terrain is very low– whereas it might be an extra source of error and unnecessary complexity.

3.1.1.2 North Sea and time horizon

The region studied is the Southern North Sea. Specifically a rectangle from 57ºN 0ºE to 54ºN 7ºE, which is approximately 423.7km wide (horizontal length) x 333.6km height (vertical length) and 552.4km of diagonal. To put in perspective the dimensions of the area considered, see Figure 3.3.2 from Section 3.3.2, showing the sites a single ADO-WT would move along the North Sea for the whole month of December 2018, according to the Upper-Bound model.

For saving time of computation, December 2018 was used to calibrate the model and find the best configuration, since it was the newest data available at that time. Final results were run for the whole 2018 to have an Annual Energy Production (AEP) for that year. A broader study should be carried out in order to see the results from simulating with greater time horizons (such as 5 years, 10 and 20); since there could be potential benefits if there is a particular season or year where the *best spot* –i.e., where a Bottom-Fixed wind farm would be located– presents worse results and therefore moving to other regions with ADO-WTs might present better results.

Note that it is very important to use time series data and not Weibull distribution –as used in industry to site wind farms–. This is due to the fact that ADO-WTs must be able to change the location from one point to another, and Weibull distributions are done for a geographical aggregated region generalized for whole lifespan of the wind farm. In fact, a pre-research carried out with ERA-Interim data –not presented in this report– shown that the Extra energy obtained from moving or not the WTs was decreasing if ADO-WTs were restricted to move every few days or hours, instead of hourly.

3.1.1.3 Interpolation

Data was geographically interpolated to allow more than 1 WT to be placed nearby the best wind spots[3]. That is, imagine a matrix of 29 x 13, this could represent the wind speed distributed over the North Sea before interpolating for a particular hour (more hours would add a third dimension to the matrix). A unique maximum value may be somewhere in the matrix, having the closest cells a lower value by definition. By interpolating the 29 x 13 into a more detailed matrix (e.g. 673 x 169), it could happen that interpolated points closer to the unique maximum point might still be greater than the following maximum point from the raw matrix. Also, in real life, wind turbines are approximately 10 times the diameter far one to another, willing to study WTs independently, it is needed to interpolate, otherwise the minimum distance between WTs would be approximately 15 km or 30 km –this is the distance between points from the raw wind speed data set–. Figure 3.1.1.3 shows wind speed module for the North Sea –selected area– for a particular area, before interpolating; Figure 3.1.1.3 shows wind speed for the same hour as 3.1.1.3 but after interpolating a 2.5D x 2.5D grid.

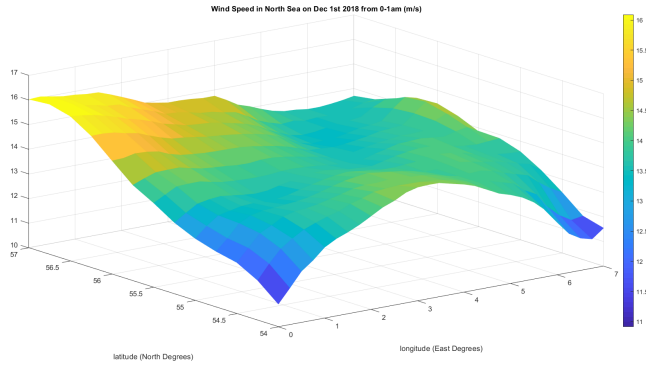

Figure 3.3: ERA-5 Wind Speed Raw Data at 1 particular hour.

[3]However, it was found that Reachable Area model results were also better if interpolated as explained in 3.2.3, 3.1.4 and 3.3.3

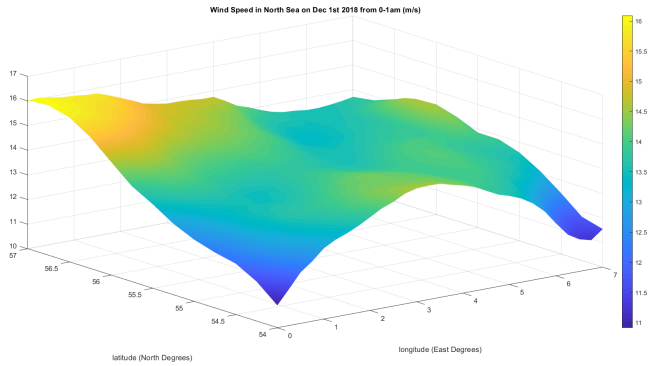

Figure 3.4: ERA-5 Wind Speed Interpolated Data at 1 particular hour.

The biggest disadvantage of interpolating is that it requires huge RAM resources, for that, a High Performance Computer was used, because interpolated variables had a weight greater that 10GB [4].

The interpolation diameter defines how close ADO-WTs –and conventional ones– can get. Since WTs will move discretely around the area "from one coordinate to another", ensuring a minimum distance between WTs is the same as defining a minimum distance between interpolated values. Raw data from ERA5 –within the selected North Sea region– is geographically interpolated . That is, initially data from ERA5 is constituted with a 15 x 30 km resolution grid and by –linearly– interpolating geographically it can be reduced to $yDxyD$ where D stands for the diameter of the wind turbine rotor and y is the diameter multiplication factor which can be 1, 2.5, 10 times the diameter.

The wake effect accounts for the decrease of wind power a WT yields due to the fact that a neighbour WT is slowing down the wind after it goes through the rotor. The effect is reduced with the distance which can be measured in relation to the diameter of the WT. According to interviews with WT wake effect researchers from Wind DTU Risø, for distances equal or greater than 10 times the diameter of a WT the wake effect can be neglected, since free wind speed goes back to initial values before entering the WT rotor. A diameter can be of 117m –for a 4.2MW Wind Turbine model V117.4.2 from Vestas, e.g.– and it gets bigger with the power. For the NREL offshore 5-MW baseline wind turbine used this is 128m [4]. Thus, the degree of interpolation could foster the need to account for wake effects or not.

In order to do that, two functions were implemented: getLonLan_interp and interpWS (see Appendices A.9 and A.10, respectively, to read the code). First function loads longitude and latitude raw vectors from ERA5 and calculates de interpolation required in order to ensure a distance equal or smaller than yD between each coordinate. Both parameters are specified in Appendix A.1, a generic function that was

[4] a whole year would have approximately 236GB for the whole North Sea if interpolating at 1D.

used by all the other functions –if required– to ensure coherence in the parameters defined only once in that file. Initially a diameter of 117m –from the Vestas model V117-4.2– was used. After getting access to NREL 5MW MW reference model, its diameter was used, being 128m [4]. After several tests –results of which are presented in 3.2.1– it was set a diameter factor of 10 which means that each turbine was at least 1280m far from each other, ensuring the absence of wake effect between WTs. The distance between coordinates was calculated with the function *haversine* created by Josiah Renfree in 2010.

Finally, depending on the parameters and the model, the interpolation may add extra computational time without providing better results. For 1 WT neither Upper-Bound nor Conventional models show any difference in their results, as explained in 3.2.1. For Reachable Area model, results will change also for a single wind turbine, since it may happen that a raw site falls out of the reachable area but not points interpolated in between (see 3.2.3, 3.1.4 and 3.3.3 for more information).

3.1.1.4 Vo2E function. Free Wind Speed to Power

This section explains how Free Wind Speed (V_0) was transformed into power and ultimately energy. Two main versions are presented. Because of a lack of data from industry, the author used theory from Wind Power Aerodynamics to translate wind speed into power and after finding NREL offshore 5-MW baseline wind turbine [4], the power curve provided in their report was integrated in the code.

From Wind Turbine Aerodynamics, one knows that the Aerodynamic Power can be expressed in terms of the relative wind the WT sees (V), the Area covered by the blades (A) also called rotor span area, the air density (ρ) and the C_P, whose limit was established by Betz in 1919 and set to 16/25 (59% approx). Notice that if the boat moves against the wind, the relative wind speed the rotor sees is the sum of the free wind speed and the speed of the boat and Bentz limit is no longer valid (see 2.3). Thus, wind power can be expressed as:

$$P = \frac{1}{2}\rho A V^3 C_P \tag{3.1}$$

Notice that the power is proportional to the wind speed to the power of three. In a first approach, and due to the lack of data, it was used this function to transform wind speed data (from ERA5) to wind energy used in the models.

Firstly, equation (3.1) was used by the three models (Conventional, Upper-Bound and Reachable Area models) and then upgraded with [4] power curve. Huge differences were found, being the upgrade the one presenting worst results in terms of extra energy (Upper-Bound dropped approximately by 1/3 with the new power curve, from approximately 90% extra energy to 30% in a month).

In real life application, each Power Curve changes for every location –even in the same wind farm WTs have differences in their Power Curves– after interviewing Bruno Kotovich [5]. Nevertheless, current wind turbines have a system to stall (actively or

[5]Project Manager and wind farm developer at Vestas

passively) and keep the power at rated values from a certain wind speed onwards (called rated wind speed). That means, the power output for a wind speed of 15m/s is the same as 20m/s in most of the cases. Figure 3.1.1.4 shows the function finally used to transform V_0 to Power, in $Vo2E$ function the energy output was obtained by multiplying the power by the time, which was 1h, 3600s to be consistent with the units.

Please, refer to [27] for more information. However, key words and concepts are briefly introduced. A common power curve has three known points; on the X-axis, i.e., V_0: V_{cut-in} (cut-in Wind Speed) is the V_0 from which the WT starts generating power (i.e., for lower V_0 the WTG is off); V_{rated}, until which the power increases from the initial value at V_{cut-in} until rated power (5MW in this case). From V_{rated} to $V_{cut-out}$ WT generates at rated power, this is mainly in order to avoid huge mechanical loses which increase the possibility to early fatigue symptoms. For wind speeds greater than $V_{cut-out}$ the wind turbine is shut down, producing no energy; for grid stability reasons mainly, some WTs shut-down gradually.

Very interesting conclusions are discussed in Chapter 5 from analysing results from the Power Losses model. Cut-out wind speed could be moved further or the pitch control could be coordinated to not limit the power output, by allowing the WT to move with the wind, seeing a relative wind speed lower than the actual one and using water turbines to slow down the whole ADO-WT by capturing energy. Refer to 5 for more information.

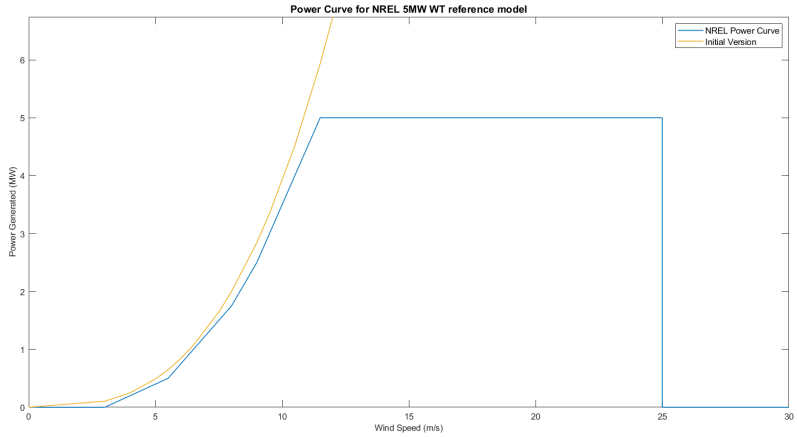

Figure 3.5: Power Curve (MW electric) of NREL 5MW Wind Turbine reference model.

3.1.1.5 Extra Energy: Main Indicator

The main indicator used to interpret the results from Upper-Bound and Reachable Area models is the relative Extra Energy. Even though the interesting value is the total extra energy which could be obtained for the whole horizon, for the sake of understanding its evolution, Extra Energy was calculated for every hour as the energy computed from hour 1 to each hour k_t, whose last value will be the time horizon. Extra Energy is thus defined as follow:

$$E_{extra\_model}(k_t) = \frac{E_{model}(k_t) - E_{conventional}(k_t)}{E_{conventional}(k_t)} * 100 \tag{3.2}$$

Where k_t refer to the hour up to which the outcome is being calculated (i.e., from hour 1 to the floating horizon k_t). $E_{model}(k_t)$ is the sum of energy yield for the models (either Upper-Bound or Reachable Area) from hour 1 to k_t (Eq. (3.6) for Upper-Bound model and for Reachable Area); $E_{conventional}$ is the energy obtained in the reference model using Eq. (3.5).

As mentioned, unlike Upper-Bound and Reachable Area, which do not modify previous hourly-values, $E_{conventional}$ is updated every hour. In other words, even though Upper-Bound and Reachable Area may change the site every hour, the energy yielded in the previous hours does not change. However, for the Conventional model, since bottom-fixed WTs are located only in one place, depending on where the best spot is, every hour the best spot is susceptible to being changed, meaning that all the previous hours must be updated.

Note that if there are several WTs, the summation of the whole *wind farm* for every hour is introduced in equation (3.2).

Finally, capacity factor was used also to compare results found in this research with current values for offshore wind turbines. It is defined as follows:

$$c = \frac{AEP(MWh)}{8670 P_n(MW)} * 100 \tag{3.3}$$

Where c is the capacity factor (in %), AEP is the annual energy production (in MWh) and P_n is the rated power in MW (5MW in this case). 8670 represents the total hours of a year.

3.1.2 Conventional model. Method

Industry sites Wind Farms using methods based on probabilistic distribution such as Weibull distributions accounting for probabilistic levels of wind speeds for a particular site, based on historic values. Combining the probability of having each level of wind speed – e.g., from 0m/s to 30 m/s– and the power curve –which changes from one WT to another–, an Annual Energy Production (AEP) is obtained for the whole lifespan, 20-30 years, for a particular site. This value (AEP), among others, are used to compare potential sites where installing a wind farm.

However, the two models describing the proposed technology –ADO-WTs– are designed to freely change the time horizon, that is, instead fo 20 years, it can be run for 1 month, 1 year, etc. As discussed in 3.3, for the implemented models, computational time rises with time horizon; it could take months to run 20 years of lifespan, depending on the parameters used in the models. Therefore, it was decided not to use the current methodology to site WTs as a reference to compare the other two models, since different input data would be used for the reference and the other two models. Therefore, a model was developed with the goal of comparing the Extra Energy obtained using the proposed technology –modelled through Reachable Area and Upper-Bound models– and the current Bottom-Fixed Offshore Wind Turbines (BFOWT).

The Conventional model comprises the ADO-WTs particularities of working –time series– with the mindset of how industry sites currently WTs. In a few words, if it was possible, WTs would be sited at the location offering more energy during the whole lifespan. And it is precisely this what is implemented in this model.

Wind Energy is obtained by transforming Free Wind Speed –got from ERA5 Data (read 3.1.1.1)– for each coordinate from the North Sea –selected area– and hour to Wind Power and multiplying this by the time –an hour– the energy is obtained, as explained in 3.1.1.4.

Therefore, values of potential wind energy for the North Sea –selected region–, at every location, for every hour comprising the time frame are obtained ($E(x, y, t)$ from now one). Summing all the potential Wind Energy at every spot (coordinate) for every hour gives a final *map* of wind energy resources ($E(x, y)$). Conventional WTs would be sited where the maximum values of Wind Energy were, and this is what the model does. Mathematically, for the whole time horizon the potential Wind Energy at every spot (coordinate) for every hour is summed:

$$E(x, y) = \sum_{t_0}^{t_{horizon}} E(x, y, t) \tag{3.4}$$

$E(x, y)$ is sorted from maximum to minimum values. The first $numWT$ values –of the sorted vector– correspond to the energy that would be obtained at spots where conventional WTs would be sited. Where $numWT$ is the number of WTs simulated. Both the energy and the location were saved to compare the outcomes from the other two models. Refer to 3.1.3 to read how the maximum was implemented and Appendix A.2 to read the code. In addition, it was studied how the Extra Energy was affected by the different number of WTs simulated (results are presented in 3.2.2) and, due to computational time, final results were computed for a single WT. To compute the total energy yield from this model, the whole energy for all WTs for the time frame was summed; mathematically, this is:

$$E_{conventional} = \sum_{1}^{t_f} \sum_{1}^{numWT} E_{conventional}(k_t, k_{WT}) \tag{3.5}$$

Where $E_{conventional}(k_t, k_{WT})$ is the energy production by k_{WT} BFOWT according to this model, at hour k_t. If the time horizon is the whole year, $E_{conventional}$ can be seen as the AEP for such year.

However, because it was found interesting to study the evolution of the extra with the time, Eq (3.4) had to be calculated every iteration of the loop. This can be seen as a summation with a floating limit. This was done because sites (where conventional WTs would be installed) were susceptible to change and so would the energy yielded. Thus, every loop, the wind energy potential geographic resources vector ($E(x, y)$) was computed and sorted and the maximum $numWT$ values –representing the energy yield from hour 1 to the current hour of the loop (k_t)– were used to compare the energy output by other models –up to that hour (k_t)– by calculating the Extra Energy obtained from Upper-Bound and Reachable Area models, compared with this model. See 3.1.1.5 for the definition of Extra Energy.

3.1.3 Upper-Bound model. Method

Upper-Bound model is less complex that the Conventional one in regards of the algorithm. If Conventional model was implemented to establish a reference, Upper-bound was developed in order to draw a limit, i.e., the maximum energy that one could get, given a region and a time frame, by moving ADO-WTs in a perfect world. It does not account for losses or time it would take to move such turbines. In a few words, it repeats the procedure implemented in the Conventional model, but removing the summation; i.e., every hour it gets the maximum value –or $numWT$ values if more than 1 WT– of the wind energy potential vector at every hour (i.e., $E(x, y, t)$).

Several approaches were studied to tackle this model, resulting the most convenient the one explained and implemented here: to sort a provisional vector with the values of Energy at every location –for that hour–, and get the first –best– numWT positions (i.e., first cells from 1 to the number of wind turbines studied, which can be 1, 10, 100, etc.). In the Upper-Bound model, the whole pretreatment of data is the same as in the Conventional one. From $Vo2E$ function, i.e., having already the energy distribution at every coordinate for every hour within the time horizon, the Upper-Bound model gets the maximum wind energy at every hour and stores both the energy obtained and the location where it is yield. Using the same notation than in 3.1.2, the following procedure is repeated for every hour –from $k_t = 1$ to the time horizon–:

1. A provisional array-variable gets all the potential wind energy in the North Sea, for every interpolated coordinate $X = E(:, :, k_t)$;, only at that hour k_t

2. The X variable is sorted from maximum to minimum values, $[X, I] = sort(X(:), 'descend')$; keeping the I index array to be able to trace the spots [6].

[6] I contains the pointer tracing the location of such maximum, by using $ind2sub$ of the first

3. First –best– numWT spots are selected $E_{upper}(k_t, 1 : numWT) = X(1 : numWT)$;.

Two main outputs are saved: the location where ADO-WTs would be placed according to the Upper-Bound model and the energy that would be yielded at every hour. After going through every hour from the time horizon, the hourly energy vector ($E_{upper}(k_t, :)$) was summed giving a unique value. This can be expressed as:

$$E_{upper_T} = \sum_{1}^{t_f} \sum_{1}^{numWT} E_{upper}(k_t, k_{WT}) \tag{3.6}$$

Please refer to the Appendix A.2 to read the whole code. Other methods were studied with the intention to reduce complexity and computational time. An alternative considered was to avoid the interpolation of the whole region only exploring nearby points, and checking for every WT the best location, making sure that such site was not taken previously. Nonetheless, since for the conventional model it was required to compute the Energy at every hour and coordinate, anyway, it was used this approach, simplifying enormously the task of checking whether the spot was taking by another WT before. Notice that because the whole wind farm is set at once getting the best $numWT$ spots from the sorted array, two WTs cannot be placed at the same spot.

3.1.4 Reachable Area model. Method

This model is the most complex of the three Wind Energy Yield Assessment models. In Upper-Bound, the whole North Sea –selected area– is available every hour to harvest wind energy. Since in Upper-Bound model travelling time was not taken into account, ADO-WTs could freely choose to move to the best spot every hour, even if it was ridiculously far. In Reachable Area model, ADO-WTs need to move only to spots they can reach, which means that a compromise must be taken. Therefore, this model includes the time it takes for ADO-WTs to move, even though power losses while travelling are not taken into account. To sum up, Reachable Area does not consider the following:

- Energy spent on travelling
- Energy Storage System
- Wind direction
- Any dynamics

The fact that the ESS is not modelled means that neither the energy lost due to charging, discharging or self-discharging, nor the travelling to discharge when fully

$numWT$ values they can be transformed back to a matrix index and therefore obtain the real longitude and latitude.

charge –or nearly– are implemented. As already mentioned, this would be features to include in future works. Nonetheless, and despite the fact that the algorithm implemented works pretty well in terms of results –computational time should be checked–, a real implementation would require forecasted data –and therefore uncertainties–, it is believed that other decision-making techniques such as machine learning or genetic algorithms could offer good results at that stage.

The algorithm developed is the result of a screening process to find the best of several approaches with different logic but the same goal of making sure ADO-WTs only move towards spots they can reach at a certain boat speed; set to 10 knots (5.2.3 presents how Extra Energy changes with the boat speed). The complexity is found in the fact that there is a maximization algorithm, where the overall energy is willing to be maximized, but the bigger the time horizon gets, the more combinations appear and therefore the computational time would skyrocket.

If formulated as an optimization problem, the objective function would be to maximize the energy yield –energy generated by the wind turbines– during the whole time horizon, taking into account that the distance from the current spot to the next should be smaller or equal than to 1 hour times the speed –assumed to be 10 knots–. Other constraints could be included and energy losses could be added to the objective function with a minus sign; the biggest disadvantage of this approach was the time horizon. Different approaches were thought through as well, such as interpolating only between nearby points, clustering several wind turbines, characterizing the wind energy map in zones, etc. The objective was not to develop the most advanced decision-making algorithm, but to implement one good enough to check whether moving ADO-WTs would foster greater yields. Future works could explore other approaches, like formulating the optimization problem and finding genetic algorithms, using machine learning techniques, etc.

After considering each approach, it was chosen the Reachable Area as the best and fastest method to move forwards. And therefore this section will focus on explaining this model.

Imagine a particular ADO-WT in a particular spot of the North Sea at a certain hour k_t, $lon(k_t), lat(k_t)$, –this will be called point A–. In order to decide to which spot the ADO-WT should move in the next hour –in case it is better to move–, a Utopian target –Z– is defined as the best spot to go in the following hours –Q parameter, in hours–. However, the Utopian target Z cannot be located anywhere in the North Sea, Z must be *reachable* in some hours or less from the current position of the ADO-WT –P parameter in hours–. In section 3.1.4.2 it is explained how to obtain the target Z. Once Z is known, one knows that after P hours the ADO-WT *might* be there. Nevertheless, a decision must be taken for the next hour, that is, a new location –or the same one– must be given to the ADO-WT as an input –*setpoint* or *reference*– to go in the next hour –this is called B point, in coordinates–. Notice that the B point is the target for the next hour, which means that it must be 1 hour far from the current point or less. Therefore, an area of radius $1hour \mathring{u} speed(km/hour)$ is defined centred in A –current point– and B must be within this area. Figure 3.1.4 shows the areas involved in the algorithm. This point B, must also ensure that after P-1 hours

the ADO-WT must be able to reach Z. Therefore, a second area centred in Z with radius $(P-1)$ůspeed$(km/hour)$ is defined. The intersection of both areas –which can be guaranteed– gives a few points which can be *reached* in 1 hours or less from the *current* location and which guarantee that ADO-WT could *reach* the target Z afterwards. The best spot of this intersected area is chosen as the B target and from that point, in the next hour, B would be the following current point, i.e., A, and a new Utopian target Z would be found –which could be the same as the previous Z, or not–. In order to make it more clear the following list summarizes each concept with its definition

- A it is the current point, where the ADO-WT is located in the Southern North Sea.
- B is the next-hour target, where the ADO-WT must move in 1 hour or less.
- Z Utopian Target, this is the best spot to which the ADO-WT could move within the next P hours. It is defined as the best spot for the next Q hours ´´after arrival", within an area *reachable* in P hours.
- P, it is the time in hours, defining the *reachable area*. It defines how far the ADO-WT can explore the North Sea –in this case– in order to track points. The biggest this parameter is, the further the ADO-WT is allowed to move.
- Q, it is a time parameter in hours, which helps to find Z. It is the forecast time used by the algorithm to check which spot from the *reachable area* is the best one to move, in the following Q hours [7].
- *P Area*, it is the *reachable area*. It is an area centred in A, with radius P times the speed at which the ADO-WTs can move. It represents all the sites the ADO-WT could *reach* in P hours or less.
- *P-1 Area*, it is an area centred in Z, with radius P-1 times the speed at which the ADO-WTs can move. It represents an area where the ADO-WT should be in the next hour in order to be able to reach Z in the left hours (P-1).
- *1h Area*, it is the area centred in A, with radius 1h times the speed at which the ADO-WTs can move.
- *Intersection area* between *1h Area* and *P-1 Area*. B point must be found within this intersected area.
- Speed, it is the speed at which the whole ADO-WT can move. Even though it could vary, in this study it is assumed to be constant. Initially it was assumed to be 10 knots (approximately 5m/s). It is also called boat speed (V_b).

[7] In new versions, forecast time could be defined as P+Q-travelling time; notice that the travelling time is different for every different potential site.

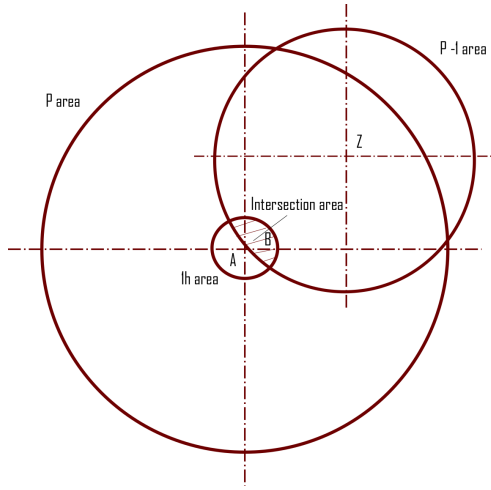

Figure 3.6: Schematic of Areas involved in *Reachable Area* model.

The algorithm goes through the following steps:

1. Get *P Area* (the so called *reachable area*)
2. Get Z Utopian Target
3. Get *P-1 Area*
4. Get *1h Area*
5. Get *Intersection Area*
6. Get B target

After finding the Point B, this is then the new A and the procedure is repeated to calculate the next hour's target. Note that the energy got every hour is entirely the transformation of the wind resources at that hour an location (with $Vo2E$ 3.1.1.4) and the next hour is assumed to be ´´already" in the next spot harvesting. This is assumed to be alright, since this spot is as much 18.5km far from the previous one, at 10 knots.

The following sections presents each of the functions implemented.

3.1.4.1 *getArea*

In this section, the main characteristics of the function implemented to calculate the Area is explained. The purpose of *getArea* is to explore around one point (also called coordinate, site or location) to check if the points next to it are nearby –certain

hours or less further from the central point–. Mathematically, in order to define a circumference, two variables must be known such as centre and radius, this function receives these two inputs plus three extra. Go to Appendix A.5 to read the code. In total, these are the input variables *getArea* –coded in Matlab– receives:

- Centre Point. This can either be the current point A or the Utopian Z point. The circumference will be centred at this point.
- Radius in hours. This will be P, P-1 or 1 depending on the step which is running.
- Longitude vector, containing the absolute coordinates of longitude interpolated in the North Sea [8].
- Latitude vector, containing the absolute coordinates of latitude interpolated in the North Sea [8].
- Spots taken, containing the sites already taken by previous wind turbines for that hour (important if the number of wind turbines is more than 1)

Note that other parameters such as the boat speed are defined in another file which each of the functions explore in case they need it (see A.1 from the Appendix).

It is important to bear in mind that the domain in computational applied mathematics is discrete, which in this case means that the circumference will not be as drawn in paper. In fact, the Area will be defined with a matrix of 0 and 1. If a cell –representing a coordinate– is P hours or less far from the centre A this cell will contain a 1, otherwise there will be a 0. Two vectors containing both longitude and latitude coordinates are required to link each matrix position (also called indices or pointers) with an actual coordinate (defined by a longitude and a latitude). Outputs of *getArea* are both shown in Figure 3.7 and listed below. Note that *getArea* gives only a single output, which is a variable type structure –cluster of variables– called Area. This variable includes:

- Area.State, it is a matrix of 0 and 1 collecting the information of whether a coordinate is within the reachable area.
- Area.Taken, similar to State, it is a matrix stating if a spot is already taken by another wind turbine for that hour (only in case of studying more than 1 WT).
- *Area Pointers*: these specify the four edges defining the Area, these are:
  - Area.North is a value (in latitude) stating how far from A the ADO-WT can go North in a straight line.
  - Area.South is a value (in latitude) stating how far from A the ADO-WT can go South in a straight line.

[8] If interpolating, otherwise absolute coordinates from ERA5 North Sea –selected region–

  - Area.East is a value (in longitude) stating how far from A the ADO-WT can go East in a straight line.
  - Area.West is a value (in longitude) stating how far from A the ADO-WT can go West in a straight line.

- Area.lat is a vector, containing the coordinates from South to North defining the Reachable Area.

- Area.lon is a vector, containing the coordinates from West to East defining the Reachable Area.

Since it is both important to calculate real distances and work with matrices (summing, looping over, updating wind speed resources, etc.), it is crucial to both keep track of real coordinates magnitudes (within Area.lon and Area.lat vectors) and matrix and vector pointers –or indices– (rest of variables stored in Area).

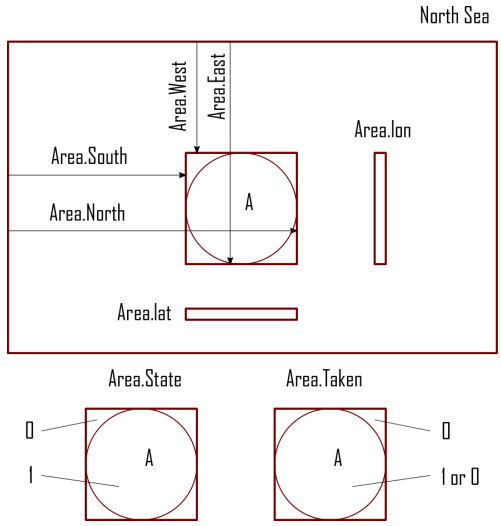

Figure 3.7: Schematic of some outputs of *getArea* function.

getArea goes through different stages to calculate the discrete circumference Area around the Centre Point, these can be clustered in three steps. The following explanation uses the case of calculating *P Area* as an example to illustrate the function. These are the three main blocks of *getArea*:

1. Determine the *Area Pointers* (north, south, east, west) defining the rectangle centred in A which constitutes the exploring matrix. In this step, Area.North, Area.South, Area.Est, Area.West are found.

2. Determine the relative coordinates vectors. In this step, Area.lat and Area.lon are found.

3. Go through the exploring matrix to check whether a site is within the reachable area (i.e., P hours or less far from A). In this step, Area.State is defined.

4. Check that the spot was not taken before. In this step, Area.Taken is found.

It is very interesting to comment that in order to guarantee intersection of areas P-1 and 1h, the radius P (in hours) sent to *getArea* to calculate the first area (namely *P Area*), is reduced by 5%. That is, instead of allowing the ADO-WT to explore an area P hours far from it, ADO-WTs can only go to 95% of P far in every direction, as maximum. The next radius sent to *getArea* (i.e., P-1 hours and 1 hour) are not reduced and empirically it is been proved that it guarantees intersection.

After finding *P Area*, the Utopian target Z can be computed.

3.1.4.2 *getZ*

As mentioned, *getZ* has the goal of finding the Utopian target Z which is the best spot the ADO-WT can reach within the following P hours. For that, *P Area* is being computed before and sent to *getZ*. All the inputs sent to *getZ* are:

- AreaP, this is the outcome from *getArea* when centred in A with radius P. Basically it is the area which *getZ* will go through to find the best wind spot.

- Wind Speed interpolated-and-updated resources for *P Area* (i.e., not the whole North Sea) from the current time plus P until the current time plus P and Q.

Wind Speed interpolated-and-updated resources refers to the wind speed matrix, which is a selection of the North Sea V_0 (third box from Figure 3.1.1) for the selected time $[k_t + P, K_t + P + Q]$ and area from *getArea*; updated with the Area.State and Area.Taken from *getArea*. That is, in order to avoid the WTs to move to one spot already taken or out of the reachable area (e.g. the corners of the WS matrix), wind speed values are set to zero and therefore the maximization function will not choose them. This has been proven successfully.

Therefore, what *getZ* does is, given the updated wind speed resources for the selected region and time frame, uses $Vo2E$ to transform wind speed into energy per site and hour. Summing all the hours for the considered time gives a 2D matrix of *forecasted* energy[9] for the available spots and, by finding the maximum value, the location where this maximum lies represents Z. Formulating this mathematically:

$$E^{max}(x_z, y_z) = max\{ \sum_{t_0+P}^{t_0+P+Q} E(x, y, t); \forall\{x, y\} \in AreaP\} \tag{3.7}$$

[9]It is not forecasted, since historic data is being use in the algorithm, even though in a real life application it would be forecast data. Reason why P and Q values were restricted not be very high.

The value of maximum energy itself is not important. What is important is the location of such maximum, that is (x_z, y_z), which defines the coordinates of Z.

Notice that what this function does, mainly is to find the maximum spot given an area and wind speed resources. In fact, after getting the intersection between P-1 and 1h Areas, B point (next-hour-site) is obtained calling this function sending the new WS resources and the *Intersection Area*.

3.1.4.3 *getIntersection*

Given the Utopian target Z, two new areas are needed to be computed: *P-1 Area* –centred in Z– and *1h Area* –centred in A– (see Figure 3.1.4.3), for which *getArea* is used, introducing the right arguments.

This section explains how the intersection of both *P-1 Area* and *1h Area* is computed. In order to do that, getIntersection has those two input arguments:

- *P-1 Area*
- *1h Area*

There is only one output variable clustering "sub-variables" used to define an area as done in *getArea* 3.1.4.1 and represented in Figure 3.7.

Figure 3.1.4.3 shows two schemes, both of which show several areas. Note that these are represented by rectangles, since it is how they are interpreted by the code in Matlab.

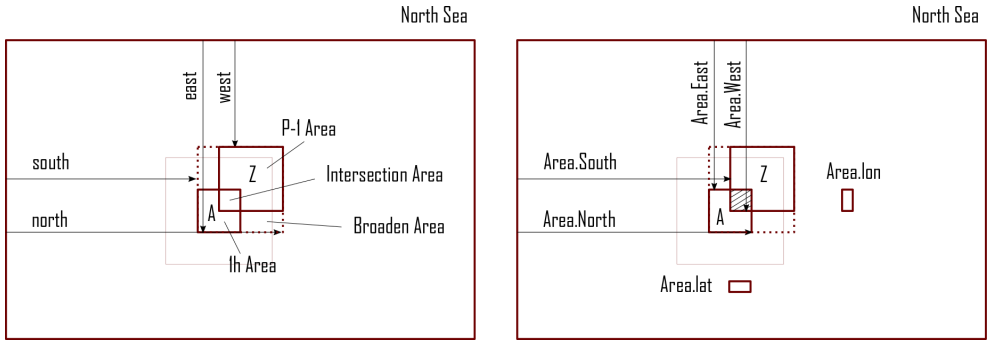

Figure 3.8: Schematic of getIntersection function methodology.

In order to obtain the intersected area, the following procedure is carried out:

1. Determine Broaden *Area Pointers* (north, south, west and east values shown at the scheme on the left).

2. Determine the intersection *Area Pointers* (north, south, west and east values shown on the right scheme).

3. Determine the relative coordinates vectors lon lat for *Intersection Area*.

4. Determine State and Taken matrices for the *intersection Area*.

Appendix A.8 shows the whole code. Briefly, all the *Area Pointers* are defined using *min* and *max* functions from Matlab and given the North Sea absolute coordinates vectors, Area.lon and Area.lat vectors are defined using its respective pointers.

A loop goes through the whole Broaden Area in order to check whether there is intersection. Calling i the index going through longitudes (from east to west or up to down) and j the index going through latitudes (from south to north or left to right), as in Appendix A.8. First, it is checked if the index combination (i, j) lies within the respective limits for each area (otherwise an error would appear), if this happens for both Areas, it means that (i, j) is within the *Intersection Area* rectangle. Notice that this does not necessarily mean that there is an intersection, since –and specially in the corners– the State matrices are usually rounds of 1 with 0 on the corners (see Figure 3.7). Thus, checking that (i, j) lies within the intersection rectangle is not sufficient, also checking if the respective Area_A.State and Area_Z.State (for 1h and P-1 Areas, respectively), in that position (i, j) is 1. Similarly, it is done for determining Area.Taken, but, instead of requiring an *AND* condition, it is done with an *OR*.

3.1.4.4 *getB*

Having the intersection, *getZ* is called to find the B point for the next hour, giving the *Intersection Area* and the updated wind resources for the next hour. Energy values from the B point are stored for that wind turbine and that hour.

Then B is the new A and the procedure is repeated to calculate the next hour. Note that the energy got every hour is entirely the transformation of the wind resources at that hour an location (with $Vo2E$ 3.1.1.4) and the next hour is assumed to be "already" in the next spot harvesting; which is acceptable since this spot is as much 18.5km far from the previous one, sailing at 10 knots. After the time horizon is gone through the total energy production is summed:

$$E_{reachable_T} = \sum_{1}^{t_f} \sum_{1}^{numWT} E_{reachable}(k_t, k_{WT}) \tag{3.8}$$

3.2 Wind Energy Yield Assessment model. Results

This section shows the most interesting results found after running simulations with the models. Since the three models were new created by the author, first, it was studied how models reacted to each parameter with the goal of finding the best

configuration to run a final test. Thus, results from the model outcomes –namely Extra Energy but also computational time– are presented. A final test was run, with the whole WEYA calibrated, for Southern North Sea during the whole 2018. Note that some of the characterization studies can be seen as sensitivity analysis.

WEYA has two interpretations, on the one hand, it assesses how much energy can be extracted, compared with the conventional model (as explained in 3.1.1.5), this is useful in this stage of R&D as an indicator of whether it is worth it to keep researching on this field. On the other hand, it shows an example of what could be the control algorithm calculating the reference or *setpoint* of each of the ADO-WTs in a coordinated manner with the objective of maximizing the energy yield during the whole time horizon. Following the mindset defined, both the methodology and the results perspective will aim at the first stage: assess how much extra energy one could get by moving WTs, the so-called ADO-WTs. Since the objective is, on this stage, to establish how much extra energy one could get, rather than having a set point value –coordinates– for each ADO-WT. A few studies were carried out to understand which parameters the model was more sensitive to with the purpose of simplifying the model, reduce computational time and be able to carry out more studies.

In this regard, several studies were carried out in order to see how the main outcome –extra energy– was affected by:

- Interpolation of Wind Resources
- Number of wind turbines
- Avoiding Interpolation module for 1WT analysis. Results
- P & Q parameters
- Vo2E: old version vs new version of Power Curve
- Boat Speed

However, a special attention was also paid to computational time.

3.2.1 Interpolation of Wind Resources. Sensitivity Analysis

With the Upper-Bound model, which is faster than Reachable Area, it was studied both for 10 and 100 WTs if the extra energy was changed by interpolating with different grid. Grids 2.5D x 2.5D resolution, 5D x 5D and 10D x 10D were studied for 10 WTs (Table 3.1) and 2.5D x 2.5D and 10D x 10D were studied for 100 WTs (Table 3.2).

Upper-Bound model was launch for December 2018 ERA5 (see 3.1.1.1) changing the y diameter multiplication parameter (for both $numWT = 10$ and $numWT = 100$). As explained, the wake effect is not modelled. This section justifies why.

For the finest grid, 2.5D x 2.5D –i.e., WTs could get up to 2.5D close one to each other both vertically and horizontally–, 89.79% of extra energy was obtained

for 100WTs –slightly more for 10WT: 90.16%– comparing the Upper-Bound model with the conventional one. Note that for distances of 2.5D between WTs there would be wake effect –having both bottom-fixed as ADO-WTs a lower output indeed–. For a 10D x 10D grid, the extra energy obtained was 88.29% for 100WTs –89.88% for 10WT–, which is mostly the same. Tables 3.1 and 3.2 also show the computational time in minutes. For 10WT simulations, there is a quite inversely linear relation between the grid resolution and the time it takes to run the code, reducing by 4 the diameter factor (i.e., from 10 to 2.5), computation rises by 4.3. Whereas for 100WTs this difference is higher, reducing by 4 the diameter multiplication factor, from 10D to 2.5D, computation time rises almost 7 times more. This is because a 10D x 10D grid has much less points than a 2.5D x 2.5D.

Therefore, a 10D x 10D grid avoids the need to implement a wake model and it saves computational time.

Simulation for 10 WT			
Diameter multiplication factor	2.5	5	10
Extra Energy	90.16	90.07	89.88
Computational time (min)	10.0	3.4	1,4

Table 3.1: Sensitivity analysis of geographic interpolation distance $numWT = 10WTs$.

Simulation for 100 WT		
Diameter multiplication factor	2.5	10
Extra Energy	89.79	88.29
Computational time (min)	9.7	2.3

Table 3.2: Sensitivity analysis of geographic interpolation distance $numWT = 100WTs$.

3.2.2 Number of Wind Turbines Sensitivity Analysis

The computational time is very sensitive to changes in the number of wind turbines simulated, the more wind turbines simulated, the more time it takes to run the code. Therefore, if results for 1WT were similar to 100WTs, only 1 WT would be simulated and then, one could extrapolate results for the 100.

Test were run with the following configuration:

- Models: Conventional and Reachable Area
- Vo2E: Old version: Eq. 3.1
- P=Q=24 hours

- Dec 2018 ERA5 North Sea (see 3.1.1.2)

- Boat speed: 10 knots

Figure 3.2.2 shows a time series of the extra energy that can be extracted from the wind according to Reachable Area model, for different numbers of WTs. Table 3.3 shows the main results from the tests. Extra Energy shown is at the end of the month[10]. In terms of Extra Energy, there is no much difference between 1 and 100

numWT	1	2	10	100
ExtraEnergy	47.50%	48.37%	49.02%	49.50%
Computational time	3.0 hours	5.2 hours	22.2 hours	15 days

Table 3.3: Sensitivity Analysis: Extra Energy vs number of wind turbines. ERA5 Dec18.

wind turbines. 1 ADO-WT presents 47.5% more energy than 1 conventional one –with the old version of the power curve–. The best trend line found fitting the Extra Energy as a function of numWT is $f(x) = 0.004ln(x) + 0.4784$, for Reachable Area results with the old version of *Vo2E*.

In regard to the computational time, it follows quite a linear function. It was obtained with *tic* and *toc* functions from Matlab. For just computing 1 WT during the whole month of December 2018, for both Conventional and Reachable Area models, it takes 3 hours (approx 10% of the month), whereas for 100 WTs it takes 15 days approximately. The trend line showing computational time as a function of the number of WTs is $f(x) = 3.6428x - 5.3958$.

Interesting interpretation of results are that the outcome for 1WT is a lower bound in terms of extra energy for Reachable Area. The more number of WTs, the more Extra Energy yield, even though the difference is not as high (2% extra energy comparing 1 and 100 WTs. Results are very positive in this regard, since it takes way less time to run 1 WT than 100 and it can be easily extrapolated.

[10]Note that time horizon is reduced by P and Q parameters

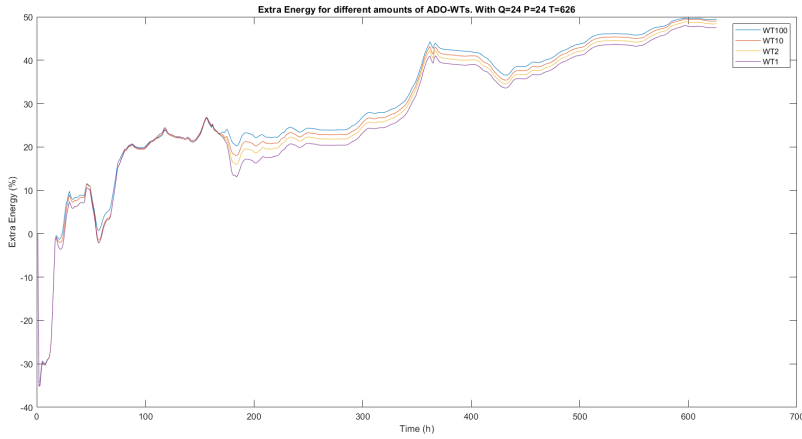

Figure 3.9: Extra Wind Energy for different number of ADO-WTs and time horizon.

Therefore, from that point onwards, studies were carried out for only 1WT. Moreover notice that negative values happen when Conventional model Energy Yield is greater than Reachable Area model, which happens within the first hours under this configuration. However, since the old version was used, final results cannot be inferred to 100WT using the trend lines found.

3.2.3 Avoiding Interpolation module for 1WT analysis. Results

With the intention to reduce even more the computational time, it was tried to eliminate the geographical interpolation function (see 3.1.1.3), which increases size of variables (more than 10GB for a single month), computational time, etc. Since every point in between would be smaller or equal than the input values for the interpolation, and for 1WT the highest value would be chosen –and since there is no second wind turbine, there is no need to get closer to such point–. Nevertheless, despite the fact that this is true for the *Upper Bound* model, it is not for the *Reachable Area*, since at every point, an area is *drawn* to find potential best spots for the next P hours –and then for the next hour–, these points may fall between two input coordinates for the interpolation function and therefore, it may happen that, if at the following raw coordinate wind speed is higher than in the current one, but such point is out of the *P area*, it will not be considered and a points in between –considered if interpolating– would present higher wind speed values the closer they get to the outer location. If no interpolation is done, WT may potentially loose these better spots, in fact, results confirmed this.

Test were run with the following configuration:

- Models: Conventional and Reachable Area
- Vo2E: Old version: Eq. 3.1
- Number of WTs: 1 WT
- Interpolating and no interpolation
- P=Q=24 hours
- Dec 2018 ERA5 North Sea (see 3.1.1.2)
- Boat speed: 10 knots

Figure 3.2.3 shows the divergence commented. As commented, it takes 3 hours to compute 1WT with Reachable Area and Conventional models if interpolation is done; if the interpolation is removed from the code it takes 65 seconds to run the code, but results are difficult to correlate and thus, it was decided to keep interpolating for 1 WT. Figure B.1 in Appendix B.1 shows the relation between both curves shown in Figure 3.2.3, it can be seen that for positive values, (i.e., after the first few hours of the month), there is no clear relation.

3.2.4 P & Q parameters. Results

The most characteristic parameters for Reachable Area model are P and Q. P defines how far an ADO-WT "can explore" its surrounding area in order to find the best spot.

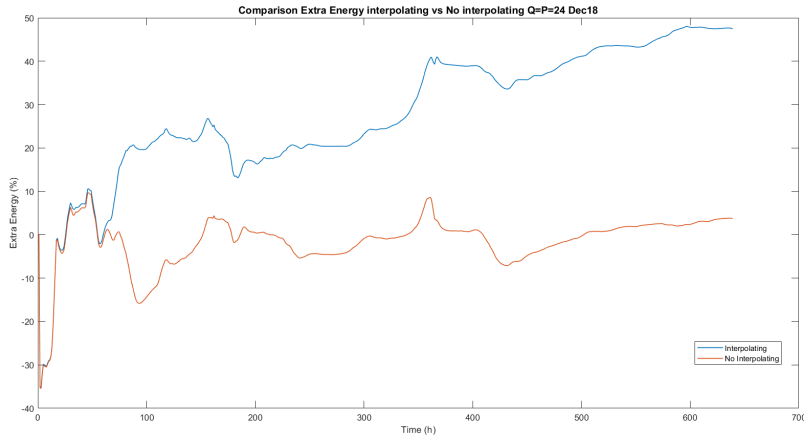

Figure 3.10: Extra Wind Energy interpolating or not interpolating for 1 WT Dec18.

Whereas Q defines the forecast time. P would be for the forecast sort of an offset lead time, in other words, ADO-WTs would analyse the wind speed forecast for Q hours after P hours from the current one. Forecasts are more accurate for shorter lead times, that is, the further one goes with the forecast, the more deviation the real wind speed will have compared with the current one.

However, two reasons force $P\&Q$ to be greater. On the one hand, ADO-WTs would base their decision in the forecast, therefore a representative sample is required to make a good choice and this means a Q great enough. On the other hand, ADO-WTs would move as far as P allows them, that is, they cannot see further than the Reachable Area, which means that if P is small ADO-WTs would be limited to explore closer to their current position, avoiding them to harvest in a location which may have very good wind resources, but could be far from their current location and thus out of their scope.

It is believed, though, that there is no such a best configuration of $P\&Q$ for all the years and sites. However, for this study, it was tested different configurations of $P\&Q$ for data from December 2018 and assumed it would work for the whole year. More research should be placed in these parameters to find a more optimal solution and understand better how it affects. Several combinations of $P\&Q$ were run in Reachable Area model with the following configurations:

- Model: Reachable Area (and Conventional)
- New Vo2E version (i.e., NREL power curve [4])
- Number of WTs: 1 WT
- No interpolation
- Boat speed: 10 knots
- ERA5 Data December 2018
- P configurations: 12, 14, 20, 24 (in hours)
- Q configurations: 12, 14, 16, 20, 24 (in hours)

Results are clustered for every P value to make the graphs more understandable. Figure 3.2.4 show the best configurations found (see Appendix B.3 to check the other results). Time is represented in the x-axis (representing hours of the whole month of December 2018). Note that the total number of hours changes slightly with $P\&Q$. This is in order to avoid errors while running the code. Extra Energy is shown in y-axis in percentage –comparing the energy obtained from Reachable Area model and the Conventional one–.

Results shown that, despite what initially was though: that the greater $P\&Q$ were, the most extra energy would be obtained (since ADO-WTs would be able to move further because Reachable Area model does not account for losses while travelling); lower values of $P\&Q$ bring better results. It is believed that fluctuation of Wind

Speed along the day would be the cause of this results. Which is sure is that lower values of $P\&Q$ would offer better results when implemented in real life, since forecast values –instead of historical– would be used, and the forecast error increases with the lead time. In fact, the best configuration for 10 knots is $P = 14$ and $Q = 16$ which means a reasonable lead time of 30 hours to find the Utopian target.

It is seen that values for $P = 14$ (always in hours) are the best ones, being $Q = 16$ followed by $Q = 14$ the best configurations for such P. Therefore the best configuration is $P = 14$, $Q = 16$ (yellow line). It is interesting to see that this configuration is the best one during the whole time, even though the second best configuration (red line), has a region where it is not the second best option. Further investigation would be required to explain this changes. Therefore, final results were run for this configuration: $P = 14$, $Q = 16$.

3.2.5 Vo2E: old version vs new version of Power Curve. Results

The whole purpose of WEYA is to quantify the extra energy obtained from moving ADO-WTs compared with conventional WTs (either bottom fixed or floating). To do that, wind speed resources need to be transformed into power and ultimately energy. This is done through the function *Vo2E*, the code of which can be read in A.4. As explained, initially data of a real power curve was not available and therefore an aerodynamic approximation was used at a first instance.

After integrating the Power Curve –from the NREL 5MW WT reference model– and therefore avoiding the Aerodynamic approximation, a huge drop of Extra Energy

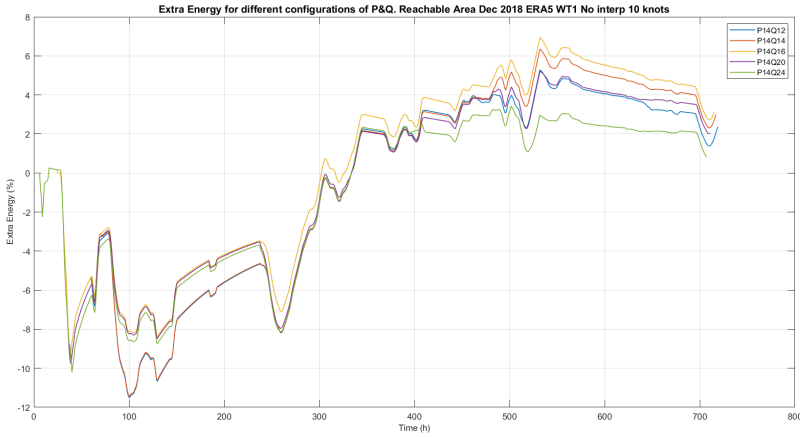

Figure 3.11: Extra Wind Energy for different configurations of Q with $P = 14$. ERA5 Dec18.

is observed for both Upper-Bound and Reachable Area. Notice that, even though the new version show worse results, these are more realistic. This section is written to shown and explain this drop. Moreover, notice that $Vo2E$ is not a parameter, is a whole function/module transforming wind speed into energy; however, since some results presented were initially obtained with the old power curve version (such as in 3.2.2 and 3.2.3) this section is included to explain how it affects the outcome (refer to 3.1.1.4 to read the method).

Figure 3.2.5 shows the Extra Energy for both Upper-Bound and Reachable Area models. Two tests were carried out: one with the old Power Curve and the other with the new power curve, for ERA5 data for December 2018, the rest of characteristics for this study are listed below:

- Models: Conventional, Upper Bound and Reachable Area
- P=Q=24 hours
- time horizon: December 2018
- ERA5 North Sea (see 3.1.1.2)
- Boat speed: 10 knots
- Number of WTs= 1 WT
- grid 10D x 10D

Regarding the Upper-Bound model outcomes –lines purple and yellow–, a huge drop is observed. At the end of the month, with the old Vo2E version, Upper-Bound outcome shows an accumulated extra energy of 93.07% whereas with the new Power Curve it drops down to 30.89%. Even though lines are slightly similar, it was not observed much correlation, Appendix B.2 show –for both Upper-Bound and Reachable Area–, correlations between both lines (with the new and the old version of Vo2E). In terms of time of computation, there is a huge difference as well. It takes 31.4 hours to run the three models (Conventional, Upper-Bound and Reachable Area) for the whole December 2018 with the real Power Curve (new version) whereas 7.2 hours if the old approximation is used.

In regards to Reachable Area model results, worse results are found. If for Upper-Bound the Extra Energy drops by 3 approximately, for Reachable-Area, the Extra Energy is 42.97% at the end of the month for Vo2E old version, whereas only 2.46% if the new version is used with those configurations.

The reason for this drop is the saturation of power from the rated wind speed to cut-out wind speed. Both the conventional model and reachable are show the same energy output if, for instance, ADO-WTs are in a location with 24m/s and conventional WTs are fixed in a location with 12m/s, because the power curve is saturated. This is a problem which lies in the way WTs are manufactured, which of course, is because of a reason. For higher wind speeds, it is required to spill some energy in order to avoid bigger loads that would generate pre-mature fatigue and even

over currents and electrical instabilities. Nevertheless, this brings a new idea, which is to avoid the spill of the extra kinetic energy from the wind by allowing ADO-WTs to move with the wind.

3.2.6 Boat Speed. Sensitivity Analysis

Boat Speed is another important parameter to take into account. The greater the boat speed, the further ADO-WTs can move. However, realistic speeds are required to be used. Discussing with Maritime Engineers from DTU and FNB (Facultat de Nàutica de Barcelona) it was found that 10 knots was a realistic assumption to start with. [5] claims that other researches used 20 knots on their studies and they use 14 knots for their research.

Therefore, several boat speed configurations were studied to see how Extra Energy would decrease if the platform could not go as fast as initially assumed.

It was tested how much extra energy could be extracted from the wind under these conditions:

- Models: Conventional, Upper Bound and Reachable Area
- Number of WTs: 1 WT
- $P = 24Q = 24$ and $P = 14Q = 16$ configurations
- Dec 2018 ERA5 North Sea (see 3.1.1.2)

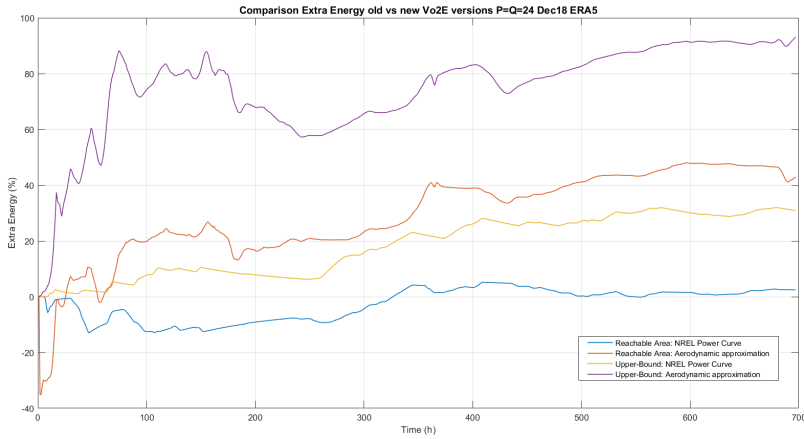

Figure 3.12: Extra Wind Energy old vs new Vo2E versions.

- Boat speed: 5 and 10 knots
- No interpolation
- New version of Vo2E (NREL 5MW WT reference model [4])

On the one hand, results of Extra Energy at the end of the month December 2018, were proven to be better for the $P = 24Q = 24$ configuration at 5 knots than with $P = 14Q = 16$, against what was expected. At 10 knots, during the whole month of December 2018, ADO-WTs would harvest 3.24% more energy; particularly, ADO-WTs would harvest 2,671.8MWh, against 2,587.9 MWh produced from the conventional model (an extra of 83.85MWh during the whole month). If ADO-WTs moved at half the speed (i.e., 5 knots), ADO-WTs would produce 0.42% less energy than Conventional wind turbines corresponding to 10.91MWh less energy by moving them, which means that, if they would move at 5 knots they would not be able to take advantage by moving during December with such configuration.

On the other hand, results for $P = 14Q = 16$ configurations shown more extreme results. Whereas at 10 knots, ADO-WTs shown 4.2% extra energy (2,696.9 MWh, 108.92 MWh more than conventional WTs); while moving at 5 knots, ADO-WTs would produce 27.17% less energy than conventional WTs, which means that it would not be worth it to move them, this is, 1,884.8 MWh for the same day.

To conclude, the model output is very sensitive to $P\&Q$ parameters, specially when combined with the boat speed. Lower values of P and V_b imply less possibility to harvest energy, because *Reachable Area* is a circumference of radius PxV_b, as explained in 3.1.4.

For the following studies, a speed of 10 knots is used, since it was seen as a realistic speed after consulting similar studies and maritime engineers from DTU and FNB. Future works could go in two directions. First –and more straightforward– , find the best configuration of $P\&Q$ parameters for every boat speed. To verify, by increasing the boat speed, results from Reachable Area model should approach the outcome from the Upper-Bound model –being this model's results the maximum limit–. Second, integrate the Power Losses model 5 in a new version of Reachable Area model. To do this, besides its module, the direction of the wind speed should be calculated for every hour and spot; for every wind speed there would be an optimal boat speed at which moving –with or against the wind–, different losses would be assessed to each trajectory and the best Energy Net would set the next hour spot.

3.3 Final Results

Previous results shown how the model output changed depending on the parameter configuration. After finding the best configuration with the aim of being as rigorous and as fast as possible, a final study was carried out. Results and discussions are presented in this section.

As said, WEYA does not account for neither energy losses for moving ADO-WTs nor losses regarding the storage system (neither charging nor discharging or storing).

First, separate results are presented for each model of the integrated Wind Energy Yield Assessment model. A final section discusses all results put together. WEYA was run with the following configuration:

- Models: Conventional, Upper-Bound and Reachable Area
- ERA5 data (read 3.1.1.1)
- No interpolation for Conventional and Upper-Bound models. Interpolating for Reachable Area model.
- Time horizon: the whole 2018
- Number of WTs: 1 WT
- New Version Vo2E with 5MW NREL Power Curve [4]
- Boat speed: 10 knots
- $P = 14$ & $Q = 16$

The reason for not interpolating in Conventional and Upper-Bound models is to avoid high computational time as explained in 3.2.3, since they offer same results for 1 WT as with interpolation. Moreover, notice than the boat speed as well as $P\&Q$ parameters only affect Reachable Area model.

In addition, time horizon is a very important parameter to take into account. Firstly, ADO-WTs were envisioned with the purpose of extracting more power from the wind by moving to better spots when wind did not blow at the site where a conventional wind farm would be placed, within the 20-30 years of lifespan. However, due to time constraints, results for 2018 are presented. Future work should explore longer time horizons.

3.3.1 Conventional model. Results

Conventional model is used as a reference. Figure 3.13 shows the geographic distribution of potential Wind Energy over the whole 2018 for the selected area of the North Sea. Energy was obtained using the last version of Vo2E (i.e., NREL offshore 5-MW baseline wind turbine [4]) for every hour at every location and then summed up together as explained in 3.1.2 and 3.1.1.5. It can be appreciated from the graph that data is not interpolated. This is done in purpose in order to speed up the computational time. However, because there is only one WT, results are exactly the same as if interpolating was done. This is only true for Conventional and Upper-Bound models simulating 1 WT (as explained in 3.1.1.3).

Last step of the Conventional model algorithm consists of choosing the best spot – or spots if more than one WT were simulated–, that is, the coordinate providing more

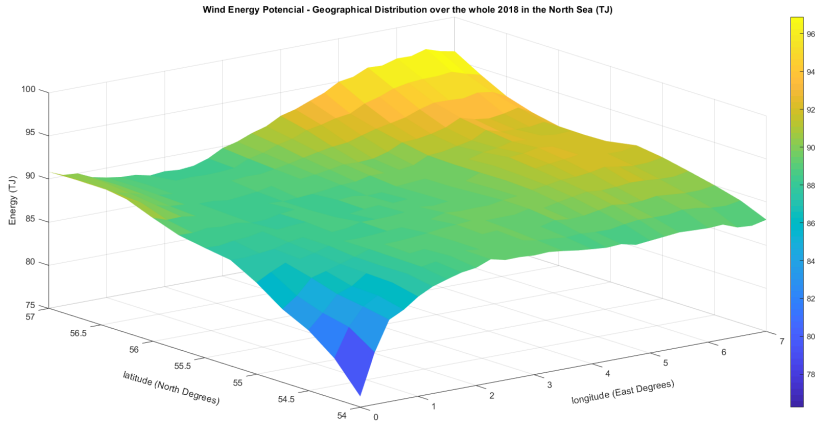

Figure 3.13: Wind Energy Potential - Geographical Distribution over selected North Sea region and the whole year 2018 for NREL offshore 5-MW baseline wind turbine [4].

energy output, after summing all the hourly production for the whole time horizon. Therefore, Figure 3.13, from the decision making algorithm point of view can be seen as the matrix to go through in order to find the maximum value, which is close to the top right corner. Thus, the single bottom-fixed WT would be located specifically at coordinates 6.5ºE and 57ºN., close to the west coast of Denmark, since there is the maximum Energy output for the whole time horizon. Keep in mind, though, that this is not the methodology used to site wind farms in real life, as explained in 3.1.2.

Results are been proven valid, which suggest a new process to site bottom-fixed wind turbines –even though this was not within the scope of this master thesis–. The total energy that the conventional WT would produce is 96.89 TJ (2.6914×10^{10} Wh), which is the same order of magnitude as results from [28] which also use NREL 5MW WT reference model [4] located in the North Sea. [28] uses the Weibull distribution –as industry does– to generalize the AEP (Annual Energy Production) from wind resources got from the NASA. Particularly, their research foresee an AEP of 2.5309 $\times$ ^{10} Wh after their proposed improvement and 2.4371 $\times$ 10^{10} Wh without it. In fact, they chose to site their WT at Hywind wind farm, the first world's commercial floating wind farm built at the moment and the biggest nowadays. Hywind is located approximately at 57.2ºN 1.20ºW [29], slightly further north and west from the top left corner from Figure 3.13. The Wind Energy potential for the closest coordinate available in the selected North Sea region from this research –i.e., the top left corner– is

90.83 TJ (2.5231×10^{10} Wh) at this location. Results from this model differ 3.53%[11] from the ones found in literature and therefore the reference model is validated .

3.3.2 Upper-Bound model. Results

As explained, Upper-Bound modes does not account for losses travelling nor time it takes to move from one site to another. In other words, if an ADO-WT was in location A at hour 1, because this is the one presenting the best wind resources at that hour and at hour 2 there was a location B presenting the best wind resources, even if B was 400km far from A, the ADO-WT –from Upper-Bound model– would be at location A during the whole hour 1 and in location B during the next hour (and no losses are accounted for such displacement). This is why it is called Upper-Bound, one cannot get more extra energy by moving WTs in the selected area of the North Sea for the chosen time frame, with 5MW ADO-WTs with [4] power curve. Future studies could explore how the Upper-Bound model would vary by increasing the wind turbine generator size; however, it has to be kept in mind that the more power harvested, the more energy required to store and this requires a compromise with the storage system, which represents a huge part of the whole system weight.

Interesting results were found while analysing the total distance travelled by ADO-WTs over the year for this model. The total distance travelled would be 339,080.07km– during 8731 hours– See 3.2.4 for an explanation of why this number is not 8760.. Even though in average the speed is 20.6 knots, which is similar as the one proposed by some studies referred in [5], if one checks the speed per hour, it can clearly be seen that speeds reach unfeasible values. Figure 3.14 is presented to illustrate this –it is not the purpose to dig into small details–. It shows the speed ADO-WTs would need to have, every hour, for every month in 2018 in order to reach the best spots. The maximum speed is 298 knots, which is the speed required to cross the diagonal of the North Sea –selected area– in 1 hour. Notice, in addition, that at this speed the whole hour would be spend on travelling, which means that unless the following hour at that spot was the best –or good enough– as well, the whole travel would have no sense –or it would need to sail at an even higher speed–. Obviously these sailing speeds are ridiculously high and this is why Reachable Area was developed, to let ADO-WTs move only to spots that are reachable. Another conclusion that was extracted is that ADO-WTs need to be able to produce power while travelling. Other studies such as the ones currently carried out in Central Nantes consider this as well. Roshamida Abdel Jamil [12] developed an algorithm to optimize sailing routes in order to maximize the capacity factor of what they call FARWIND energy ships [23].

[11] Calculated referred to the AEP without the improvement. To be consistent with calculations for Reachable Area model, which only reach the 8731 hour, both Conventional and Upper-Bound models are computed until that hour, which means that 29hours of 2018 are missing. If accounting for the energy that would be generated at that location –57ºN 0ºE– for the last 29h of the year 2018, the deviation is 4.14%, which is still accepted.

[12] PhD student from Central Nantes.

Moreover, some months –such as September and October, e.g.– present a few zero speed values, which means that the best spots did not change (see Figure 3.14). In some cases, this location differs from the location where the conventional wind farm would be sited. To illustrate this, for example from September $8^t h$ to September $11^t h$ the best location is at 57ºN 0ºE, which is very close to the world's first commercial floating offshore wind farm's location, called Hywind wind farm [29]–, but not where the BFOW farm would be sited according to the conventional model.

Figure 3.3.2 shows the sites an ADO-WT would move according to the Upper-Bound model within the whole December 2018, for the selected area of the North Sea. Notice that the location of the single BFOWT is also shown. ADO-WTs would move all over the North Sea –selected area– if there were no time constrains (i.e., if it could teleport). Figure B.5 from Appendix B.5 shows the sites a single ADO-WT would move each month according to the Upper Bound model.

Regarding the main indicator, results from the Upper-Bound model shown that ADO-WTs would have 45.24% more energy for 2018. As said, this represents the upper bound to the other models. However, it may be increased if the new Power curve proposed in 5 would be implemented, which would not be straight forward as already mentioned in the chapter. An interesting point of view is to convert the Extra Energy into the number of ADO-WTs that would produce the same power as conventional WTs. Under these conditions, if the Annual Energy Production (AEP) of 2018 was representative for the following 20-30 years, 10 ADO-WTs would generate as much power as 15 of the conventional WTs. However, as it is explained this is only an ideal case.

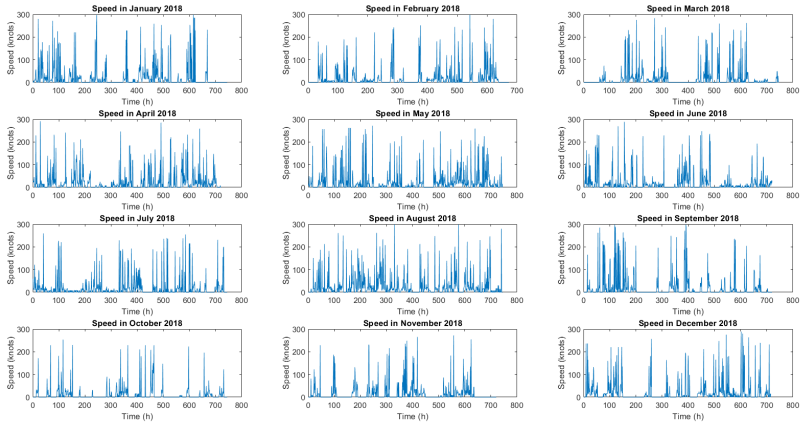

Figure 3.14: Speed the ADO-WTs should move in order to reach spots from Upper Bound model per month of 2018.

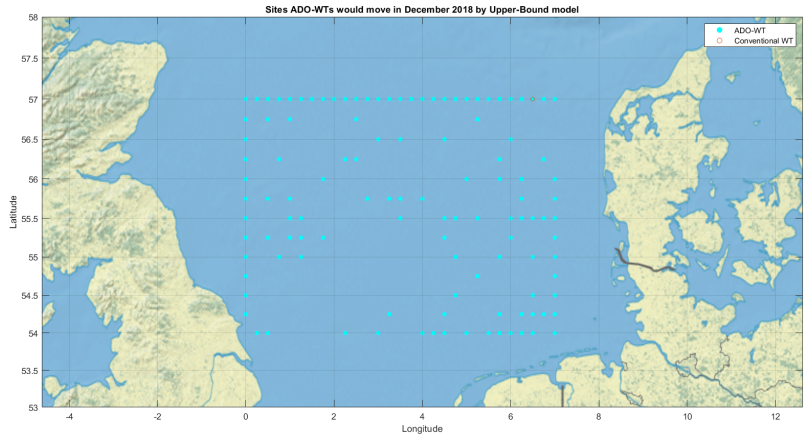

Figure 3.15: Sites a Single ADO-WT would move during Dec2018 along the North Sea delimited area according to the Upper-Bound model.

Another interesting study which could be carried out in future works would be to define a strategy to divide ADO-WTs to minimize the distance travelled, based on pre-found spots where wind is found to be good. For that, it should be found areas –close to each other– which complemented each other in terms of wind energy; that is, whenever wind does not blow in one of these areas, it does in the other. This would make these areas unattractive to BFOWT but it could be utilized with this technology. Moreover, harvesting the far wind, where BFOWT could not reach due to high O&M expenditures, installation and equipment –think of the export cable, e.g.–, would be another interesting to study to carry out in future works.

3.3.3 Reachable Area model. Results

Reachable Area model brings the Upper-Bound to a more realis tic scenario. In this model, ADO-WTs only travel to spots accessible, i.e., every hour ADO-WTs only move to a maximum distance they can reach in this hour, given the speed as a parameter. As already stated, it was modelled a boat speed of 10 knots (approximately 5 m/s), after discussing with several sources; as an example [5] proposes even higher speeds, which might however incur in high frictional losses. Despite the upgrade it represents to the Upper Bound model, as any model, it has some limitations (see 3.1.4).

Figure 3.3.3 illustrates the sites where the simulated ADO-WT would move according to results from Reachable Area model during the month of December 2018. The north region concentrates many locations where ADO-WTs would go. This sug-

gest to broaden the selected region towards the north, in future works. For December 2018, a vertical region close to the west coast of Denmark (longitudes from 5ºE to 7ºE) and another from longitudes 2ºE to 4ºE present good wind spots. It was observed that for some months (such as October 2018) ADO-WTs would not harvest wind power at the location where BFOWTs would be sited. Figure B.5 in Appendix B.5 presents results per month. Moreover, notice that some spots would represent huge costs for BFOWT or FOWT due to the export cable. Future research should also focus on water depths and draft ADO-WTs would have –ensuring stability– to check which regions would be available, besides other restrictions such as permits, sailing routes, etc. Perhaps the far offshore could offer less issues on those regards, as claimed by [5].

ADO-WTs would have 20.98% more energy annual energy production during 2018 under the stated conditions. If 2018 could be inferred to the whole lifespan, this means that 5 ADO-WTs would produce more than 6 BFOWT, omitting the simplifications. Moreover, it is seen that results from Reachable Area improve with the number of wind turbines (see 3.2.2), therefore 80 ADO-WTs would yield approximately the same energy than a wind farm made of 100 BFOWTs during the whole 2018.

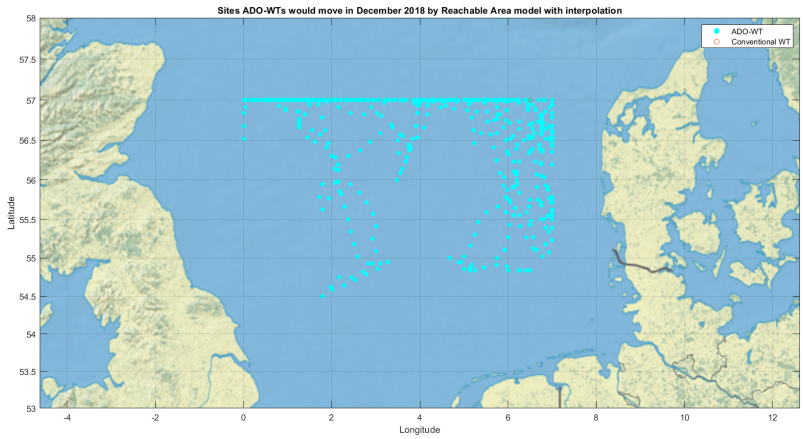

Figure 3.16: Sites a Single ADO-WT would move during December 2018 along the Southern North Sea according to the Reachable Area model.

3.3.4 Comparing three models and discussing results (WEYA model)

Regarding sites where ADO-WTs would move according to each model outcome, results from Reachable Area model show that ADO-WTs would not go as far as in Upper-Bound. For example, in December 2018 (see Figures 3.3.3 and 3.3.2, respectively), it is believed that the south west areas present temporary high wind speeds, whereas the north and east present constantly better good wind resources; reason why Reachable Area, where ADO-WTs are restricted to travel to nearby sites move primarily around those areas. Another interesting conclusion is that the best overall fixed-location is not the best site for every hour. In fact, in September 2018, according to Reachable Area results, ADO-WTs would not to the top right corner, where BFOWTs could be located– within the whole month, in October 2018 they would not even get close and in November only temporary they would pass by that location, although they would rather stay at the north west. Figure B.5 in Appendix B.5 presents sites per month from the Reachable Area model whereas Figure B.5 shows sites from the Upper-Bound. Future works should explore areas where BFOWT would not be sites due to high costs, variability of wind, etc. and calculate if ADO-WTs could yield enough wind power to make the project feasible.

Figure 3.3.4 shows the accumulated energy the three models present during the whole 2018. Reachable Area energy yielded lays in between the reference model and the Upper-Bound. It is very positive to prove that by just moving WTs one could get 5.6467 GWh more in a year, per wind turbine, these would generate huge more revenues that worth it further research. The extra energy is 12.1759 GWh per wind turbine and year compared with the Upper-Bound model. It is believed that for WT with greater power this difference could even be higher.

Expressing the annual energy output as a capacity factor (i.e., $\frac{AEP(MWh)}{8760x5}$), results are very promising as well: Conventional model presents a capacity factor of 61.45%, Reachable Area model 74.34% and Upper-Bound 89.24%. Notice that the capacity factor of the conventional model is more common for floating offshore wind turbines than to BFOWT; this model represents turbines which cannot move, without specifying the type of foundation, a deeper study would need to dig into the terrain conditions at that location as well as broaden the time horizon to find definitive results. Another interesting conclusion is that the evolution seen, in terms of capacity factor, from onshore wind (22% in 2018 [6]) to bottom-fixed offshore (37% in 2018 [6]) and floating [13]. ADO-WTs may bring the capacity factor to values higher than 70%.

Finally, future works should also deal with integrating in the decision making algorithm from a new version of *Reachable Area*, the Energy Losses for every new location target. To do so, first the direction of the wind should be taken into account,

[13] 65% is the capacity factor Statoil states Hywind had within the first months of operation; found online in `https://www.4coffshore.com/windfarms/project-dates-for-hywind-scotland-pilot-park-uk76.html`.

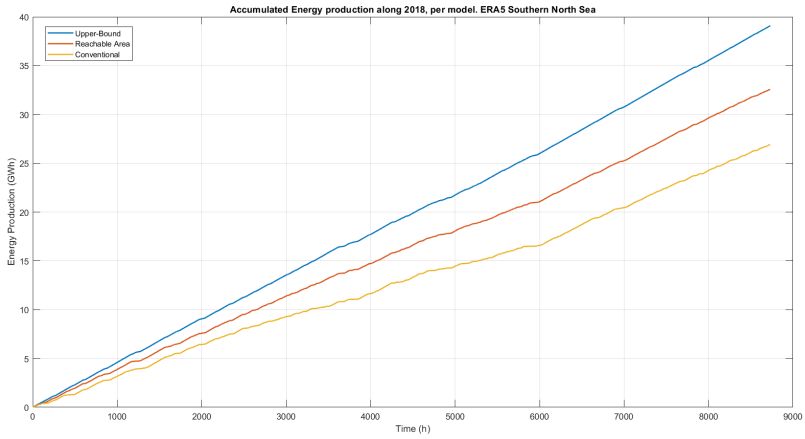

Figure 3.17: Energy Accumulated for 1 WT during the whole 2018. Comparing the three models.

a control loop would set the boat speed reference value at which it should go with or against the wind (other cases would be incorporated in upgraded versions), this would mean different time arriving at the location and therefore, more or less time to harvest energy on that spot. At the same time, losses accounted for the travel would be taken into account, as well as extra power reached for free wind speeds greater than the cut out wind speed, since the boat would go with the wind, making the rotor see a lower relative wind speed.

CHAPTER 4

Energy Storage System

The storage system will affect the buoyancy and stability of the system, since it will be the major part of the overall weight. Since ADO-WTs are envisioned as an autonomous entity, able to freely move with no limits due to connections, ADO-WTs will have no cables, which leads to the conclusion that all the energy yield must be stored on board, this will represent a mass that cannot be neglected and therefore a key parameter to study in this report. Different technologies can be used for this purpose, this section identifies the potential best fit Energy Storage System (ESS) for the ADO-WTs. There are several energy storage technologies the author went through in order to identify the most appropriate.

4.1 Energy Storage System – Methodology

This section presents the methodology used to analyse the Energy Storage System. The main goal of this analysis is to include suitable ESS to the analysis by accounting for the energy losses while travelling due to the extra weight the ESS represents as well as to include associated costs in the cost analysis. The method used was:

1. A list of specifications for ADO-WTs ESS was detailed and used to discard technologies not suitable for ADO-WTs.

2. Electric ESS State of Art was reviewed to make sure that every possible technology was considered.

3. Three electric ESS technologies were selected and introduced in the Hydrodynamic model (find results in 5)

4. Two electric ESS outputs from this research were used in the costs analysis (find results in 6)

This chapter presents results from the literature review and the preselection of technologies. Moreover, characteristics of the three preselected technologies are presented as well as a discussion of which parameters are used for the Hydrodynamic model. Results from the Hydrodynamic model and Costs analysis can be read in 5 and 6, respectively.

An ADO-WT is envisioned as a buoyant mobile system whose main purpose is to harvest energy –in a more cost and environmental efficient manner-. Therefore, its storage system must have the following characteristics:

- On board: The Energy Storage (ES) must be able to be carried by the ADO-WTs system on board.
- High energy capacity: since Wind Turbines rated power is getting bigger and bigger [15], the storage system must have a high capacity in order to allow ADO-WTs to stay harvesting energy for enough time before going to the discharging substations.
- Low weight: The system is floating and moving on the sea, the energy lost by moving increases with the mass of the boat since the total mass makes both the displacement greater –and this fosters greater water resistance–. In addition, the force required to move the system is proportional to the product of its mass and acceleration.
- Long storage duration: ADO-WTs must be able to harvest energy for a few days before coming back to discharge the energy, therefore the ES must be able to keep the energy with the less losses as possible during as much time as possible.
- High Power (fast charging discharging): Wind Turbines
- Low volume: the lower the volume is, the less draft for the hull and therefore ADO-WTs would be able to move around shallow waters, dock closer to shore, etc. lowering overall costs.
- Mild operation temperature: the storage system may be compatible to work at water temperatures, which can be from 4ºC to 8ºC in winter and from 16ºC to 19ºC in summer in the Southern North Sea [30].

In this stage of R&D, costs constitute the final factor to consider, first technical specifications for this applications were identified in order to discard technology technically unfeasible. In addition, as already mentioned, the maturity of the technology was not a requirement –even though it was checked–, since the proposed technology is not mature either. Thus, it is believed that by the time ADO-WTs might develop, storage system state of art might have evolved as well. It is true though, that lack of data due to low maturity or the fact that a certain technology was used in different industrial applications, forced the rejection of such technology, even though they might be suitable or transferred –after a few adaptations– to ADO-WTs. This is the case, for instance, of CRYObattery or CAES.

4.2 Energy Storage System – State of Art

A first classification of energy storage identifies two big groups which are electrical and thermal energy storage. Electrical storage class includes every type of energy

which will be transformed into electricity while it is discharged –even though it might be stored as thermal energy, for instance–, whereas thermal energy storage includes only thermal energy stored to release heat [31].

Because of ADO-WTs technical needs, heat storage system is discarded before even going through the State of Art, because the energy produced by the wind rotor is mechanical firstly and then converted to electricity –unless it is seen that it is more efficient to use this mechanical power to store energy in another way–. In either case, the energy produced would not be heat and by the definition in [31] the remaining storage technology available is the electrical one.

Since electricity is not storable as such, it needs to be transformed into a more stable energy form which it will be transformed back into electricity –or to power a vehicle, e.g..-. Thus, in this classification, by electrical storage one understands all type of storage containing an energy carrier in an energy form transformed from electricity and used either to produce electricity afterwards or not. For example, hydrogen could be stored and used later as a vehicle fuel and contribute to align the transport sector towards a sustainable transformation. According to literature, electrical storage state of art can be sub-classified as following.

4.2.1 Mechanical Energy Storage

These are electromechanical systems such as flywheels, pumped hydro energy storage, gravity power module, compressed air energy storage and liquid-piston energy storage.

4.2.1.1 Flywheel

A flywheel ES is mainly a rotational mass with shape of a wheel, providing more inertia to the system and therefore storing the energy. Nevertheless, due to friction losses, they are not good for long term energy storage. After charging, a flywheel can have an efficiency of 85%, which drops to 78% after 5h and to 45% after one day [32]. Thus, an even before considering energy density or other characteristics, flywheel is discarded as a plausible ES.

4.2.1.2 Pumped Hydroelectric Energy Storage (PHES)

Pumped Hydro consist on using electricity to pump water to a higher altitudes. Energy is stored as water with potential energy which can be realised afterwards to move a turbine and produce electricity. Because the ES must be carried on board, this technology is discarded, since it would either need to be incorporated to a natural reservoir (river or lake) at another location or have a water deposit as high as possible and as heavy as possible to carry as much energy as possible, making the whole ADO-WTS system very unstable. Just for the sake of illustrating this, a storage able to carry 1 week of electricity production at 5MW rated power would need 3.024 PJ, which has to be stored as potential energy (i.e., $E_p = m\mathring{u}g\mathring{u}h$, that is the product of mass, gravity and height). This fosters that the product of mass and height must be

30.8257E10 kg · m, meaning that if the centre of mass of the deposit is at 100m of height, e.g., the storage would weight 3,082,569 tonnes which is completely ridiculous.

4.2.1.3 Gravity Power Module (GPM)

Due to some limitations of Pumped Hydroelectric Energy Storage (PHES), namely need of water and topographical requirements, other technologies are studied, even though they are in phase of development [31], there are the so called Gravity Power Module (GPM). However, the concept is the same as in PHES: use electricity to lift a mass at a certain height which will be released whenever the energy is required later. The same reasoning explained in PHES can be applied, regardless of the energy carrier, the product of total mass times height would be too much to carry. Thus, for such amount of energy to be stored in a buoyant platform, these technologies cannot be used.

4.2.1.4 Compressed Air Energy Storage (CAES)

Compressed Air Energy Storage (CAES) uses electricity to compress air and store it in a highly pressurised reservoir which can either be underground (i.e., a cavern) or above the ground in a pipe or vessel. CAES efficiency is about 70% and a lifespan around 40 years [33],[34] its energy density is between 30 and 60 Wh/kg. Moreover, according to [5] they meet long storage duration requirements, even though it is not specified how much time in their paper. Also in [34] it is stated that their self-discharge is very low, nevertheless, the technology is mainly developed to be used onshore in huge areas where a lot of energy can be stored in order to compensate the infrastructural costs. It requires an air purifier section, a motor –that would be the wind turbine in case of choosing this ES technology– powering the compressor that pumps the air into a high pressure tank. No evidences in literature have been found of portable systems or a market around compressed air that could lead to consider this technology. It is the belief of the author that it could technically be implemented, the air would be stored and pumped into a bigger storage in the discharging substation (either offshore or onshore) which would have the gas to power convert to generate electricity and supply the power system; nevertheless, the lack of literature in this regard made the author discard this option for the moment.

4.2.1.5 Liquid-Air Energy Storage (LAES)

Highview Power developed a technology called LAES in some papers and Cryogenic Energy Storage in other. Read 4.2.5 to find this information.

4.2.1.6 Liquid-Piston Energy Storage (LPES)

Liquid-Piston Energy Storage (LPES) consists of a liquid and gas vessel, which stores energy; the liquid is pumped into the vessel containing the gas (usually nitrogen)

compressing it from 100 bar up to 250 bar. The energy density is about 3.2 to 5.55 Wh/kg [31] which would mean 151,351 tonnes for 1 week of production at rated power. Even though compared with PHES or GPM, LPES would be better regarding total weight, it is still too heavy to carry on board with acceptable water frictional resistance.

4.2.2 Chemical Energy Storage

In Chemical Energy Storage, the stored chemical compounds are created using electricity, their energy density is greater than Hydro Pumped or Compressed Air which makes them very attractive to constitute the ADO-WTs ESS [31].

4.2.2.1 Hydrogen Energy Storage (HES)

Hydrogen is a gas that, unlike electricity, can be stored. In fact, one of the ways of producing hydrogen is by water electrolysis, breaking-down every molecule of water H_2O into H_2 and $\frac{1}{2}O_2$, achieving pure hydrogen (>99.99%) [35]. Hydrogen is stored and when mixed with the air –which contains Oxygen– it gives water, power and heat. Its huge advantage is its high energy density of 800-10,000 Wh/kg [31], however, it also presents high costs ($6–$20/kWh) [33] and a very low overall efficiency, since by breaking down water molecules only around 60% is converted into H_2 and once this hydrogen is mixed with oxygen, around 50% of it is transformed directly into electricity [31] and the leftover is heat at low temperature so it is difficult to re-use to generate electricity; giving a final round trip efficiency of 20–50% [33]. Regarding the energy density reported in [31], the HES able to store 1 week of production at rated power (5MW) would weight between 84 and 1050 tonnes. If the performance of producing Hydrogen stated in the same paper is considered (i.e., 60%) in order to store 840MWh of Hydrogen (which would equal to 1.67 weeks producing at 5MW) the storage would weight from 140 tonnes up to 1,750 tonnes.

Even though following the classification proposed in [31] Hydrogen ESS is seen as a carrier to be transformed in electricity, it can also be directly used as a fuel for transportation or as an energy carrier. In principle, Hydrogen can be produced from water and then further converted to synthetic methane by reacting with CO_2 [25]. The author believes, Hydrogen would be a good solution if used directly as a product. It could contribute to the decarbonization of the transport sector which represents a huge share of CO_2 emissions (25% of EU-28 in 2017 according to Eurostat, including aviation [36]), by powering cars, ships and even planes [5].

Moreover, this technology has been proposed by similar studies such as the one being carried now in Central Nantes in France [5].

4.2.3 Electro-chemical Energy Storage

This category of ES can be subdivided in Supercapacitor energy storage, which will be discarded and Battery Energy storage, exposed in detail. Supercapacitors have very low energy density (about 10 Wh/kg [31]), which means 84,000 tonnes of storage considering 1 week of production at 5MW. Moreover, even though their efficiency is about 95%, they possess a daily self-discharge of 5%, which means that almost half of the energy harvested would be lost in a week.

Therefore, this section will focus on the state of art of battery energy storage. A battery energy storage is an electro-chemical device with the ability to deliver electricity. [37] authors claim that Battery system is the most widespread energy storage device for power system applications.

4.2.3.1 Sodium Sulphur (NaS) battery

NaS battery is used for commercial energy storage in distribution grid support and wind power interaction [38]. It has high energy density of 151-170 kWh/m^3, 2500 cycles of lifespan up to 90% depth of discharge, an efficiency of about 85% but short discharge period for ADO-WTs application (6 hours). In addition, it operates at 300-350^{o}C and it is combustible if exposed to water [31] and therefore it is not considered as an appropriate technology for ADO-WTs application.

4.2.3.2 Sodium Nickel Chloride ($NaNiCl_2$) battery

Even though environmental concerns associated to the toxicity of cadmium, lead or mercury are avoided in Sodium Nickel Chloride batteries; like NaS Batteries, NaNiCl batteries operate at high temperatures of about 270-350^{o}C [38], reason why it is not considered further. A NaCl solution –also know as *common salt*– is mixed with Ni forming $NiCl_2$ and 2Na. A ceramic wall constitutes the electrolyte allowing Na^+ to go through leaving electron gaps in the other side.

4.2.3.3 Flow batteries

Flow batteries consists of two electrolyte reservoirs from which the electrolytes are circulated –by pumps– through an electro-chemical cell, where the chemical energy is transformed into electricity when both electrolytes flow through it [37]. It has low maintenance costs and the ability to be deep charged without affecting the life span. However, it needs pumps, sensors power management [31]. It can achieve efficiencies of 85% [39] and their size can easily be customized keeping both the energy and power requirements fulfilled. Their power rating and long storage duration meet the requirement of far-offshore wind energy converters [5]. The energy density is characterized by the size of the tanks whereas the power density depends on the rate of the chemical reactions [37]. It is claimed in [37] that flow batteries can go from

charge to discharge in about 1ms. The author highlighted two technologies from literature:

- **Flow batteries - Vanadium RedoxBattery (VRB)**: Despite its good performance (78%), lack of self-discharge (100% Depth of Discharge), and relatively long lifespan 15-20 years, it is not a good solution for mobile systems because of its energy density, which is around 25-35 Wh/kg [34]. This means a storage 24,000-33,600 tonnes of weight for a week of production at rated power (considered as 5MW).

- **Flow batteries - Zinc Bromine (ZnBr)**: During the charge mode, Zn is deposited as a thin film on one side of the electrode, whereas during the discharge, Zn and Br combine into zinc bromide [37]. Even though the sum up of their relatively high energy density, between 75-85 Wh/kg, a high energy efficiency and long cycle life of 2000 cycles at 100% of Dead of Discharge with no damages [34] made it a really attractive candidate for ADO-WTs system, environmental concerns made the author reject it. In fact, with such life cycle, the storage would last 38 years if cycles are weekly or 166 years if monthly, which means that it would not be as limiting factor for the ADO-WTs. Also, their energy density would make them weight 10,000-11,200 tonnes for a week producing at rated power (5 MW) or 4 more times for a monthly, which is a bit worse than the Li-ion battery in this regard. Moreover, the system is made of recycled plastic allowing low cost production and high recyclability [34]. As a flow battery it has no self-discharge and the two aqueous solutions based on Zn and Br are stored in separate tanks, which could be places for instance in both sides of the catamaran hull structure. Nevertheless, as it was found in [34] that a tank failure would expel bromine gas which is toxic, the author discarded this technology for this research. Nevertheless, risks of such failure should be quantified in a further research to fully reject it.

4.2.3.4 Zinc Air (ZnAir) battery

This technology presents the major disadvantage that has low efficiency 50% and lifespan, only a few hundreds of cycles. Another big challenge is the purification of the air coming into the battery. Even though potentially they are the less expensive type of battery [31]. In addition, the anode in this battery is made of zinc, which is a common and available metal [37]. According to [5], metal-air batteries are an option for energy storage for far offshore wind energy converters, their capital cost fluctuates from 10-60$/kWh but their lifecycle is about 100-300 cycles. Nonetheless, this means 1.9-5.7 years if ADO-WTs cycle was a week but 8-25 years if it would finally be a month. The target would be a month and it is the belief of the author that the technology may improve getting closer to the current upper bound or beyond. Even though in [37] it is stated that it is very difficult and inefficient to recharge, which would foster the rejection of this technology for the ADO-WTs application.

4.2.3.5 Lead Acid (PbO_2) battery

This is the oldest rechargeable battery for households an commercial applications. Even nowadays, they are broadly used; their energy density is of 30 Wh/kg and efficiency greater than 85% [31]. Nevertheless, they present an environmental concerns regarding the toxicity associated to lead [40]. Thus it is been refused to use this technology.

4.2.3.6 Lithium ion (Li-ion) battery

Their energy density ranges from 90 to 190 Wh/kg, according to the sources used in [31]. Their high efficiency and low self-discharging makes them suitable for Electric Vehicles solutions [41]. Their major drawbacks are their capital cost ($900-1300/kWh) –even though they are cheaper than Hydrogen ESS–, as well as the internal protection they need in order to avoid overload. Moreover, their life cycle is affected by the temperature [31]. They have a limited environmental impact since the lithium oxides and salts can be recycled. In addition, new Li-ion batteries are capable to produce 10 times electricity of existing Li-ion batteries.

Moreover, the author found two cases, one already build and the other to be build, of Li-ion batteries plant next to wind farms to, mainly supply frequency response, which means short duration storage times. On the one hand, Vattenfall has a 22MW Li-ion battery storage plant in operation since May 2018 in South Wales connected to National Grid and Pen y Cymoedd Wind Farm. The plant, called Battery@pyc, is made up of six shipping container sized units, five of which house 500 i3 BMW manufactured battery packs. Battery@pyc goal is to supply frequency response. The author tried to contact the project manager to gather more information, but did not succeed [1]. On the other hand, ScottishPower –part of Iberdrola group– is planing to build a 50MW Li-ion battery ESS plant to complement wind fluctuation of the already existing onshore wind farm Whitelee to be fully operational by the end of 2020, by stating that it is the most cost-effective storage technology for renewable electricity [2]. The battery system is expected to provide ancillary services such as reactive power and frequency response to the National Grid. It is also claimed that the battery will as well be able to store excess energy from the wind farm.

Even though Li-ion are used to compensate wind fluctuation and they are already being built commercially in big scale, the main focus is to supply frequency response, not store energy for long time durations; in fact, [34] reports a self discharge rate of 1-5%/day and [37] a lower value of 1% month. After discussing with DTU researcher, it was selected as one of the possible technologies for ADO-WTs, even though its self-discharge may end up being a decisive rejecting reason. For more information refer to [39].

[1] All information was found on their website `https://group.vattenfall.com/uk/what-we-do/our-projects/battery-pyc`

[2] Found in Iberdrola home page: `https://www.scottishpower.com/news/pages/super_battery_plan_to_boost_uks_biggest_onshore_windfarm.aspx`

4.2.3.7 Nickel Cadmium (NiCd) battery

Even though Nickel Cadmium batteries are one of the most developed nickel based batteries [31], the presence of Cadmium rises environment concerns due to its toxicity and associated recycling issues [42]. Therefore they are not considered.

4.2.4 Superconducting Magnetic Energy Storage (SMES)

Superconducting Magnetic Energy Storage uses a magnetic field to store energy. It is discarded because of the operation temperature, the filaments inducing the magnetic field must be kept at -270ºC [43] which require extra energy for operation. This implies a reduction of the overall efficiency and higher operation costs.

4.2.5 Cryogenic Energy Storage

Highview Power developed a patent describing this technology [3]. Initially, electric refrigerators cool down the pre-cleaned atmospheric air until it gets liquid (about -196ºC). The liquid air is stored at large low pressure tanks at -196ºC, up to 12 hours, and then used to produce electricity. Since the air occupies about 700 hundred times more space in gas phase than in liquid phase, the liquid is expanded in a turbine producing power. Moreover, the liquefied air, before expanding requires some heat to turn into gas phase, this energy can be used for cooling purposes. Nevertheless, the technology is used as a power system storage able to be charged during off-peak demands and discharge power during peak hours. Moreover, the system is more profitable when it gets bigger, currently the company is building a 1.2GWh plant able to supply 200MW of power. They state to have proven that their technology –also called CRYObattery– is able to store huge amounts of power for months at a time in any location, at a far cheaper price than any other energy-storage system. However, this technology is envisioned to be sited on land, with huge and heavy equipment, not being neither the space nor the weight a restriction. Even though from a technical perspective, the author sees it technically feasible to place a smaller system with the power to gas and storage modules without including the gas to power unit on board, it is not the target of the company so for now, this solution is discarted for ADO-WTs.

However, in several interviews [4] Javier Cavada, CEO of Highview Power, states that their technology will have an LCOE of $50/MWh by 2030. This technology seems very promising for onshore projects. In fact, Javier Cavada mentioned that they are looking at projects on Islands. The author see the North Sea Wind Power Hub as a very good match for this technology, even though it does not seem appropriate for ADO-WTs.

[3] which is briefly explained in their website `https://www.highviewpower.com/technology/`

[4] See, for example: `https://www.rechargenews.com/transition/1821297/liquid-air-storage-offers-cheapest-route-to-24-hour-wind-and-solar`

4.3 Energy Storage System – Selection of best technologies

After going through the State of Art, most of the current technologies were automatically discarded since they did not fulfill technical requirements for ADO-WTs. From the first screening, only three technologies were considered for a further analysis: Li-ion batteries, Hydrogen ES and Zinc-Air batteries. Tables 4.1 and 4.2 summarize the main characteristics of these three Energy Storage Systems.

It was observed differences in literature and therefore, minimum and maximum values shown for every paper are shown. The hydrodynamic analysis considered both limits. However, further analysis are focused on the best values of the current state of art since it is assumed that these would correspond to the scenario some years ahead, when ADO-WTs may be implemented.

Technology	**Energy Density (Wh/kg)**	**Round trip efficiency (%)**	**Power Density (W/kg)**	**Power rating**
Hydrogen Energy Storage	800-10,000 [31] 100-1,000 [34]	20-35 [31] 40-50 [31] 35-42 [34]	>500 [31]	0-50 MW [31] 0.1-50 MW [34]
Lithiom-ion Battery	75-200 [31] 80-200 [34] 90-190 [37]	85-90 [31] 78-88 [34] 100 [37]	500-2,000 [31] 245-2,000	0-100 kW [31] 0.1-50 MW [34]
Zinc-Air Battery	150-3,000 [31] 450-650	50-55 [31] 50 [37]	100[31]	0-10 kW [31]

Table 4.1: Characteristics of the three pre-selected ESS technologies *suitable* for ADO-WTs. Table 1/2.

Technology	**Self Discharge**	**Life Time (years)**	**Life Time (cycles)**
Hydrogen Energy Storage	None [34]	5-15 [31] 15 [34]	1,000 [31] 20,000 [34]
Lithiom-ion Battery	1-5%/day [34] 1% month [37]	14-16 [34]	1,500-3,500 [34] 3000 (at 80% DoD) [37]
Zinc-Air Battery	Neglectible [37]		A few 100

Table 4.2: Characteristics of the three pre-selected ESS technologies *suitable* for ADO-WTs. Table 2/2.

4.3.1 Results of the research

Table 4.3 shows both bottom up and down values obtained from 4.1 and used for the Hydrodynamic model.

Technology	**Low energy density (Wh/kg)**	**High energy density (Wh/kg)**	η_{Low}	η_{High}
Hydrogen Energy Storage	100	10000	20%	50%
Lithiom-ion Battery	75	200	78%	90%
Zinc-Air Battery	150	3000	50%	55%

Table 4.3: Summary of properties of the *pre-selected* ESS technologies.

In order to define the storage system, regardless do the technology used, a main parameter need to be determined: the storage size. Given the WT rated power (5MW according to NREL reference model [4]), two alternatives could be used to size the ESS: either by setting a common storage system for all three technologies, which, due to their different round trip efficiencies would foster different days WTs are free to harvest energy –at rated power– before going to discharge its power; or the number of days ADO-WTs are envisioned to be harvesting energy is fixed which would foster different storage sizes for each technology or, in other words, each technology would store different amounts of energy. It was chosen to keep the energy store as a common factor, so that energy density would be the determining factor, letting the days ADO-WTs are free to harvest determined by the performance.

In order to determine the size of the storage system it was chosen to be able to harvest at rated power (i.e., 5MW) during 20 days, this means 2400 MWh.

Given the storage size (MWh), by using the energy density of each technology (kg/MWh) the total size of the storage system was determined by:

$$Weight = E_{density} \times E_{storage\_size} \tag{4.1}$$

It is assumed that the ADO-WTs will keep harvesting until fully charging the storage which would take 20 days of production at rated power, before going to discharge the energy to the substation. Nevertheless, since technologies present losses, in order to fully charge the ES, the ADO-WTs will be more days harvesting. The time it takes to charge a given ES size (MWh) charging at a rated power P_n and performance η is:

$$t = \frac{E_{storage\_size}}{\eta \times P_n} \tag{4.2}$$

Since the Energy Storage size can be express as a product of time and rated power:

$$E_{storage\_size} = t_{design} \times P_n \tag{4.3}$$

Where t_{design} is the time it would take to fully charge the storage at rated power P_n and ideally conditions (performance of 100%). The time it takes to fully charge the ES with some efficiencies can be expressed as:

$$t = \frac{t_{design}}{\eta} \tag{4.4}$$

The common parameters each studied technology shares are listed below:

- Rated Power of the ADO-WT: 5 MW [4]
- Design days: 20 days
- Storage Size: 2400 MWh [5]

As mentioned, the amount of days ADO-WTs would be harvesting depends on each technology performance, since there are two performance limits specified in 4.3, two values are given per technology. These results are shown in Table 4.4. First column of Weight was obtained using the low density limit –causing a higher weight– whereas the second was obtained with the high density value. Regarding days to fully charge, its first column was obtained using the low performance (round trip efficiency) whereas the second one used the high performance.

ESS technology	**High Weight tonnes**	**Low Weight tonnes**	**Days to fully charge**	**Days to fully charge**
Hydrogen ESS	24000	240	100	40
Li-ion Batteries	32000	12000	25.64	22.22
Zn-Air Batteries	16000	800	40	36.36

Table 4.4: Case 1. Energy Storage weight per technology and adjusted days to fully charge.

It is interesting to comment a few aspects regarding these results. Hydrogen ESS represents the lighter weight if checking the high density values (second column), 70% less than Zn-Air batteries and 98% less than Li-ion batteries. As commented in 5, higher weights represent a greater hull structure which causes greater losses while travelling. Moreover, it will also determine huge costs for the hull and propelling system, which creates a huge disadvantage specially to Li-ion batteries (see 6).

Days to fully charge values are shown to illustrate how each technology would foster huge differences in the sailing dynamics, which would ultimately affect Yield Energy Assessment models. However, it was not taken integrated in neither these models nor in the Hydrodynamic one. Future works could introduce a model of the storage State of Charge which would determine the need to go to the substations to discharge the energy before harvesting: studies to find the best time to discharge regarding both wind resources and energy prices forecasts would be interesting aspects to take into account.

[5] Ideally, 20 days charging at 5MW

For the high performance (last column), Li-ion batteries would present the best results in days of fully charge. ADO-WTs would be slighly more than 20 days harvesting before going to release the energy –no self discharging was taken into account in the calculations–. Note that revenues come from the energy stored, this means, under this simplifications Li-ion batteries would receive almost twice the income of Hydrogen based ADO-WTs (neglecting market price fluctuations among others). In numbers, Li-ion would receive approximately 80% more incomes than hydrogen and 60% more than Zn-Air batteries. This highlights a major drawback of ADO-WTs: whereas conventional WTs are connected to the grid and their losses are minimized, ADO-WTs require energy transformations which causes big losses in some cases, this directly detriments the revenues of ADO-WTs.

Regarding the Hydrodynamic model inputs from this research, each technology will deliver two inputs –low and high values of weights–. Weight will be used to calculate the total displacement, the volume of the hull, its dimensions and finally the energy losses while travelling (see 5).

4.3.2 Hydrogen vs Electricity

Both Hydrogen and Li-ion batteries or Zn-Air batteries seem to be technically feasible solutions for ADO-WTs in this preliminary research. However, they do not store the same type of energy. Future analysis could focus on costs, to have more accurate data and perform feasibility studies using revenues for each energy carrier. Nonetheless, this section is written to illustrate some of the differences these energy carriers present, how they can be compared and how this relates with ADO-WTs. The information exposed here was obtained through interviews with Martin Hartvig[6] who also provided some references.

When analysing an energy carrier, a Transmission System Operator would focus on three dimensions which are:

- Price
- Transportation costs
- Storage costs

All three aspects are important and thus a compromise between these three points must exist. H_2 has higher value than electricity due to the fact that it can be stored and it is cheaper than electricity to transport. Regarding transportation costs, it is approximately 20 times cheaper to transport gas than electricity [44]. In fact, hydrogen can be injected in the form of an admixture to the natural gas grid, used to produce synthetic methane for injection or injected directly into a hydrogen grid. The admissible hydrogen contents in a NG pipeline varies from country to country and for industries (concentrations up to 30 % in volume are considered feasible, however some

[6]Senior Engineer from Energinet (Danish TSO)

industrial branches, such as chemical companies which employ hydrogen as a feedstock for their production, hesitate to accept H2 concentrations exceeding 1 Vol.% [44]). Moreover, pipelines presents lower transmission losses, approximately 4% in power transmission lines [25, 45] while 1% for gas pipelines [25]. The volumetric losses of hydrogen by leakage are always larger than those of NG, but the energetic losses are always smaller [46]. In addition, existing gas infrastructure can provide large seasonal storages which can be greater than 350 times greater than transmission lines [44].

Nonetheless, electricity presents better results in price. In fact, one of the processes of obtaining hydrogen is by electrolysis of water using electricity from renewable energies, which is expected to contribute to the future decarbonization of the energy sector in EU [44]. This means that, such process of producing H2 will carry electricity costs on top of which other costs would be added, making electricity cheaper to be produced.

This can also be seen an advantage of ADO-WTs producing hydrogen, since they would use the advantage of producing cheap electricity from the wind to transform it into hydrogen, storable and cheaper to be transported.

CHAPTER 5

Power Losses model

As mentioned, Wind Energy Yield Assessment model does not account for losses while travelling. The fact that ADO-WTs are envisioned to be able to move is a very particular feature of this technology and therefore it was decided to study this in detail, with the purpose of both quantifying this losses and also understanding to which variables affect travelling losses –referred too as power losses– the most. This chapter shows methodology, results and discussion of the power required to move the whole ADO-WT system. This is made of the wind turbine rotor, nacelle and tower, energy storage system (ESS) on board, floating platform (hull) and the propeller. First, the methodology is exposed followed by the results and discussion. Results for the three selected ESS technologies (see Chapter 4) are shown. However, due to a lack of data regarding costs for Zinc-Air batteries as well as the fact that none of the experts neither from the industry nor academics shown particular knowledge about this technology, no further analysis was made. However, since no evidence of Zn-Air batteries being incompatible with ADO-WTs was found, results for this technology regarding Power Loss are still shown in this chapter. Perhaps in the future this technology is found useful for ADO-WTs. Moreover, both low and high values of energy density are used for each technology with an attempt to show more robust results. For the costs analysis, only high density values –causing low weights– were used assuming that in the future energy densities will be equal –or better– than the best ones currently found in the state of art.

5.1 Power Losses. Methodology

The main goal of any type of wind turbine (WT) is to harvest energy. The author envisions a new concept where WTs move to harvest more wind, the so-called ADO-WT (from Autonomously-Driven Offshore Wind Turbines). Nonetheless, some energy is required to move these WTs. This energy is considered a loss from the WT point of view, since it is spilled so as to move the wind turbine from one point to another and therefore it is neither stored nor directly injected into the power system.

In order to calculate the Power Losses, concepts from Maritime Engineering and Naval Architecture are required. Basically, the Power Losses are constituted by the energy required by the propelling system to move the boat (i.e., from a Naval engineer perspective thi would not be considered as loss but as the power required to propel the system). This will mainly depend on the boat design speed and the morphology

of the hull itself. Thus, a simplified hull must be designed in order to quantify the energy lost by ADO-WT to move from one site to another in order to harvest more wind.

To design a hull, the first step that one must take is to calculate the displacement. The displacement is the whole system weight, which must be equal to the volume of water the hull –hydrodynamic floating structure– needs to displace in order to make the system float. The displacement is used to design the hull dimensions and in order to assess it, the total mass of the ADO-WT must be quantified, for which the storage mass needs to be known. Consequently, the weight calculated in the Energy Storage (see 4) is an input for this model. Knowing the displacement, the hull dimensions can be designed, which will determine both the Reynolds number –which is used to calculate the friction coefficient– and the wet area, enabling the calculation of the energy required to move the system, which is the energy loss to move ADO-WTs from this research point of view.

Therefore, to obtain the Power Losses, the following methodology has been followed:

1. Calculate the displacement
2. Calculate the hull dimensions
3. Calculate the friction coefficient
4. Calculate the Energy Loss

5.1.1 Displacement

Archimedes principle states that the upward buoyant force exerted on a body immersed in a fluid is equal to the weight of the fluid that the body displaces. Moreover, according to Newton's second law, in order to keep an equilibrium of vertical forces, the gravitational force of the whole ADO-WT system -rotor, tower, storage, floating platform, etc.- must be equal to the buoyancy force. Therefore, the total mass of the system must be computed first and then, taking into account the water density, compute the volume of water that must be displaced in order to generate a force able to compensate the whole system weight. Thus:

$$V_{design} = \frac{Displacement}{\rho_w} \tag{5.1}$$

As said, the *Displacement* is the system total mass, including the hull –which is meant to be designed– and ρ_w is the density of the water. V_{design} is therefore, the volume the hull must have in order to ensure buoyancy. Nevertheless, this process is iterative. Since in order to design the hull the total mass –including the hull's– must be known, pre-designing methods are elaborated. For that, first three definitions must be introduced. In naval architecture, three weights are defined for pre-designing a ship. Using the definitions from [47]:

- *Lightweight* or LW. It is the weight of the ship when it is empty. It includes the hull and machinery weight. In this analysis, it is the unknown term that must be quantified in order to calculate the displacement.
- *Deadweight* or DWT. This is the weight that a ship carries. Its cargo, fuel, food and water, passengers crew, etc. In an ADO-WT there is no food or crew. It will be assumed, though that the DWT is the storage and the Wind turbine systems, since it would represent the cargo (i.e., source of revenues).
- *Displacement* it is the sum of the Deadweight and the Lightweight, for a normal ship. As mentioned, it represents the weight of the volume of water that the ship must displace in order to float.

In naval architecture, the ratio Deadweight vs Displacement is used for pre-designing boats. This is:

$$C_D = \frac{Deadweight}{Displacement} \tag{5.2}$$

Following the recommendations from DTU naval architects, a Ro-Ro Ferry has been chosen to pre-design the ADO-WT system. A typical ratio of *Deadweight/Displacement* for a Ro-Ro Ferry is $C_D = 0.3$ [47], which means that the lightweight (hull plus propeller, mainly) represents 66% of the total system mass. This is probably conservative, but due to the fact that the ship proposed in very unconventional, a whole dedicated study should be carried out by a naval architect. For the sake of comparison, other ships present higher *Deadweight/Displacement*, which would foster lower loses at the end; for instance, $C_D = 0.82$ for the Ore Carrier [47]. Future works could focus on designing a more realistic hull in order to minimize losses which will constitute a direct improvement of ADO-WTs overall performance.

The Deadweight is assumed to be the whole system mass except from the hull and propelling system. Thus, knowing the WT mass and the ESS's –using outputs from 4–, the Deadweight can be computed.

$$DWT = M_{WT} + M_{ESS} \tag{5.3}$$

Finally, the displacement can be obtained by using the C_D parameter:

$$Displacement = \frac{DWT}{C_D} \tag{5.4}$$

And finally, dividing by the density of the water, the hull design volume with (5.1) is obtained. Therefore, the procedure followed to obtain the displacement is as follows:

1. Get the whole WT mass M_{WT} (see Table 5.1)
2. Calculate the DeadWeight for each ESS technology –for both limits–, using Equation (5.3)

3. Compute the Displacement using Equation (5.4)

4. Calculate the total hull volume using Equation (5.1)

Table 5.1 shows the wind turbine mass from [4]. It was not found evidence in the report for accounting the step up transformer in the tower mass. ADO-WTs might not need a transformer since the power generated would be directly injected either in the battery (transforming it into DC) or in the cells to generate hydrogen. Future works could focus on modelling more accurately the whole system mass (i.e., whole WT, hull and propelling system and energy storage system).

Moreover, Froude number needs to be introduced since it is a basic parameter to take into account while designing ships. ADO-WTs would have low Froude numbers, which account for lower wave making losses as seen in 5.1.3. Any book of naval architecture presents the formula, which in this case was obtained from [48].

$$F_r = \frac{V_b}{\sqrt{g \times L_{pp}}} \tag{5.5}$$

Where V_b is the speed of the boat (10 knots, approximately 5.14 m/s), g is the gravity (9.81m/s^2) and L_{pp} is the length of the hull (100m). For the specified conditions, the Froude number –non-dimensional– is 0.1642.

5.1.2 Hull dimensions

This sections presents the method deployed to design the hull in order to make the whole ADO-WT float. Therefore, the total volume defined by the hull must equal the displacement calculated using the method explained in 5.1.1.

Different research studying a similar concept chose a catamaran vessel to support wind turbine structures, like [19, 21], even back in 1983 it can be found a patent showing a sailing Wind Turbine on top of a catamaran vessel [18]. In addition, [49] claims that catamaran vessels give good stability due to the separation between the catamaran side hulls whereas its slenderness provide better resistance characteristics. Therefore, a catamaran hull is been chosen to support the ADO-WT.

Item ID	**Mass (kg)**
Tower	347460
Nacelle	240000
Rotor	110000

Table 5.1: Weight Constants for the Displacement Calculation Model. From [4].

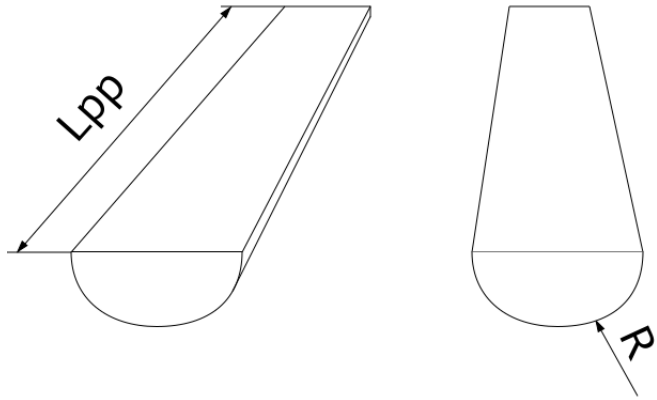

Figure 5.1: Hull Outline.

Figure 5.1 shows the sketch of the catamaran hull. In this simplified model, each catamaran side hull is made of a semi-cylinder. The hull dimension model can therefore be simply defined with two variables (note that the distance between each side hull does not affect the water displaced). Therefore the total volume of the Catamaran can be computed as the volume of a whole cylinder:

$$V_{hull\_catamaran} = \pi R^2 L_{pp} \tag{5.6}$$

Where L_{pp} is the catamaran length and R is the radius of the semi-cylinder –note that there are two semi-cylinders–. As explained in Section 5.1.3, the water frictional losses depend, among others, on the wet area (A_w), which for the design hull shown in Figure 5.1 can be expressed as:

$$A_w = 2\pi R^2 + 2\pi R L_{pp} \tag{5.7}$$

Determining the hull dimensions, even for a simplified model like this, is not a trivial task; because it affects the water frictional losses which will worse off the overall performance of the ADO-WTs. Therefore, even though in a future research more emphasis shall be placed in this topic, a good enough design must be implemented in order to obtain satisfactory results.

From an optimization point of view, this would be a problem whose objective function is the minimization of frictional losses –expressed in Eq. (5.15)– subjected to fulfil that the volume i.e., Eq. (5.6) equals the Eq. (5.1). This can be expressed as:

$$\min_{L_{pp},B,R} \quad F_w = \frac{1}{2}\rho_w V_b^2 A_w C_f \text{s.t.} \qquad V_{hull\_catamaran} = V_{design} \tag{5.8}$$

Where $V_{hull\_catamaran}$ is as expressed in (5.6) and V_{design} will be given for every different ESS technology (since each will have a different weight and therefore the

total volume of water to displace will vary). This can be fully expressed, using the expressions Eq. (5.15), (5.16), (5.6), (5.7)

$$\min_{L_{pp},B,R} \quad \frac{1}{2}\rho_w V_b^2 \left(2\pi R^2 + 2\pi R L_{pp}\right) \frac{0.075}{log_{10}\left(\frac{V_b L_{pp}}{\nu} - 2\right)} \text{s.t.} \qquad \pi R^2 L_{pp} + 4BRL_{pp} = V_{design} \tag{5.9}$$

Note that this is a very complex optimization problem not lineal at all. In fact, the L_{pp}, the length of the catamaran hull appears in the lower side of the fraction as an argument of the logarithm. Therefore, instead of trying to solve this optimization problem straightforward, another approach is proposed.

Moreover, note that only two variables are to be computed, the problem would increase in complexity by just adding a third variable –such a prism on top of the flat face of the semi-cylinder– or, in a real case, a more complex hull structure.

Variable R affects only the wet area, whereas L_{pp}, besides affecting the total wet area, it also affects the frictional coefficient $C_f = \frac{0.075}{log_{10}\left(\frac{V_b L_{pp}}{\nu} - 2\right)}$. Therefore, first a value of L_{pp} will be assessed using reasonable values seen in literature for similar cases. And then the radius can be computed (from Equation (5.6)) as:

$$R = \sqrt{\frac{V_{design}}{\pi L_{pp}}} \tag{5.10}$$

Then the optimization problem was approximated through a heuristic iterative procedure, as follows:

1. Set a total length L_{pp} (values given were 100m, 150m and 200m)
2. Compute the Radius using Equation (5.10)
3. Calculate the water frictional losses for each case
4. Identify the L_{pp} which lower losses

According to findings of William Froude [48], the longer a plank was (L_{pp} in this case), the lower the frictional losses were for a given speed. However, with the simplifications effectuated in this model, results did not confirm this (see 5.2.1 for the explanation). After discussing with maritime engineers from DTU it was found that values between 100m and 200 meters were a good initial approach.

Therefore, three cases were defined for each value of L_{pp} (i.e., 100m, 150m and 200m); the radius was computed and the water frictional losses were calculated for each value of boat speed from -15m/s to 5m/s. This was re-adjusted after observing that results for optimal values of boat speeds did not exceed these limits. It was observed that for every technology, $L_{pp} = 100m$ presented better results, results and discussion are explained in 5.2.1.

At this stage of research, the material used for the hull is unknown. Because of the available data found for the costs analysis it was assumed to be steel, even though

glass reinforced plastic would foster a lighter structure. In fact, some vessels used for O&M of current offshore wind farms are made of GRP (glass reinforced plastic), which is a much lighter material and has been used for the construction of a number of vessels which have proven to be more economic than aluminium vessels but lighter vessels have other limitations. [1]

5.1.3 Power Losses model

In order to assess the energy required to move the platform, a model quantifying the main forces applying to the ADO-WT system while moving through the sea is formulated. For that, Second Newton's law was formulated for a system composed by a boat floating on still water, with a propeller and a wind turbine on top. The system is represented in Figure 5.2. For the sake of an easy understanding, it is shown only the case at which the ADO-WT moves against the wind and commented the case of ADO-WT going with the wind stream. However, wind coming from other directions are not studied in this research. Future works could adapt the Power Losses model to account for any wind direction, which would be required to integrate Power Losses and Wind Energy Yield Assessment models.

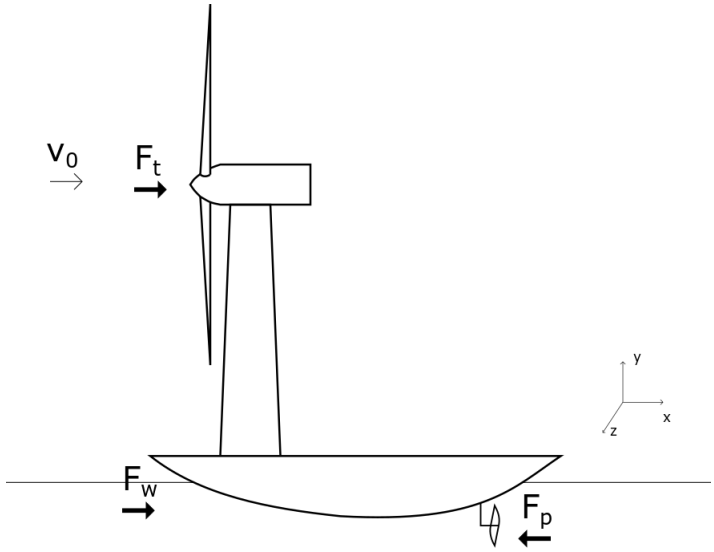

Figure 5.2: Scheme of horizontal forces.

Assuming that vertical forces are in equilibrium -ensuring buoyancy- and not considering the forces perpendicular to the draw (lift force from wind speed, producing

[1] Found in https://www.4coffshore.com/windfarms/an-introduction-to-crew-transfer-vessels-aid2.html

the turn of the rotor), since these are the one generating power, but not slowing down the structure. Assuming only horizontal forces in x-axis and that the whole ADO-WT moves against the wind, the equilibrium of forces according to Second Newton's Law is:

$$M\frac{\partial V_b}{\partial t} = F_p(V_b + V_0) - F_t(V_b + V_0) - F_w(V_b) \tag{5.11}$$

Where M is the total mass of the whole system (i.e., including on-board storage, hull and propelling system, wind turbine, tower, etc.), V_b is the relative speed of the boat-system, F_p is the propulsion force, the one meant to be obtained, F_t is the Thrust force, created by the wind –pushing the rotor towards the wind stream– and F_w is the water friction resistance. Note that the variables of the right hand side of the equation depend on the speed, which in some cases are both the speed of the boat plus the free wind speed -V_0-. Moreover, two forces are neglected in this system: the pushing force the wind generates on the tower –since the area of the bottom part of the tower is negligible compared with such– and the wave making resistance, created from boat moving through the water, which for a low Froude numbers can be neglected (note that the boat moves very slow and the length of the catamaran is quite large, so Froude number is of 0.16 (from Eq. (5.5) for $V_b = 10knots$ and $L_{pp} = 100m$). Note that even in smooth new ships, frictional resistance accounts for 80 to 85 percent of the total resistance in slow-speed ships and 50 percent in high-speed ships [48]. ADO-WTs are envisioned to move very slow in order to minimize losses so in a first approach it is reasonable to neglect wave making losses given such small Froude number. Note that even though the water frictional resistance force will always be opposite to the direction of movement (slowing down the system), the thrust force, in some cases, will contribute to accelerate it (minimizing losses), this is discussed in the results section 5.2.

At the steady state, there is no acceleration and therefore the propulsion force can be derived as the sum of the resistances. Future works could study the differential equation to study the transient. The author contacted with the department of Applied Mathematics from the School of Industrial Engineering from the Universitat Politècnica de València (UPV) who proposed to approach the solution considering, first both F_p and V_0 as constants and for the boundary conditions, consider the boat starts still (i.e., $V_b(0) = 0$) and that it speeds up until a constant speed of design ($V_b(end) = 10knots$, for instance). The problem could be complicated by considering the propulsion force depending on the boat speed and relating it with the energy generated (which depends on V_0). Moreover, V_b could be expressed as a function of V_0 and run it for different wind speeds. However, this is out of the scope of this research and therefore it is only studied the steady state. Equation (5.12) shows the Eq. (5.11) in steady state:

$$F_p(V_b + V_0) = F_t(V_b + V_0) + F_w(V_b) \tag{5.12}$$

From Wind Turbine Aerodynamics, one knows that the Thrust force can be expressed in terms of the relative wind. Since the boat is moving against the wind, the relative

wind speed the rotor sees is the sum of the free wind speed and the speed of the boat:

$$V = |V_0 + V_b| \tag{5.13}$$

Where V_b is considered positive when the ship moves against the wind stream and negative when it goes with the wind stream. Even though (5.14) was not used for computing the Thrust force, since NREL offshore 5-MW baseline wind turbine [4] was used instead, for the sake of understanding the dependency of this force with the relative wind speed, it is presented:

$$F_t = \frac{1}{2}\rho_a(V_0 + V_b)^2 A_{rotor} C_t \tag{5.14}$$

Where ρ_a is the air density, V_0 is the free wind, V_b is the speed of the boat, A_{rotor} is the area of the wind turbine rotor and C_t is the thrust coefficient, which even though depends on $V_b + V_0$, one knows its relationship and it can be obtained from tables. Nevertheless, as already mentioned, in this research a reference wind turbine has been used to transform free wind speed in thrust force –as well as for the power generated–.

The water friction resistance force can be expressed –and it was computed– as:

$$F_w = \frac{1}{2}\rho_w V_b^2 A_w C_f \tag{5.15}$$

Where ρ_w is the water density, A_w is the total wet area, V_b is the speed of the boat and C_f is the frictional resistance coefficient. Note that when transferred to power, F_w is multiplied by V_b which means that water frictional losses increase with the power of 3 with the boat speed. The frictional resistance coefficient is calculated following the recommendations from the ITTC [50]:

$$C_f = \frac{0.075}{log_{10}(Re) - 2} \tag{5.16}$$

Where Re is the Reynolds number which can be computed as:

$$Re = \frac{V_b * L_{pp}}{\nu} \tag{5.17}$$

Where V_b is the speed of the boat, L_{pp} is the boat length and ν is the cinematic viscosity of the water $1.012 \cdot 10^{-6}\ m^2/s$.

Therefore, one can see that in order to obtain the frictional resistance and get the propulsion power –and therefore the energy required to move the ADO-WT system–, one needs to define the hull length and its morphology, in order to calculate the wet area (see section 5.1.2).

Therefore, knowing both forces, the power required to propel the whole system, which represent the power loses for moving the ADO-WT, can be computed as the boat speed times the sum of the resistive forces:

$$P_{losses} = V_b(F_t + F_w) \tag{5.18}$$

Moreover, the Net Power is defined as Power Generated by the WTG minus the ADO-WT travelling losses. Thus:

$$P_{net} = P_{gen} - P_{losses} \tag{5.19}$$

Where the Power generated was computed according to the power curve for a NREL offshore 5-MW baseline wind turbine [4]. Since Power Losses depend on both free wind speed and boat speed forces. For each ESS technology –and both of their Weight limits–, Power Losses were studied for every combination of free wind speed, from 0 to 35m/s and boat speeds, from -15m/s to 5m/s. The convention used to define the boat speed sign is V_b>0 if the boat goes against the wind and V_b<0 if it goes with the wind stream. For each combination (V_b,V_0) a different value of P_{net} was obtained. Finally, the optimal Boat Speed (V_b) is defined as the speed at which the Net Power is the highest, for every Free Wind Speed (V_0).

5.2 Power Losses. Results

This section presents results from the Power Losses model. First, results from designing the two hull dimensions –from the simplified design used– are presented (5.2.1). This determines the best hull length (L_{pp}) found for the three combinations studied. Further sections presents results from the model having set L_{pp} at 100m. The net power for every combination of free wind speed and boat speed are presented in 5.2.2. 5.2.3 presents the optimal boat speeds at which the net power is the highest and 5.2.4 shows the maximum net power (if sailing at optimal boat speeds). Further research should explore the performance when not sailing at optimal boat speeds.

Knowing the dimensions of the hull, the energy lost for travelling at a certain speed with a frontal wind speed (against or with), the power losses can be computed (see 5.1.3). Subtracting this power to the one generated by the wind turbine –for each relative wind perceived by the wind turbine and the power curve defined in [4]– one get the net power (Eq. (5.19)), for every (V_0,V_b) combination. For each V_0, it was found the maximum value of P_{net} –and the boat speed at which this happens–. Thus, ADO-WTs are envisioned to have a control strategy module finding the –optimal– boat speed reference value for each wind speed –similar as it is done with current pitch control– at which harvesting maximum net power. This reference value would be obtained by carrying out analysis similar to the one shown here.

The greatest advantage that can be derived from this whole analysis is the fact that ADO-WTs would be able to generate power at free wind speeds greater than the original Power Curve's cut out wind speed, for any ESS technology studied. Since the relative wind speed that the rotor sees is smaller than the free wind speed –because the boat goes in the wind stream direction, pushed by the proper wind speed (see 5.8)–, the WTG can keep producing whereas current wind turbines (i.e., BTWTs), would be shut down, since V_0 is greater than V_{cutout}. This can also be seen in Figure 5.6 showing the relative wind speed for an ADO-WTs moving at the optimal boat

speed at every V_0. However, there are also two regions where it is worth it to spend some power on moving the whole platform in order to change the relative wind speed the rotor sees and ultimately gain more power. Other researches [16, 19–21] confirm this property of moving in a fluid while extracting energy from another, proving that one can even go faster than the wind, going against the wind and extracting energy from the wind, which may look like a perpetual motion machine, but it is not.

5.2.1 Preliminary results. Lpp design

This section summarizes results obtained while designing the hull structure. The whole model was run for three combinations of L_{pp} 100m, 150m and 200m. Water frictional losses were computed for every case –every technology and every limit bound found in literature–. Figure 5.3 shows the results.

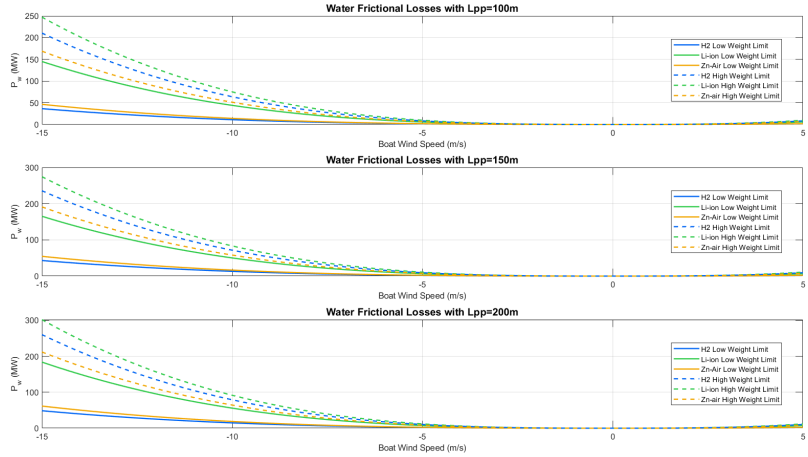

Figure 5.3: Water frictional losses for different values of hull length (L_{pp}).

By just checking at the y-axis one can see that water frictional losses increase with the length of the hull (L_{pp}). This happens for every technology. To put it with some numbers, looking at the blue line –which represents low weight hydrogen based ADOWTs–, it has $P_w = 36.47$MW at $V_b = -15$m/s for $L_pp = 100$m, at the same speed, for $L_pp = 150$m it has $P_w = 42.99$MW and for $L_pp = 200$m it has $P_w = 48.53$MW. It is not worth it to extract further conclusions, since the model is very simple.

For the sake of understanding, though, the reason of this is that the wet area (A_w) is a non-linear function and that values of L_{pp} are one order of magnitude higher than R. Note that the radius of the semi-cylinder changes for each technology.

As mentioned in the methodology, water frictional losses are the product of the boat speed in module –since they always subtract power– and the water frictional force, which is proportional to the A_w and the water frictional coefficient (C_f). Note that even though F_w is proportional to V_b^2 which means that P_w is proportional to V_b^3, this remains the same for the three cases studied. The wet area affects more than C_f to the final losses and A_w is greater for $L_pp = 150m$ and even more for $L_pp = 200m$.

Results for $L_{pp} = 100m$ are presented and discussed in the following sections 5.2.4, 5.2.3 and 5.2.4. Particularly, Figure 5.7 shows the Net Power Curve for $L_{pp} = 100m$.

Therefore, $L_{pp} = 100m$ was chosen as the best configuration. Since the objective was not to develop the best catamaran hull structure but one giving satisfactory results, it would be future works to find a better geometry minimizing weight and frictional losses. Note that even though the tendency was to increase the net power by decreasing L_{pp} it could not be reduced more, because the platform should ensure stability, even though this study is out of the scope of this research.

It was checked that the non-linearity of the minimization problem was the major cause of $L_{pp} = 100m$ presenting better results than greater values of L_{pp}, contradicting Froude experiments found in literature. Wet area is more sensitive to values of R which are to the power of two, rather than L_{pp}, taking into account that values of L_{pp} have one order of magnitude more than R.

Finally, to have some order of magnitude, with a hull length of $L_{pp} = 100m$, a low weight hydrogen ADO-WTs would have a $R = 3.1m$ ($R = 16.0m$ for the high limit), a low weight Zn-Air batteries ADO-WT would have a $R = 3.9m$ ($R = 13.2m$ for the high limit) and low weight Li-ion batteries ADO-WTs would have a $R = 11.5m$ ($R = 18.4m$ for the high limit). However, the focus is not put onto the hull dimensions, which are a step required to calculate the power losses for moving ADO-WTs.

5.2.2 Net Power Generated. Results

For every technology pre-selected (Li-ion batteries, Zinc-Air and Hydrogen) it was used the higher and lower values of energy density found in literature. This means a total of 6 studies, two per technology. Dimensions of the hull are as specified in 5.2.1.

Figure 5.4 is shown to illustrate the shape of a Net Power 3D curve, as a function of Free Wind Speed (V_0) and Boat Speed (V_b). In particular it is shown the one for the highest density value found in the State of Art for Hydrogen –which represents the ESS with lowest weight carrying the same amount of energy–. From now on, 'low weight' followed by the type of technology is used to refer to the best energy density found in literature –i.e., the highest value of energy density found– for the specified technology. Note that the flat region where no 3D curve is seen, represents combinations of (V_0,V_b) at which P_{net} values are negative, which means that it would cost more energy to move the WT than the one extracting from the wind or, in other words, that the ESS would be discharging. As explained5.1.3, for each value of V_0 the maximum P_{net} was found and as well as the boat speed at which this maximum is.

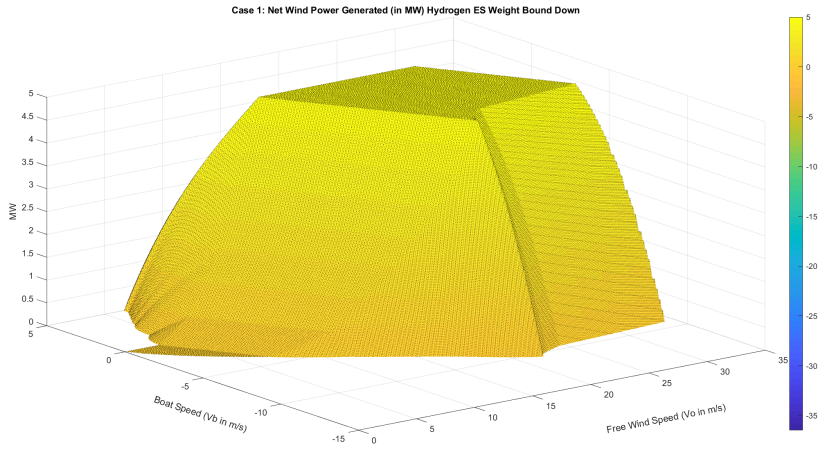

Figure 5.4: Net Power (MW) for every Boat Speed (Vb) and Free Wind Speed (V_0) for Hydrogen Energy Storage.

5.2.3 Optimal Boat Speed. Results

The optimal Boat Speed giving the maximum Net Power for every Wind Speed is shown in Figure 5.5. A new Power Curve $P_{net} = f(V_0)$ –represented in Figure 5.7– is obtained assuming the boat goes at its optimal sailing speed for every free wind speed as represented in 5.5. The relative wind speed that the Wind Turbine Generator (WTG) would percive if the boat moved at the optimal wind speed is represented in Figure 5.6. Figure 5.5 shows the speed at which the boat should move in order to maximize the net power extracted –i.e., $P_{gen} - P_{travelling\_loss}$– for every free wind speed. It is seen that for V_0 lower than 3 m/s, ADO-WTs tend to move with the wind, pushed by the thrust force, speeding up the whole system until reaching a speed creating a force with same magnitude but opposite direction –which is the water frictional loss-, compensating the thrust force. Nevertheless, this movement would be originated by the wind *for free*, only precautions should be taken to avoid collision with the shore or other sailing boats –or ADO-WTs–; to illustrate this, in 15 minutes ADO-WTs would traverse 1800m. However, a deeper study of the system dynamics should be carried out in order to state this with more certainty.

I From 0m/s to 3.1m/s the optimal boat speed obtained from the simulation is to go with the wind (reason why it is negative), even though it generates neither power nor losses. In a real application ADO-WTs would most likely be set to be still since no power is generated.

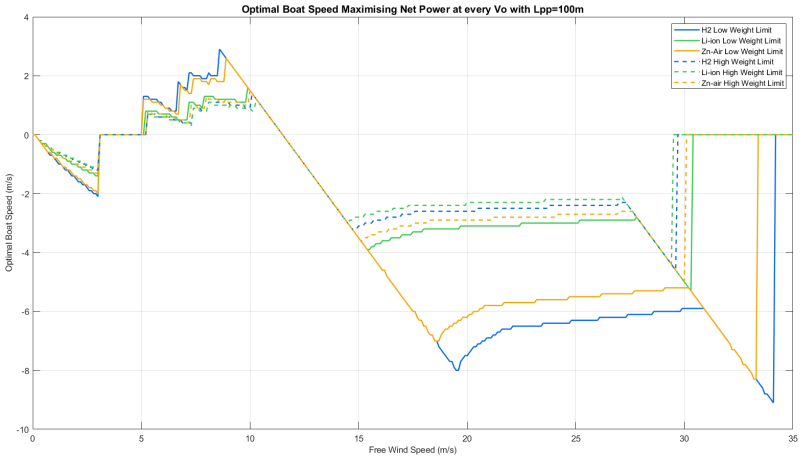

Figure 5.5: Optimal Boat Speed maximizing Net Power for every Free Wind Speed.

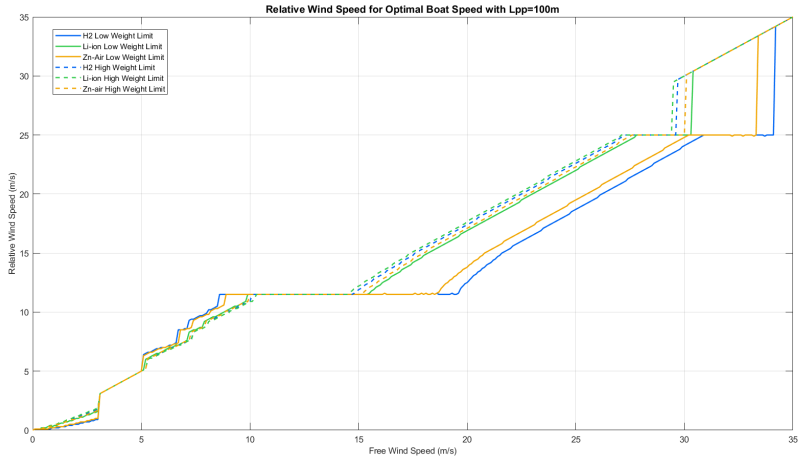

Figure 5.6: Relative Wind Speed seen by the rotor at Vb* for each Technology.

II From 3.1m/s to a range between 5m/s and 5.2 m/s, the optimal boat speed is zero for every ESS considered and from that point ADO-WT moves against the wind. This means that ADO-WTs would be still on the sea ($V_r = V_0$ or $V_b = 0$) from 3.1m/s to approx 5.2 m/s, this can be seen, respectively in Figure 5.6 as a function of type $f(x) = x$ for that range and in Figure 5.5 as a function type $f(x) = 0$ for that range. It is observed a tendency of the lightest technologies H_2 and Zn-Air low weights to start to move at lower values of V_0 (both starting at 5m/s), Li-ion low weight starts at 5.1m/s and for all the heigh weight cases all three technologies would start at 5.2m/s.

III From approximately 5.2m/s to 11.5m/s (which is the rated wind speed), boat speeds are positive for every technology. This means that the boat moves against the wind –and therefore there are power losses (see Figure 5.8)–. By increasing the relative wind speed the rotor perceives, the wind turbine generator (WTG) extracts more power. It is observed a tendency to have a relative wind speed of the lowest wind speed at which the WTG gives the rated power, that is, the rated wind speed. In other words, results from the simulations confirm that an optimal ADO-WT would spend the minimum power required to produce at rated power. If looking at Figure 5.6, similar conclusions are found. It is observed that low weight of hydrogen reaches a relative wind speed of 11.5m/s (i.e., producing the maximum power) at a free wind speed of 8.6m/s –and it keeps this relative wind speed until 19.6m/s, by letting ADO-WT move with the wind from $V_0 = 11.5$m/s–. For the case of low weight Zn-Air batteries, $V_r = 11.5$m/s is reached at $V_0 = 8.9$m/s and for Li-ion low weight this happens at $V_0 = 9.9$m/s, close to the results seen for hydrogen and Zn-Air batteries heigh weights.

IV From $V_0 = 11.5m/S$ to a V_0 which changes for each ESS technology ($V_0 = 15.4m/s$ for Li-ion batteries low weight-ADO-WTs, $V_0 = 18.6m/s$ for Zn-Air batteries low weight-ADO-WTs and $V_0 = 19.5m/s$ for hydrogen low weight ADO-WTs), ADO-WTs would change the direction –from moving against the wind to move with the wind– increasing the relative wind speed (V_b in negative values). This tendency to increase the boat speed happens for all technologies studied until 14.5m/s approximately, at which the heaviest ESS technologies-ADO-WTs tend to decrease the boat speed in order to reduce water frictional (see Figure 5.9). At $V_0 = 15.4m/s$ Li-ion low weight-ADO-WTs –which would be moving at $V_b = -3.9m/s$ – would start to decrease their speed for the same reason. Anticipating what is explained in 5.2.4, Figure 5.9 shows a thrust increasing linearly –because of the pitch of the blades to keep the rated power at 5MW– whereas water frictional losses increase with V_b to the power of three (as discussed in 5.1.3). Since ADO-WTs go with the wind –from $V_0 = 11.5m/s$–, thrust power contributes to move them, however, due to the steep increase of the water frictional losses, ADO-WTs based on heavy ESS technologies need to slow down at V_0 lower than the ones at which ESS ligh technologies do. Regardless of the V_0 at which V_b is reduced, all technologies studied find a

certain stability –or equilibrium– until the next range. Before explaining this range, it is interesting to point out that for low weight hydrogen ADO-WTs V_b tend to get higher in module until $V_0 = 19.5m/s$ –as already mentioned–. At this V_0, ADO-WTs based on hydrogen would move at $V_b = -8m/s$ which in knots is 15.55 approximately, this value is faster than the assumption used in the Wind Energy Yield Assessment model and up to this values there are no power losses associated (see Figure 5.9). For low weight Zn-Air batteries based ADO-WTs, this would happen at $V_b = -7m/s$, 13.61 knots approx. –also higher than the 10 knots assumed on the yield assessment research–. Even though in this region the boat speed is being reduced, the relative wind speed is still increasing (since free wind speeds are getting higher). In fact, in this region, the relative wind speed increases approximately at a rate of 1.2 –with V_0–, this happens until the relative wind speed reaches the cut-out wind speed, which is $V_0 = 25m/s$. The equilibrium seen in this region is broken when the relative wind speed reaches 25m/s, WTG would shut down if V_r increased 25m/s.

V Moving with the wind –for the established sign convention– V_b are negative. In order to keep V_r at 25m/s, for greater values of V_0, V_b needs to be higher. This can be seen in Figure 5.5 as a slope after the relative equilibrium commented already. In this region, ADO-WTs optimal boat speed increase with the free wind speed in order to avoid the relative wind speed overpass the cut out –forcing them to shut down– or, in other words, to keep the rotor generator at 25m/s and therefore producing power. However, this will generate losses since the thrust cannot supply enough power to keep ADO-WTs at such speeds. This regions can also be seen in Figure 5.6 as an horizontal line at $V_r = 25m/s$. As explained, this requires power to propel the system and the increase of sailing speed occasions the rise of water frictional losses until a point from which the power net would be negative.

VI This can be seen as the vertical line bringing the boat speed to zero (Figure 5.5) and in Figure 5.6 as a $V_r(V_0) = V_0$ function as in the previously seen region at which ADO-WTs were still.

VII For greater V_0 ADO-WTs would be shut down and the optimal boat speed would be zero (for low weight hydrogen ADO-WTs this happens at $V_0 >= 34.2$m/s)

As a final conclusion, it is seen that boat speed tends to increase in this final stage to avoid the shut down of the WTG and for every technology studied, the speed reached at this point is greater than the one seen in the previous slope –where the power to propel the system was entirely supplied by the thrust force–. Moreover, lighter technologies allow greater boat speeds, which would allow ADO-WTs to go to further regions were harvesting power.

Future works could also study the compromise between staying at the optimal boat speed and the need to go at other speed –or even in other directions– in order to harvest wind at other spots. This could be done by integrating both the Wind Energy Yield Assessment model and Power Losses model.

5.2.4 New power curve: Optimal Net Power Curve. Results

As already introduced, a new Power Curve is defined for every V_0, assuming the boat goes at each optimal wind speed –and only for the the steady state–. This Power curve –represented in Figure 5.7– is obtained by calculating the maximum value of P_{net} at every V_0 and, therefore, transforming the 3D curve –shown in Figure 5.4– into a 2D curve. Note that Figure 5.7 includes the original power curve for a static case, which is, basically, the power curve of Bottom-Fixed Offshore Wind Turbines (BFOWT) from NREL offshore 5-MW baseline wind turbine [4] –also used in the Energy Yield Assessment model–.

The Net Power Curve is easier to understand than the boat speed's. The represented power curve is the result from subtracting the energy losses to the power generated –which can be maximum 5MW in this case–. Moreover, this curve would characterize ADO-WTs moving at the optimal boat speed –which is different for each value of V_0–. One needs to bear in mind that this study is done under steady state conditions, which means that a sudden change in the free wind speed (from 10m/s to 12 m/s, for instance) would not cause an immediate change in power as seen in the curve, since in order to have such net power output, the boat would need to change from the speed it was going at 10m/s following the example –which is in fact against the wind– to the optimal boat speed for a $V_0 = 12$m/s which is different both in module and in sign. This on of the reasons why future works could focus on the dynamics of this system.

Regardless of the speed at which the boat should go, steadily, the first conclusion one can draw is that even for the worst case found in the the state of art, ADO-WTs would be able to generate at rated power at higher wind speeds than BFOWT without compromising the wind turbine (since the wind it would perceive is the same it would *see* a BFOWT with at $V_0 = 25$m/s). To illustrate this, the in worst case, ADO-WTs would be producing a net power of 5MW even at a $V_0 = 27.2$m/s, (2.2m/s more) shutting completely down at 29.4m/s). Low weight Li-ion batteries ADO-WTs would still produce a net power of 5MW until 27.9m/s from which it would be progressively produce less power until 30.4m/s at which they would be shut down. Low weight Zn-Air batteries ADO-WTs would produce at rated power at free winds lower or equal than 30.2m/s from which it would be reduced until 33.4m/s. Low weight hydrogen ADO-WTs would produce at rated power until 30.9m/s, being definitely shut down at 34.3m/s. Notice that for the best case –lower weight hydrogen–, ADO-WTs would be able to produce with a net power equal to the rated –since there are no losses 5.9– for wind speeds almost 6m/s higher than current wind turbines.

As explained in 5.2.3, there are seven different regions, which cannot be identified in the Net Power Curve. These are discussed below from the net power curve perspective:

I A first region where ADO-WTs would be moved by the wind, with neither production nor losses (from 0m/s to 3m/s).

II A region where ADO-WTs would be still –which can be seen in Figure 5.7

as a slope from 3m/s to 5m/s–. In this region both ADO-WTs and BFOWT would produce the same, since in fact, ADO-WTs would not move at optimal conditions.

III A region where ADO-WTs would tend to move against the wind to increase the relative wind speed (see 5.2.3), from [5,5.2]m/s to 11.5m/s. It is interesting to point out that even for the worst value found in the state of art for the three technologies considered –which corresponds to the heigh weight value of Li-ion batteries–, the WTG would start to produce at rated power at free wind speeds at least 1.2m/s lower than the current rated wind speed ($V_0 = 11.5$m/s). However, as it can be seen in the Net Power Curve 5.7, it is not until free wind speeds are greater than the actual rated wind speed that the net power equals the rated power. This is due to the fact that by moving against the wind, part of the energy harvested needs to be spent on the movement itself [2]. Even though there are losses while moving against the wind, net power is greater than the one bottom-fixed wind turbines (BFWTs) would generate. To illustrate this, at $V_0 = 10m/s$, BFWTs generate 3.5MW –for the given Power Curve–, whereas for the same wind speed, ADO-WTs with hydrogen storage could generate 3.86MW of net power, 10% more power, and for the worst case seen ADO-WTs would generate a net power of 3.7MW, almost 6% more power.

IV For wind speed values greater than 11.5m/s, moving against the wind would not increase net power since even though the relative wind speed would increase, the power generated would be limited to 5 MW (black line from Figure 5.7 or blue line from Figure 3.1.1.4), nonetheless, travelling losses would increase –both the thrust and water frictional losses– causing the net power decline. At this region, ADO-WTs would move with the wind increasing the boat speed and the net power would be 5MW (first region of the horizontal line of Figure 5.7).

V As explained, at some point –which differs for each technology– frictional losses would foster the slight reduction of the boat speed, even though it would still move –with the wind ($V_b < 0$)–. However, net power would still be rated one, since there are no losses (which means that ADO-WTs would travel *for free*). This region, which cannot be identified in Figure 5.7 corresponds to the last region of the horizontal line of the same graph (up to 30.9m/s for low weight hydrogen ADO-WTs, e.g.).

VI For higher wind speeds, the relative wind speed the boat requires to keep producing at rated power (not net power, though) could no longer be supplied by the thrust power from the wind and therefore, the propeller system should do

[2] This phenomenon may look like a perpetual motion machine, however, several studies support this theory as already mentioned. Studies found started in 1969 and up to 2017 there were found publications [16, 19–21]. In fact, Mac Gaunaa [3] competes every year in a race of cars moving against the wind and exclusively propelled by wind power with other colleagues and students from DTU.

it, this would cause a drop of the net power –and an increase of power losses, see Figure 5.9–. ADO-WTs would tend to have higher boat speeds in order to stay within the generation curve (i.e., $V_r <= 25$m/s). This can be seen as the drop from 5 MW to 0 MW

VII Next region would be 0MW, with ADO-WTs shut down and still. However, future work should study the dynamics of the system, focusing on the movement traversed of ADO-WTs for different boat speeds aiming at finding if it would be possible to stay at a best wind spot –or go to– without incurring in extra losses for not sailing at optimal boat speeds.

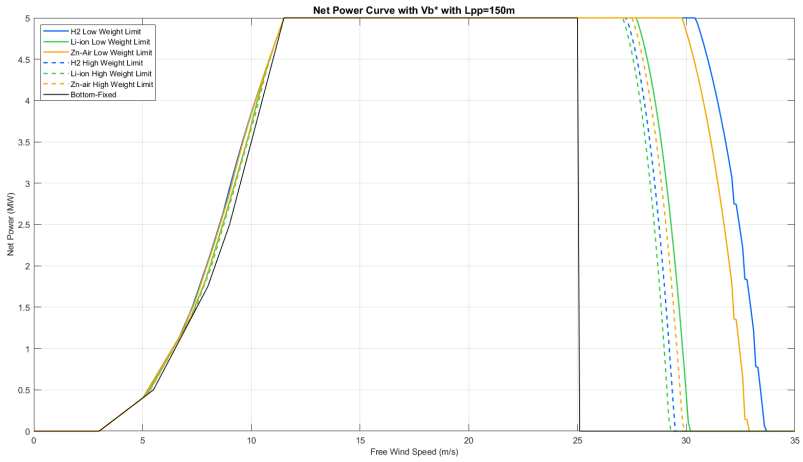

Figure 5.7: Net Power curve for every technology considered compared with Bottom-Fixed WTs, for every Free Wind Speed.

Figure 5.8 shows, for each optimal boat speed Power Losses in percentage of the Power Generated, Power Generation and Power Losses, for each of the technologies studied –for both the highest and lowest value of energy density–. Notice that subtracting the Power Losses to the Power Generated, one would get Figure 5.7.

The bottom graph from Figure 5.8 shows that, from 13m/s to 31m/s approximately, there are no losses for the low weight hydrogen ADO-WTs represented by the blue line. Low weight Zn-Air batteries ADO-WTs –in golden yellow– shows no losses from 13m/s to 30m/s, approximately; whereas low weight Li-ion batteries ADO-WTs start having losses at 28 m/s. This means that ADO-WTs could travel without expending energy, however, only in the direction of the wind to maximize the net power. Figure 5.8 also confirms that the worst numbers found in the state of art for both

H2 and Zn-Air technologies present similar results than the best numbers of Li-ion state of art. As already discussed in the Net Power Curve explanation, low weight hydrogen ADO-WTs would still produce power with no losses from 25m/s to 31m/s –at which Bottom-Fixed WT would be off–. This is because the optimal boat speed is the difference between the cut-out wind speed (25m/s) and the free wind speed –from 25 m/s to 31m/s–, which means that ADO-WTs' generator would supply at rated power (5MW) being the thrust force the responsible for the propulsion of the system, at zero power cost.

This can be understood better by checking the balance between water frictional resistance losses and thrust resistance losses (Figure 5.9), since when the boat goes with the wind, water frictional resistance is opposed to the movement of the boat but not the drag from the wind –in some cases–, which is pushing the whole ADO-WTs towards the wind stream (i.e., helping the wind turbine to move); for such thrust pushing the boat (when free wind speed is greater than the boat speed –going with the wind– in absolute value), the optimal boat speed is the generating water frictional losses as great as the thrust, since it is not considered that the propeller can extract energy from the water. Therefore, the equilibrium is found when the boat, speeded up by the wind, reaches the speed that creates a water frictional force (F_w) equal to the F_t generated by the wind. At this moment the ADO-WTs moves *for free*, thanks to the drag generated by the wind. In fact, every time E_{loss} is zero is because thrust force compensates water frictional force.

For boat speeds greater than 6m/s going with the wind (i.e., $V_b < -6m/s$), the water frictional resistance exceeds the thrust from the wind and therefore the pro-

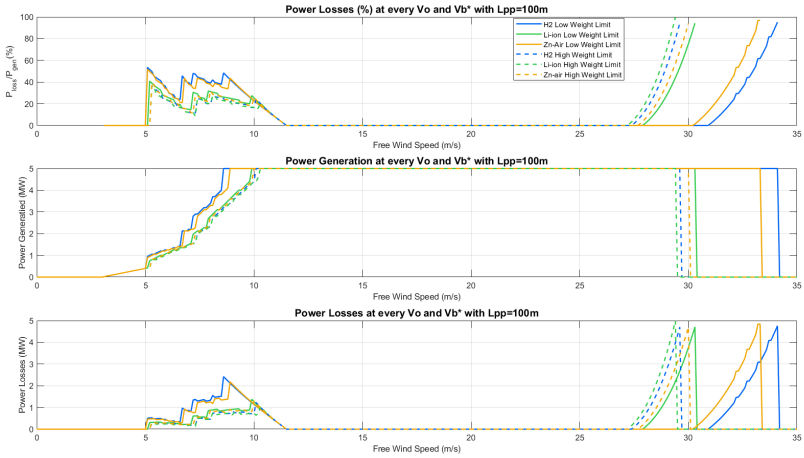

Figure 5.8: Power Losses while Travelling for each Technology.

peller needs to work to move the ADO-WT. When the free wind speed reaches a certain threshold (31m/s for the low weight hydrogen ADO-WTs), in order to keep the relative wind speed within the operation range (i.e., below 25m/s), the boat must reach greater speeds that generate water frictional forces greater than the thrust forces. Therefore, the propelling system must inject energy to make the boat faster so as to be able to keep generating at rated power (<=25m/s). When V_0 reaches the other limit (34.2 m/s for low weight hydrogen ADO-WTs), water frictional losses are greater, not only than the thrust, but the power generated and therefore the net power would be negative, using energy to move the wind turbine. Therefore, the boat is brought back to 0 m/s. With this philosophy, cut-out wind speed is pushed almost 6m/s at no power losses expenses. Future studies would need to dig more into this phenomenon to quantify in a more realistic model how big this margin would be –as well as if it would be worth it to move ADO-WTs against the wind for $V_0 < V_{rated}$–, quantifying as well the wave making losses, propeller performance, etc.

Finally, note that in both graphs (Figures 5.8 and 5.9) there are some asymptotes, this happens when the Energy Generated by the rotor is zero, since the coefficient is calculated dividing by that term. Moreover, Figure 5.9 shows a "negative" power loss, this was avoided by limiting the propelling power to be either positive or zero. However, this region represents a potential source of power, since it shows that thrust from the wind is greater than water frictional losses tending to accelerate the whole system. A smart solution seems to be to use a water turbine to subtract this power while slowing down the system. Thus, future research could study the usage of water turbines to slow down the structure by extracting energy from the water and keeping

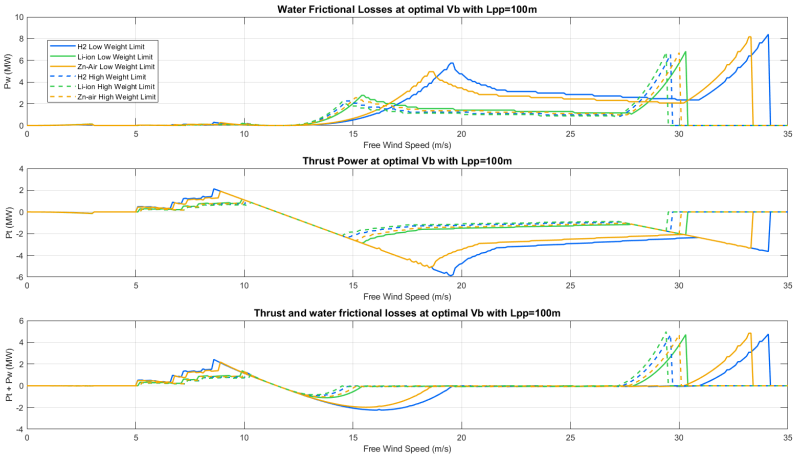

Figure 5.9: Frictional Losses due to water and wind resistance for each Technology.

ADO-WTs relative wind speed right above rated wind speed in order to keep the WTG at rated power production. A system like the one being currently studied by researchers from Central Nantes among other seems to be an interesting starting point[4]. However, the stability would be a major aspect to take into account, from the author point of view for the ADO-WTs with a water turbine.

Moreover, it is proven that the lighter the ESS is, the faster the ADO-WT can go and as seen from results from WEYA (see 5.2.3), the faster the ADO-WT can sail, the greater the Energy Yield will be. Moreover, if ADO-WTs can move faster –for being lighter and having less losses–, the Net Power Curve shows an extra advantage not implemented in the Wind Energy Yield Assessment model, which is the extra energy ADO-WTs can get at rated power for wind speed higher than cut-out wind speed.

Finally, it is interesting to point out that despite the fact that travelling losses rise since both thrust and water frictional losses decline the overall performance, net power is greater by moving the ADO-WT against the wind, for those V_0 values. It can also be pointed out how the lighter the system is, the more extra energy can be obtained. Therefore future works could study ways of minimizing mass of the whole ADO-WT system.

Perhaps a final solution could integrate both [5] and the one presented here: a WT to extract power from the wind and a water turbine/propeller for either moving the ship –for certain range of wind speeds and for other operation and maintenance purposes– or slowing it down by getting energy from the water, for wind speeds greater than the rated power. The goal would be to keep the WTG at rated power by targeting a relative wind speed close to the rated free wind speed and capturing the extra energy from the wind –which nowadays is spilt– with the water turbine.

[4]Refer to results presented in the International Offshore Wind Technical Conference, 2018, San Francisco [22]

CHAPTER 6

Cost Analysis

In any engineering project, profit has the last word. A new technology or any project will not have green light unless it is proven that it will be profitable. This chapter is an attempt to quantify the costs of a wind farm made of ADO-WTs and compare it with a wind farm made of Bottom-Fixed Offshore Wind Turbines (BFOWTs), already consolidated. Moreover, this chapter also aims at clarifying which Energy Storage System is more cost-effective: either Li-ion batteries or hydrogen. LCOE is used to compare each case.

It has been very challenging to find realistic costs. On the one hand, regarding wind turbines, wind farm development and hull & propelling system it was difficult to find real costs because this information is very sensitive to the industry. On the other hand, regarding the Energy Storage System (ESS), its lack of maturity was the main reason of finding unrealistic costs. Thus, rather than a final number, this chapter shows an initial approach to quantifying the real costs of this new technology. In the future, a feasibility analysis could be carried out, including the price of selling each energy carrier.

This chapter presents: the assumptions taken and method carried out to estimate costs –both CAPEX and OPEX– 6.1; LCOE results 6.4.1 and costs share per component 6.4.2; discussions comparing with other reports 6.4.3 and rough targets for hull & propelling system and ESS to make ADO-WTs competitive 6.4.4.

Through interviews with Magdalena Zajonc [1] it was found that papers and reports usually inflate costs. However, no alternative was found except from assuming an industrial benefit (8% to 12%) and discounting this from the bidding price of current wind farms already commissioned –whose data is free and available to everyone– in order to estimate the overall costs. However, a detailed break-down cost of each item would be required to disaggregate this number into individual costs. Multiple sources state that costs greatly vary from project to project, making it very hard to find an appropriate comparison. Moreover, from conversations with Magdalena Zajonc it was found interesting to find a relationship between WT wear, lifespan and O&M (extra costs) and the increase of capacity factor (extra revenue) for future research.

After discussing with people from the industry (experts in Power to Gas from Energinet, Danish TSO) and Energy Storage experts from the Elektro Department in DTU, Zinc-Air batteries were discarded. This does not mean that they cannot

[1] Magdalena Zajonc works as business developer and consultant at PEAK Wind. She also does OPEX modelling and R&D.

fit the ADO-WT system, but neither industry nor research sector thought it was a realistic solution due to the lack of development. In addition to that, not reliable papers were found publishing costs of Zn-Air batteries. Regarding hydrogen and Li-ion batteries, industry shown more interest in the former solution, because it has less losses for long term storage whereas DTU researchers express as a more realistic solution a Li-ion battery, since hydrogen has a lot of losses while converting Power to Gas (found in literature as PtG or P2G as well) and it is more dangerous to operate. Therefore, both options were studied forwards, leaving out of the analysis the Zinc-air battery storage system. Nevertheless, it must be point out that current large scale Li-ion batteries are used for frequency control not for long term storage. This could definitely mean that Li-ion batteries are not a good technology for this ADO-WTs.

6.1 Costs Analysis. Methodology

The costs analysis was carried out assuming that the proposed technology –ADO-WTs– were already matured. Notice that this was done in order to find if, ADO-WTs would be able to compete with current alternatives, after a proper R&D phase and market consolidation. Of course, in case the ADO-WT concept was developed further, first years it would be more costly, as it happened with any other technology.

6.1 presents the main sources used in this chapter as well as the reference project used by NREL to compute wind farm related costs. 6.1.1 describes each different case studied. Based on NREL report [51] –including the new features of ADO-WTs–, wind farm costs were broken down into:

- CAPEX
  - Wind Turbine CAPEX
  - Balance of Plant
  - Financial Costs
- OPEX
  - Wind Farm
  - Energy Storage System
  - Hull & Propelling System

The Capital Expenditures of both the ESS and the hull & propelling system are included in the Balance of Plant, since to some extend they would substitute intra-array cables –and export cable for case 3– as well as the foundation, respectively.

Moreover, the lack of detailed data forced to make many assumptions as well as not go deeper in areas of which more data was collected. David Johnsen [2] provided

[2]David Johnsen is Senior Director of Copenhagen Offshore Partners, electrical engineering specialized in High Voltage by DTU.

detailed information about the cable layout configurations of current offshore wind farms, however such level of detail was not found in other items (such as the substation, WT, hull, etc.) so items were aggregated as in [51].

Sources and reference projects

NREL report [51] provided the most accurate breakdown costs structure of wind farms (onshore and offshore) and thus it was used to entirely estimate case 1 and partially cases 2 and 3 (read 6.1.1).

Most accurate data for Li-ion was found at [25], however, it is believed that it is conservative; hydrogen costs were found more detailed, realistic and relevant for ADO-WTs in [5]. Regarding the hull & propelling system costs, it was first consulted [52]; however, after interviewing Manuel Ventura[3] it was used information provided by him to quantify its CAPEX –cases 2 and 3–, even though he made it clear that they were rough approximations.

The offshore reference project used in [51] is located in the North Atlantic region of the United States with same parameters for BFOWT and floating wind farms (except from water depth); consisting of 107 wind turbines rated at 5.64 MW with a 140-m rotor diameter –equating to a 600-MW wind power plant capacity–. This is similar to the ADO-WTs modelled in this research, which are 5MW and 128m of diameter. Lifespan is assumed to be 20 years, with no catastrophic O&M events. BFOWT are assumed to be installed in water depths of 30 m with monopile substructure, whereas floating WTs are assumed to be installed in water depths of 100 m semisubmersible substructure. The array cable system and electrical line connecting to the offshore substation is of 33-kilovolt. The export cable from the offshore substation to the land substation is assumed to be 220-kilovolt. Moreover, notice that [10] claims that overall costs increase with distance to shore, which would not affect ADO-WTs but BFOWTs wind farms.

Regarding costs of hydrogen. [5] presents a detailed costs split for four cases of fleets of far offshore hydrogen-producing wind energy converters, which inspired this analysis. In [5] four cases are studied, combining compressed and liquefied hydrogen and a terminal –to which wind energy converter would sail to unload the hydrogen– which could be onshore or offshore. In case it was offshore, ship carriers would collect the hydrogen from the offshore terminal and bring it to a second terminal onshore. In addition, [5] studies the distribution on land of the hydrogen, although this is not relevant for this research. Moreover, [5] estimates the cost of producing electricity with the LCOE from floating wind turbines (of 0.11€/kWh) to which costs of mooring system, installation and BoP (of 30%) are subtracted and, finally, assuming that FOW has a capacity factor 50% whereas their proposed system would have 90% they arrive to a final cost of 0.04€/kWh. It is believed that a capacity factor of 90%

[3]Manuel Ventura has a PhD. in Naval Architecture, by the Technical University of Lisbon (2005), MSc. in Naval Architecture, by the University of Glasgow (1996). He holds a degree in Naval Engineering by the Technical University of Lisbon (1982) and a degree in Mechanical Engineering by the Instituto Superior Técnico (1978).

might be too high for their concept, where 4 Flettner rotors installed in the same catamaran would extract energy from the wind to propel the system, which obtains energy from a water turbine; the biggest concern found is the wake effect that each rotor would create between each other. Since more detailed data was in [51] regarding wind farm calculations, only costs related with hydrogen electrolysis, compression –or liquefaction– and storage are considered from [5]. In addition, [5] proposes ship carriers to transport LH2, however, fossil fuels power currently this ships which is not an ideal solution. Instead, a pipeline would be installed for this purpose, which could be amortized during the lifespan of the ADO-WTs and even further if new ADO-WTs would be "installed". Notice that ADO-WTs are independent one from each other which would decouple the lifespan of each system. Legislation should be studies in Future works could focus on checking which legislation would apply to ADO-WTs, since they would be boats and WTs at the same time and current re-powering of wind farms require a to deliver a whole new project (including a new EIA, etc.).

All costs are converted to USD from the original reported year exchange rate –if they were not in USD already– and then inflated –or discounted– to 2017 USD using the Consumer Price Index, as proceed in [51].

6.1.1 Description of case scenarios

Case 1 represents the conventional wind farm with BFOWTs whereas cases 2 and 3 model two possible typologies for an ADO-WT wind farm. An ADO-WTs wind farm is ideally foreseen with an onshore substation, since it would present less overall costs, complexity to construct, operate and maintain and decommission, besides lower risks and safety for the technician workers. Nevertheless, some sites might present prohibitive water depths forcing the installation of an offshore substation/terminal. Moreover, because ADO-WTs would need to move to the substation to discharge every time, an offshore substation might allow them to go to the far offshore and compensate the extra cost of the substation. Therefore, these cases have been studied:

6.1.1.1 Case 1: Hundred 5MW BFOWTs with offshore substation

Case 1 represents a Wind farm made of 100 BFOWTs 5 MW each, with an offshore substation. AEP production was obtained from results of the Conventional model from Wind Energy Yield Assessment simulated for the whole 2018. BFOWT are assumed to have monopile foundation, they would be electrically connected to the substation through intra-array cables and an export cable would connect the offshore substation to an onshore centre of transformation/substation.

6.1.1.2 Case 2: Hundred 5MW ADO-WTs with offshore discharging substation/terminal

Case 2 represents a wind farm made of 100 ADO-WTs 5 MW each with the discharging substation –or terminal– installed offshore. 'Discharging substation' will be used for Li-ion cases (carrying electricity). 'Terminal' will be used for hydrogen, as in [5]. Since two Energy Storage System (ESS) have been selected for further research, case 2 is subdivided in the following cases:

Case 2.1: ADO-WTs with hydrogen ESS and offshore terminal

In this scenario, ADO-WTs would yield energy and store it aboard in form of liquefied hydrogen (LH2). Each ADO-WTs would be harvesting at least during 40 days and go to offload the energy to an offshore terminal which would be connected to an onshore terminal through a pipeline. The offshore terminal would have 20 piers to allow 20 ADO-WTs to berth and offload their energy at a time; this means that every 8 days 20 ADO-WTs could go to the terminal to discharge their energy, since it takes 40 days to fully charge their aboard tank storage at rated conditions. No storage would be offshore, instead the onshore terminal would have a tank storage (of type Horton spheres) equal to 20% of the sum of each ADO-WTs individual capacity. From the onshore terminal LH2 would be distributed as described in [5]. In the future, an optimal design of the number of piers and storage capacity at the onshore terminal should be analysed in detail.

Case 2.2: ADO-WTs with Li-ion batteries ESS and offshore discharging substation

In this scenario, ADO-WTs would yield energy and store it aboard in Li-ion batteries. The discharging substation would not have a storage, ADO-WTs would discharge the electricity which would be transported through an export cable to an onshore substation/centre of transformation, connected to the transmission system; as the terminal for LH2, it would have 20 piers to allow 20 ADO-WTs to berth and discharge their energy at a time.

6.1.1.3 Case 3: Hundred 5MW ADO-WTs with onshore discharging substation/terminal

Case 3 represents a wind farm made of approximately 100 ADO-WTs 5 MW each with a discharging substation –or terminal– installed directly onshore; this option saves the installation of the onshore terminal or substation/centre of transformation. As case 2, this case is subdivided in the following cases:

Case 3.1: ADO-WTs with hydrogen ESS and onshore terminal

In this scenario, ADO-WTs would yield energy and store it aboard as LH2, once fully charged –or more profitable conditions–, ADO-WTs would go to shore to offload their energy at the terminal. The terminal would also have the same tank storage as the onshore terminal in case 2.1 and 20 piers as the offshore terminal in case 2.1 to allow ADO-WTs to berth and offload their energy.

Case 3.2: ADO-WTs with Li-ion batteries ESS and onshore discharging substation

In this scenario, ADO-WTs would yield energy and store it aboard in Li-ion batteries, once fully charged –or more profitable conditions–, ADO-WTs would go to shore to discharge their energy at the discharging substation which would be connected directly to the power system. As in case 2.2, it would not have a storage, but 20 piers to allow 20 ADO-WTs to berth and discharge their energy at a time.

6.1.2 Levelized Cost of Energy (LCOE)

The LCOE is computed using the simplified formula used in [51] from the original report [53]. This can be expressed as:

$$LCOE = \frac{CAPEX \times FCR}{AEP} + \frac{OPEX}{AEP} \tag{6.1}$$

Where $CAPEX$ is the overall initial investment (sum of all the CAPEX), FCR is the fixed charge rate before taxes, AEP is the Annual Energy Production and $OPEX$ is the final OPEX (sum of all the OPEX).

The AEP is obtained from the Wind Energy Yield Assessment model. For case 1, AEP is the energy outcome from the Conventional model, whereas for cases 2 and 3, this value is multiplied by $(1 + EE)$ where EE stands for Extra Energy in per unit, obtained from the Reachable Area model (which, in a few words, accounts for the extra energy that one could get from moving WTs on the North Sea –selected area–). Notice that WEYA accounted for the same region, future works including the ESS model would restrict the distance ADO-WTs can go to yield since at some point they would need to discharge their energy.

FCR represents the amount of revenue required to pay the carrying charges on an investment during the expected project life per year [51]. Note that FCR would differ from BFOWT and ADO-WTs in an initial state, due to the uncertainty of the latter technology, however, in a future scenario it would be closer depending on how competitive the market is. In fact, in the report published in 2013, offshore wind had a FCR of 11.7% facing a 10.2% for onshore wind [54] whereas in the new report [51] FCR for offshore dropped to 7% lower than the 8.6% assigned to onshore wind. Notice that floating was not included in 2013 report, however, in the new report [51] it was set to 8.2%.

For this study it is being assumed the value of 7% as the last value given for offshore wind turbines, assuming that the market will still be competitive as nowadays. Results are shown in Table 6.1

6.2 CAPEX

This sections explains the assumptions taken and final values given to each cost item, regarding the Capital Expenditures for all 5 cases. The classification used in [51] is been used to break down the wind farm CAPEX. The hull & propelling system as well as the ESS is included in the Balance of Plant (BoP) since it would substitute, respectively, the foundations and the intra-array cables –and export cable for case 3–.

6.2.1 Wind Turbines (CAPEX)

For case 1 (modelling the conventional wind farm), the WT system CAPEX used was the one provided [51] for BFOWT: $1,557/kW. Because the turbines modelled are 5,000kW the total turbine costs is $7,785,000/WT.

[51] proposes a slightly smaller cost for floating wind turbines, which is $1,521/kW. ADO-WTs would be closer to floating WTs than to BFOWT and therefore this value is used for both cases 2 and 3, summing up a total turbine cost of $7,605,000/WT for both cases.

However, despite the fact that according to Bloomberg New Energy Finance's Wind Turbine Price Index proposes a lower cost for the WT [4], which might be more realistic, it was decided to use a single source to be more coherent and [51] is the only one providing enough detailed information transferable to cases 2 and 3.

Future research could explore a new type of Wind Turbine Generator (WTG). Currently, one of the turbines most used in Offshore wind farms has a back-to-back converter which consists of a module AC/DC DC/AD used mainly to control the wind turbine rotor speed. If ADO-WTs ESS would require a DC input, it would be interesting to study a direct connection without the need of transforming the current back to AC. Moreover, this could be studied to current offshore wind farms using a DC link. However, the fact that there is only one provider in the market able to provide the power electronics required for such implementation, raises the risks of this implementations[5].

6.2.2 Balance of Plant (CAPEX)

[51] shows CAPEX costs for the Balance of Plant, which are decomposed into:

- Development cost

[4] $990/kW found in `https://about.bnef.com/blog/2h-2017-wind-turbine-price-index/`.

[5] From conversations at the first meeting of the Steering Committee for the North Sea Energy Hub, which the author of this research attended.

- Project Management
- Substructure and foundations
- Port and staging, logistic and transportation
- Electrical Infrastructure (both offshore and onshore substation, cables, components, etc)[6].
- Assembly and installation (for both electrical components and WT itself)

In addition to these items, cases 2.1 and 3.1 (referring to ADO-WTs storing energy in form of hydrogen) also include the following cost items:

- Electrolysis system
- Tank storage aboard ADO-WTs
- Offshore terminal (only for 3.1)
- Onshore terminal with a tank storage
- Pier System
- CAPEX hull and propelling system for Hydrogen

Due to lack of detailed data, cases 2.2 and 3.2 (referring to ADO-WTs with Li-ion batteries ESS) include less cost items regarding the ESS costs:

- Power Conversion System for Li-ion Battery ESS
- Storage System for Li-ion Battery ESS
- Pier System
- CAPEX hull and propelling system for Lithium

Case 1 is defined exactly as the BFOWT case in [51]. For cases 2 and 3 some assumptions were made in order to adapt values found in the report.

For both whole cases 2 and 3 (i.e., 2.1, 2.2, 3.1 and 3.2), Development costs and Project Management were assumed to be the same as in the reference case (case 1), which are \$150/kW and \$76/kW, respectively; because in a far future –with ADO-WTs being a mature technology– it is believed that it would not imply neither more nor less engineering and management hours.

[6]This is broken down as onshore and offshore substations, Array cables and export cables. Regarding this cost item, case 2.1 only considers a pipeline estimated through the cost of the export cable; case 2.2 accounts for every component except from the array cables; case 3.1 does not account for any cost and case 3.2 accounts for the Electrical Infrastructure costs from the onshore wind farm in [51].

Substructure and foundations costs were assumed to be 0 for both whole cases, since this will be accounted through the hull costs. Notice that the substructure for the offshore substation is accounted through the electrical infrastructure.

Port and staging, logistic and transportation was assumed to be the same as in Bottom-Fixed ($56/kW) for both whole cases, assuming that it represents the transportation of all the components to port. Notice that even for case 3, it is assumed that every component would be assembled on shore, even though there would be no human operation offshore during the installation costs.

From conversations with David Johnsen from COP, it is known that conventional WTs are normally connected in a long string with the first turbine connected to the substation. Behind the first turbines, the array can be routed in many ways, as long as the capacity of the line does not exceed the 70-90MW limit –for a 66kV line–. Thus each string would cluster 16 WTs, having therefore 6-7 intra-array cables for the whole wind farm. The distance between each WT is found as a compromise between the wake they create between each other –causing a decrease revenue due to the capacity factor decrease– and the cable costs, which increases with the distance between WTs –to minimize the wake effect–. This distance is approximately 8 times de diameter of the WT (which is 128m for the studied case). The Electrical Infrastructure is broken down at [10] into substation costs (9/17), array cable costs (2/17) and export cable costs (6/17). Moreover, it is assumed that clusters of 20 ADO-WTs would discharge electricity to the substation or offload hydrogen to the terminal at a time, for a wind farm of 100 ADO-WTs, due to economies of scale it is assumed that this would cause a reduction of 70% of the costs, instead of 80%. In case 2.1 a pipeline is installed to transport liquefied hydrogen from the offshore terminal to the onshore, both terminal costs become a cost item accounted in the ESS cost balance sheet and no array cables exist. Moreover, transporting gas is approximately 20 times cheaper than transporting electricity [44]. Therefore a $\frac{9+2}{17}$ is subtracted from the reference item, and the result is divided by 20, which leads to $20/kW; because only a fraction of the whole ADO-WTs wind farm would offload at a time and due to economies of scale, this value is multiplied by 0.7 which gives a final value of $6/kW and $29,276 per ADO-WT accounting for the pipeline. In case 2.2 an export cable is installed connecting the offshore discharging substations and the onshore substation, therefore only the array cables cost was subtracted from the reference item cost and the 70% of it was calculated. This leads to $293/kW and $801,667 per ADO-WT, accounting for both substations –offshore and onshore– and the export cable. For the same reasons of case 2.1 in addition to the fact that in case 3.1 there is no pipeline, the Electrical Infrastructure costs were set to zero. In case 3.2, the discharging substation would be onshore, therefore the value was taken from onshore balance sheet from [51], which is $160/kW and applied the 70%, which leads to $48/kW and $240,000 per ADO-WT.

Assembly and installation costs were assumed to be as in onshore wind balance sheet for the whole case 3, this is $49/kW and $245,000 per ADO-WT. Notice that even though hull & propelling system plus the ESS would need to be installed –whereas in onshore wind farms this does not exist–, neither foundation on land nor roads, or electrical connections between WTs would be deployed. It is assumed that

a third of this costs represents the installation of both hull & propelling system and the storage, that is \$16.3/kW. In whole case 2, assembly and installation costs were estimated by summing 50% of the reference (\$288/kW from case 1) because ADO-WT would not be assembled offshore and only the discharging substation would be installed offshore, plus the assembly costs of the hull & propelling system plus the ESS; this leads to \$160/kW and \$800,000 per ADO-WT.

Finally, the pier system was estimated as follows: Costs of offshore and onshore substation was obtained as 9/17 of Electrical Infrastructure (\$1106/kW) based on [10] cost breakdown, leading to \$585.5/kW. Onshore substation costs (\$160/kW) were subtracted, which leads to \$425.5/kW. Notice that these are already uninstalled costs so no installation factor needs to be deducted. The difference between offshore substation costs and onshore substation costs is \$265.5/kW, which is assumed to account for the whole offshore structure. Assuming that the pier would require the equivalent of 20% of that structure, this lead to a pier system costs of \$53.1/kW. Only 20 piers are assumed to be installed for the whole wind farm of 100 ADO-WTs, thus 20% of that costs leads to a final costs for the pier system of \$10.6/kW; no economies of scale apply because the whole terminal would be the sum of the pier and the terminal itself.

6.2.2.1 and 6.2.2.2 show the assumptions made to account for Hull & propelling system and ESS costs, respectively.

6.2.2.1 Hull and Propeller System (CAPEX)

Both hull and the propelling system costs were calculated following the indications of Manuel Ventura [7]. Hull costs were calculated as:

$$C_{hull} = LW \times C_{steel} \times (1 + f_{installation}) \tag{6.2}$$

Where LW is the *lightweight*, assuming that the weight of the machinery is negligible compared with the hull weight. Notice that this might not be true, in which case LW should be reduced to account only for the mass of the hull –i.e., without the propelling system–. Read 5.1.1 for the definition of *lightweight* and 5.1.2 to understand how the hull was designed. C_{steel} is the price of steel (910.8 2017USD/tonnes) inflated from [55] as indicated by the professor. $f_{installation}$ is the installation factor, which was assumed to be 1. Which means that the cost of steel is accounted twice, for the material itself and for labour costs. In addition, notice that lightweight is different for ADO-WTs with hydrogen ESS or Li-ion batteries ESS. In fact, LW for ADO-WTs based on hydrogen is 2,187.4 tonnes whereas ADO-WTs based on Li-ion batteries is 29,627.0 tonnes. Using this approach, the hull cost of Li-ion based ADO-WTs is approximately 13.5 higher than hydrogen's –penalizing enormously the low energy

[7] Manuel Ventura has a PhD. in Naval Architecture, by the Technical University of Lisbon (2005) and a MSc. in Naval Architecture issued by the University of Glasgow (1996). He holds a degree in Naval Engineering by the Technical University of Lisbon (1982) and a degree in Mechanical Engineering by the Instituto Superior Técnico (1978).

density of Li-ion batteries compared with hydrogen ESS–. Moreover, as commented in 5.1.2, the hull was over-sized which means that hull cost might be smaller.

The propelling system cost is calculated using the approximation proposed by the professor:

$$C_{propel} = 1.6 \times (\frac{P_{propel}}{100})^{0.82} \times C_{machinery} + 1600 \times (\frac{P_{propel}}{100})^{0.6} \times C_{labour} \quad (6.3)$$

Where P_{propel} is the power of the propelling system. It is assumed to be 5,000 kW, since results from the power loss model shown that the power would be always below 5MW if the boat moves at optimal speed (i.e., to avoid losing power, remember that the wind turbine is 5MW). $C_{machinery}$ is the machinery unitary cost which was assumed to be twice as the slow-speed diesel engine including shaft line plus propeller given by Manuel, because the propelling system would need to be autonomous and precise to move to the best wind locations; however, more research should be carried out to find a more precise value. Finally,C_{labour} represents the cost of man/women hours set to 29.426 2017USD/h inflated from values given by Manuel Ventura.

The final cost of the hull & propelling system was the sum of both propelling system and hull costs, increased a 10% for general expenses.

Therefore, total CAPEX for Hydrogen based ADO-WTs is 4,982,184 2017USD and for Lithium 59,964,557 2017USD, being the latter 12 times higher than the former, due to the difference in energy density from each technologies. Thus, the extra weight of Li-ion ADO-WTs solution represents a huge disadvantage for the hull and propelling initial investment, independently from ESS costs.

6.2.2.2 Energy Storage System (ESS CAPEX)

ESS CAPEX were computed differently for each technology. The reason is that more accurate data was found for hydrogen thanks to last year's publication from researcher from Centrale Nantes in France.

Both cases 2.2 and 2.3 (i.e., ADO-WTs with Li-ion batteries), have same cost regarding the storage. It was computed as the sum of the Power Conversion System and the Energy Storage cots as in [25]. Power conversion costs –expressed in USD/kW– were multiplied by the power of the WT (i.e., 5,000kW) and the storage system costs –expressed in USD/kWh– were multiplied by the storage size set to 2,400,000 kWh for both technologies (20 days producing at 5MW rated power under ideal conditions). For Li-ion Battery ESS, Power Conversion System costs are 348.90 2017USD/kW ($1,744,505 per ADO-WT) and Storage System 680.4 2017USD/kWh ($1,633,030,393 per ADO-WT) [25].

Regarding cases 2.1 and 3.1, several literature was found. In general, overall costs of ESS were mainly found as the sum of the cost of the electrolyser and the costs of storing hydrogen (such as Power Conversion costs and Storage System costs, for lithium-ion batteries):

- Regarding Power Conversion, there are commercially two available processes for water electrolysis: alkaline electrolysis cells (AEC) and polymer electrolyte

membranes (PEMEC); while solid oxide electrolyzer cell (SOEC) offers the possibility of high efficiency but are still at a development stage [56]. According to [25], costs for SOEC plants in 2020 will be 590 €/kW. However, in the same paper and in the corrigendum published a year later from the same authors, a higher value is shown without specifying which electrolyser technology is used, this value is 2395 EUR/kW for both [25, 57]. According to [56], current capital costs for electrolysers are $1300 per kW for AEC and $2500 per kW for PEMEC, although these are declining rapidly [56]. Moreover, 30% of P2G pilot plants globally use PEMEC, whose prices are likely to fall to those of AEC by 2030. Danish Energy Agency and Energinet forecast a cost by 2050 of 400 €/kW for both PEMEC and SOEC whereas 500 €/kW for AEC both in EUR2015 [8]. Finally, according to [5], long term electrolyser is 600€/kW.

- Regarding Storage System costs, [57] presents 399 EUR/kWh. A value way higher than the one derived from [5] which presents long term costs of 56€/kg excluding installation costs –accounted in the assembly and installation cost item–, leading to 5.6 €/kWh with the energy density found in [25]. Other sources such as the report from NREL [58] also present lower values closer to the used by [5].

However, as justified in 6.1, values and reasoning from [5] are used for this analysis. Costs are assumed to be in EUR2017 since the paper was initially delivered in December 2017 to Elsevier, therefore costs are converted to USD2017 to be consistent with the rest of of the analysis. For cases 2.1 and 3.1, Capital Expenditures are divided into: electrolysis system costs, tank storage aboard ADO-WTs, offshore terminal –for case 2.1–, onshore terminal and tank storage at the onshore terminal. Notice that the extra costs associated with the transportation of hydrogen from the terminal to shore are accounted through the pipeline.

Both cases 2.1 and 3.1 have same CAPEX, the only difference is pipeline costs already accounted in "Electrical Infrastructure" cost item. Thus:

- Long term electrolysis system costs is 600€/kW [5], neglecting double desalination of sea water using reverse osmosis for achieving highly purified water, as done in [5]. Assuming that the power of the electrolysis would be as the rated power of the wind turbine, this leads to 3MEUR2018.

- Long term aboard storage costs without installation costs are 56€/kg [5] of the total capacity of the storage, which is 2400MWh per ADO-WTs; for an energy density of 10kWh/kg [25]), this represents 240,000 kg, translating into a final value of 17.472 MEUR2017 per ADO-WT. Note that installation costs are included through assembly and installation costs item.

[8] From the Datablade for produktion af fornybare brændstoffer - juni 2017 - Opdateret februar 2019, which can be found online at: `https://ens.dk/service/fremskrivninger-analyser-modeller/teknologikataloger/teknologikatalog-fornybare`.

- Offshore terminal costs without pier: It was estimated using the same reasoning applied to estimate the pier costs. Costs of offshore and onshore substation was obtained as 9/17 of Electrical Infrastructure ($1106/kW) based on [10] cost breakdown, leading to $585.5/kW. Onshore substation costs ($160/kW) were subtracted, which leads to $425.5/kW. The difference between offshore substation costs and onshore substation costs is $265.5/kW, which is assumed to account for the offshore structure costs. Since only 20% of the total capacity would be installed, this leads to a final cost of $53.1/kW and $265.5 per ADO-WT.

- Storage at onshore terminal costs are 25€/kg for 3,500 m^3 for Horton spheres [5] including the offshore substructure; notice that 240,000kg of hydrogen equals 3,387m^3 of liquid hydrogen and therefore 20 Horton spheres would represent slightly more than a 20% of the total energy storage capacity of the 100 ADO-WTs. Therefore, an onshore terminal with 20% of the total capacity carried by the whole fleet comprising the wind farm would have a total of 1.2 MEUR2018 per ADO-WT.

- Onshore terminal Costs: It is assumed to be 20% of the onshore substation, which leads to $32/kW and $160,000 per ADO-WT.

This leads to a total CAPEX of 21,954,059 USD2017 per ADO-WTs for case 2.1 and 21,475,668 USD2017 for case 3.1. Compressed gas was discarded since uninstalled long term costs of storing aboard are 360€/kg for the long term including installation costs [5], leading to 103,775,040 USD2017 which is one order of magnitude greater than the whole cost of the liquefied system.

Regarding the replacement of the ESS, it is assumed that neither Li-ion batteries nor hydrogen ESS wouls be replaced. This is due to the fact that ESS lifespan is seemed to be greater than the rest of the ADO-WT system for both technologies considered. In the worst case scenario found in literature, Hydrogen ESS has a lifespan of 1000 cycles (Table 4.2) and each cycle would last at least 40 days (Table 4.4), which means that it would last almost 110 years. Li-ion batteries ESS has at least 1500 cycles of lifespan (Table 4.2) and each cycle would last 22.22 days or more (Table 4.4), which means more than 90 years. However, it was not found other applications of Li-ion batteries or hydrogen with such long cycles; perhaps they would need to be replaced once during each lifespan.

6.2.3 Financial Costs (CAPEX)

Financial costs –found in [51]– are subdivided in:

- Insurance during construction
- Decommissioning bond
- Construction financing

- Contingency
- Plant commissioning

Case 1 had same values as in BFOWT from [51].

Case 2 and 3 have been calculated assuming that operations onshore would decrease costs enormously. Case 2 has considered half the costs of BFOWT for Insurance during construction, Decommissioning bond, Construction financing and Plant commissioning, whereas case 3 has considered 20% of BFOWT costs. This is due to the fact that, case 2 will still have to commission and decommission the discharging offshore substation –i.e., workers would operate offshore–, however, in case 3 all the operations involving commission and decommission –and most of O&M– will be completed onshore, with less risks, cost overrun, etc. However, contingency was assigned 75% and 50% of BFOWT to cases 2 and 3, respectively. Costs are envisioned for an scenario where ADO-WTs would be consolidated as a mature technology. Among others, ADO-WTs present the advantage of being independent one from each other. Thus, in a scenario where the technology works normally, an unexpected fault would cause the temporary shut down of one of the turbines, whereas for BFOWT, a fault in the cable string connecting for instance 16 WTs, would cause the shut down of the whole cluster; which means that this cable will be oversized finding a compromise between risk and extra costs for dimensioning it. Even more extreme is the export cable –or LH2 pipeline–, which would still appear in case 2, but not in case 3.

Summed up, case 1 has $690/kW which means a total of $3,450,000 per ADO-WT. Case 2 has $414.75/kW and $2,073,750 per ADO-WT. Case 3 has $221.7/kW and $ 1,108,500 per ADO-WT.

6.3 OPEX

This sections explains the assumptions taken and shows the main values regarding the Operational Expenditures for all 5 cases. OPEX costs are divided in Wind Farm OPEX, Hull and propelling system OPEX and ESS OPEX.

6.3.0.1 Wind Farm. OPEX

Firstly, this section presents a brief introduction of how offshore wind farms are currently operated. Lack of data made it impossible to use the information presented below to perform a better estimation, however, it helps to have an overall picture of how Offshore O&M works and the advantages associated with ADO-WTs technology. Secondly, calculations and assumptions carried out for estimating OPEX for cases 2 and 3 are shown.

Currently, operational decisions are made on a daily basis by the site marine coordinator. Offshore wind farms O&M are mainly completed by two types of vessels called: Service Operational Vessels (SOVs) and the Crew Transfer Vessels (CTVs).

Most of the CVTs are limited to sea conditions [9]. SOVs are larger vessels that can operate in more difficult conditions than CTVs, they can remain at sea and provide accommodation for technicians and storage for their equipment. SOVs –or 'walk-to-work' ships as they have become known– are larger and more expensive but can remain at sea for long periods, provide accommodation for wind farm technicians, have significant storage space for equipment, and usually transfer workers to turbines [10]. In addition, further offshore with larger capacity turbines has changed the operational model for vessel support. SOVs and helicopter support is becoming more common, reducing the need for Crew Transfer Vessels (CTVs) [11].

Moreover, citing other sources, [51] ensures that OPEX vary between projects mainly due to the distance from the wind farm to the maintenance facilities and the meteorological ocean climate at the site. However, as already commented, this was not taken into account in this analysis, since no mathematical expression was found to calculate O&M as a function of distance to shore or water depth.

OPEX costs are generally expressed in two categories: fixed O&M costs (e.g., scheduled plant maintenance or land lease costs for onshore wind farms) and variable O&M costs (e.g., unscheduled plant maintenance) [51]. However, for simplifying or lack of data, many reports include it together as a fixed-cost term making it very difficult to disaggregate operations and maintenance costs. In fact, the most accurate report found [51] gives a single OPEX for onshore wind farms, and two OPEX (for Operations and Maintenance, separately) for BFOW and floating farms.

FOW and BFOW have same operation costs ($31/kW/year) because they have the same annual leases and fees [51]. Therefore, operations expenditures were assumed to be 31 $/kW/year (2017 USD) for all three cases.

However, maintenance expenditures differ between BFOW and FOW because they utilize a different maintenance strategy (i.e., in situ versus tow-to-shore), resulting in $127/kW/year for the fixed-bottom project and $93/kW/year for the floating project [51]. It was assumed that maintenance expenditures include both scheduled and unscheduled maintenance of the whole wind farm, comprising the whole WT system (i.e., blades, nacelle, generator, tower, step-up transformer, etc.), foundation and the whole offshore substation and cabling. Thus, for the case 1 (BFOWTs with offshore substation) maintenance was set to be 127 $/kW/year (2017 USD).

Maintenance expenditures of the wind farm for whole case 2 (ADO-WTs with discharging substation offshore) were assumed to be half of floating wind farm maintenance costs, because only the substation would have same maintenance costs as floating wind farm since ADO-WTs would go to shore *self-towed-to-shore* to be inspected and only an unexpected fault in ADO-WTs propulsion system may require the

[9] Found in `https://www.4coffshore.com/windfarms/an-introduction-to-crew-transfer-vessels-aid2.html`.

[10] Found in `https://www.owjonline.com/news/view,innovative-vessels-bridge-gap-between-ctvs-and-sovs_55757.htm`.

[11] Visit `https://ostensjo.no/fleet/eddamistral/` to see the characteristics of Edda Mistral the SOV that will soon be used in Hornsea 1.2GW wind farm, the biggest in the world, 24h a day 365 days a year during the whole lifespan of the wind farm

unit to be externally towed to shore like floating WTs (and O&M of the hull system would prevent this). This gives a final number of 27.5 $/kW/year for maintenance of the whole wind farm for whole case 2.

Maintenance expenditures of the wind farm for whole case 3 (ADO-WTs with discharging substation onshore) were assumed to be as in onshore wind farms since ADO-WTs would be *self-towed-to-shore* to be inspected and the substation is already on land. However, O&M is not disaggregated for onshore wind farms in [51]. Thus, by calculating the share of maintenance expenditures in respect to the whole O&M from case 2 (i.e., $27.5/(27.5+31) = 0.47$) and multiplying it to the whole O&M value found for onshore wind farms (i.e., $43.6/kW/year), a final value of 20.5 $/kW/year (2017 USD) was found and set as maintenance costs for case 3.

Finally, as commented, ADO-WTs would have extra OPEX compared with conventional BFOWT due to the hull & propelling system and the energy storage system which are explained in sections 6.3.0.2 and 6.3.0.3, respectively. In addition, it is believed that an extra capacity factor would cause higher CAPEX, however, for this degree of detail it was nearly impossible to compute.

6.3.0.2 Hull and Propeller System (OPEX)

In a first attempt to estimate hull & propelling system costs values found in [52] were used. However, these annual costs were of the same order of magnitude than the initial investment for the whole hull & propelling system. Therefore, OPEX was assumed to be 5% of the whole hull & propelling system CAPEX.

6.3.0.3 Energy Storage System (ESS OPEX)

Li-ion batteries ESS has a fixed O&M cost of 2.9 2017USD/kW/year and variable O&M costs of 0.0006 2017USD/kWh [25]. Variable costs –only for Li-ion batteries– are multiplied by the AEP (in kWh/year) obtained from the WEYA model. Whereas fixed costs are multiplied by 5,000kW. Thus, for both cases 2.2 and 3.2 fixed O&M costs of Li-ion batteries ESS are $14,477/year whereas variable O&M costs are $15,600 per year.

According to [25], hydrogen ESS fixed O&M costs are 23.16 2017USD/kW/year; for both cases 2.1 and 3.1 fixed O&M costs of hydrogen ESS would be $115,818/year. Moreover, [25] affirms that hydrogen ESS has no variable OPEX, which matches [56] who states that electrolysis systems variable costs are governed by the electricity source (zero for ADO-WTs on this regard). According to [5], liquefaction costs are 0.55€/kg and offloading operations at the terminal can be assumed to be as in LNG terminals; however ADO-WTs would have their own renewable source of electricity and thus, for both cases 2.1 and 3.1 liquefaction costs would be zero; notice that this would affect revenues though, which is one of the drawbacks of ADO-WTs. Storage aboard O&M costs are 1% of the storage CAPEX [5], this would lead to $175,841/year for both cases 2.1 and 3.1. Therefore, OPEX for hydrogen ESS was set to the mean of both values, which lead to $145,829/year.

6.4 Costs Analysis. Results and discussion

This section presents results: CAPEX, OPEX and LCOE for each case and cost breakdown by cost item. Moreover, LCOE results are compared with other studies and cost targets for Hull & Propelling system as well as ESS are established.

6.4.1 LCOE results

Table 6.1 presents CAPEX, OPEX, AEP, FCR and LCOE results for each case.

CAPEX per wind turbine (WT) representing the whole wind farm associated costs are: 22.68 millions of USD2017/WT for case 1 (a BFOW conventional wind farm with offshore substation); 38.94 MUSD2017/WT for case 2.1 (ADO-WTs wind farm with an offshore terminal at which ADO-WTs would offload liquefied hydrogen (LH2) stored aboard, which would be transported through a LH2 pipeline to an onshore terminal), 36.90 MUSD2017/WT for case 3.1 (ADO-WTs wind farm with an onshore terminal at which ADO-WTs would directly go to offload LH2), 1,708.17 MUSD2017/WT for case 2.2 (ADO-WTs wind farm with an offshore substation at which ADO-WTs would discharge electricity stored on Li-ion batteries installed aboard, which would be connected through an export cable to the onshore substation) and, finally, 1,705.43 MUSD2017/WT for case 3.2 (ADO-WTs wind farm with an onshore substation at which ADO-WTs would directly discharge electricity stored on Li-ion batteries installed aboard).

OPEX per WT are: 790,000 2017USD/WT for case 1, 687,439 2017USD/WT for case 2.1, 652,417 2017USD/WT for case 3.1, 3.32 millions of 2017USD/WT for case 2.2 and 3.29 millions of 2017USD/WT for case 3.2.

AEP for case 1 is 26,914 MWh/WT, which represents a capacity factor of 61.45% and 32,563 MWh/WT, which represents a capacity factor of 74.35% for the rest of the cases. As commented, case 2 may represent higher capacity factor than case 3, since ADO-WTs could go further offshore to harvest wind power as explained in [5].

With these values, and for a common fixed charge rate (FCR) of 7%, LCOE results, using Eq. (6.1), are: 88.34 $/MWh for case 1, 104.81 $/MWh for case 2.1, 99.37 $/MWh for case 3.1, 3,774.08 $/MWh for case 2.2 and 3,767.10 for case 3.2.

	Case 1	Case 2.1	Case 2.2	Case 3.1	Case 3.2
CAPEX (MUSD2017)	22.68	38.94	1,708.17	36.91	1,705.43
OPEX (MUSD2017/year)	0.79	0.69	3.32	0.65	3.29
AEP (MWh)	26,914	32,563	32,563	32,563	32,563
FCR (%)	7%	7%	7%	7%	7%
LCOE (USD2017/MWh)	88.34	104.81	3,774.08	99.37	3,767.10

Table 6.1: LCOE calculations and results for each case.

6.4.2 Cost Breakdown -results

6.4.2.1 Case 1 Cost Breakdown Results

Figure 6.1 shows the CAPEX for case 1, a conventional wind farm with offshore substation. Turbine capital costs –in blue– account for 34% of the whole initial investment. BoP –in warm colours– accounts for 50%, whereas financial costs –in green– account for 15%.

OPEX for case 1 is subdivided into General Operations (19.6%) and General Maintenance (80.4%).

6.4.2.2 Case 2.1 Cost Breakdown Results

Figure 6.2 shows the CAPEX for case 2.1, ADO-WTs wind farm with an offshore terminal where ADO-WTs would offload liquefied hydrogen (LH2) stored aboard, which would be transported –through a LH2 pipeline– to an onshore terminal. Turbine capital costs –in blue– account for 20% of the whole initial investment. BoP –in warm colours– accounts for 75%, whereas financial costs –in green– account for 5%. Balance of Plant (BoP) includes: LH2 tank storage aboard which accounts for 42% of the total CAPEX, Hull & Propelling System (13%), Electrolyser (9%) and the LH2 storage onshore (4%); the rest of BoP cost items share 2% or less of the total CAPEX

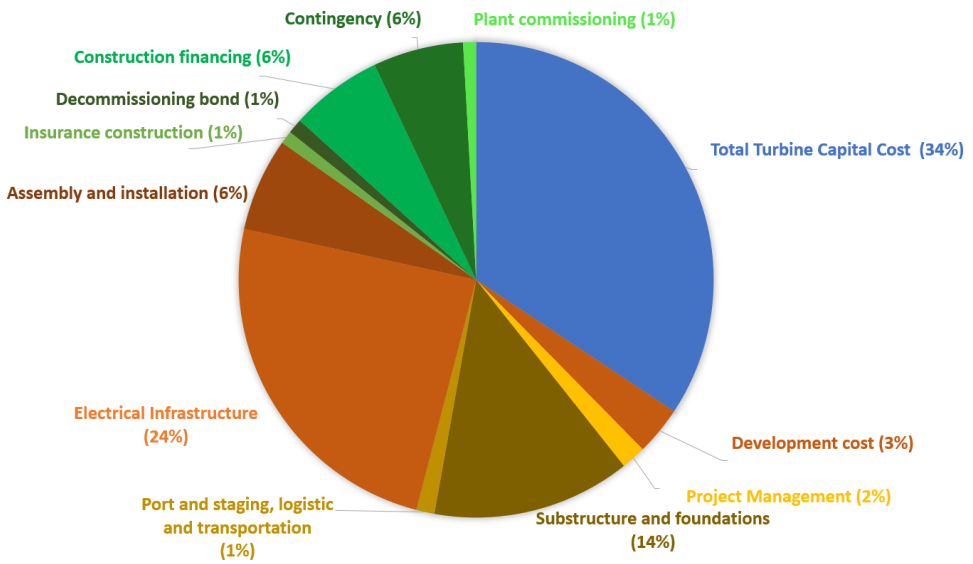

Figure 6.1: CAPEX case 1: BFOWTs with offshore substation.

(to highlight, the offshore terminal accounts for 1.43%, the LH2 pipeline accounts for 0.08% and the onshore terminal 0.74%).

OPEX for case 2.1 is subdivided into General Operations (23%), General Maintenance (20%), O&M of Hydrogen ESS (21%) and O&M of Hull & Propelling System (36%), see Figure D.1 in Appendix D.

6.4.2.3 Case 2.2 Cost Breakdown Results

In case 2.2 (see Figure D.2 in Appendix D), ADO-WTs wind farm have an offshore substation where ADO-WTs would discharge electricity stored on Li-ion batteries installed aboard, which would be connected through an export cable to the onshore substation. BoP –in warm colours– accounts for 99.4%, whereas financial costs –in green– account for 0.1%. Individually, Li-ion batteries aboard account for the major share of the CAPEX (95.6%), Hull & Propelling System accounts for 3.5%, the turbine accounts for 0.4% and all the rest represents 0.3%.

OPEX for case 2.2 is subdivided into General Operations (5%), General Maintenance (4%), O&M of Li-ion batteries (1%) and O&M of Hull & Propelling System (90%), see Figure D.3 in Appendix D.

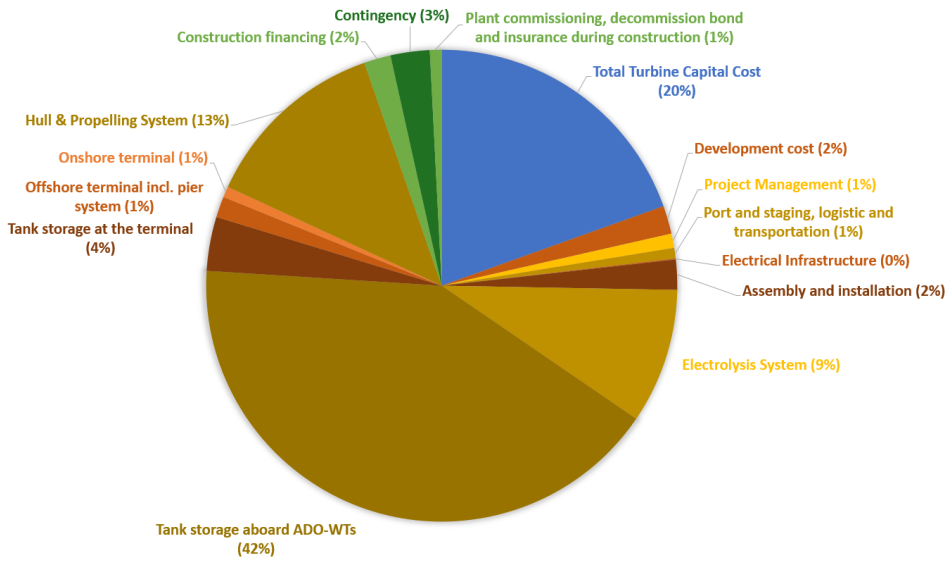

Figure 6.2: CAPEX case 2.1: LH2 ADO-WTs with offshore terminal.

6.4.2.4 Case 3.1 Cost Breakdown Results

Figure 6.3 shows the CAPEX for case 3.1, ADO-WTs wind farm with an onshore terminal at which ADO-WTs would directly go to offload LH2. Turbine capital costs –in blue– account for 21% of the whole initial investment. BoP –in warm colours– accounts for 76%, whereas financial costs –in green– account for 3%. Balance of Plant (BoP) includes: LH2 tank storage aboard which accounts for 44% of the total CAPEX, Hull & Propelling System (14%), Electrolyser (10%) and the LH2 storage onshore (4%); the rest of BoP cost items share 2% or less of the total CAPEX (to highlight, the onshore terminal accounts for 0.78%).

OPEX for case 3.1 is subdivided into General Operations (24%), General Maintenance (16%), O&M of Hydrogen ESS (22%) and O&M of Hull & Propelling System (38%), see Figure D.4 in Appendix D.

6.4.2.5 Case 3.2 Cost Breakdown Results

In case 3.2 (see Figure D.5 in Appendix D), ADO-WTs wind farm have a substation onshore at which ADO-WTs would directly discharge electricity stored on Li-ion batteries installed aboard. BoP –in warm colours– accounts for 99.5%, whereas financial costs –in green– account for 0.1%. Individually, Li-ion batteries aboard account for the major share of the CAPEX (95.9%), Hull & Propelling System accounts for 3.5%, the turbine accounts for 0.4% and all the rest represents 0.2%.

OPEX for case 3.2 is subdivided into General Operations (5%), General Maintenance (3%), O&M of Li-ion batteries (1%) and O&M of Hull & Propelling System

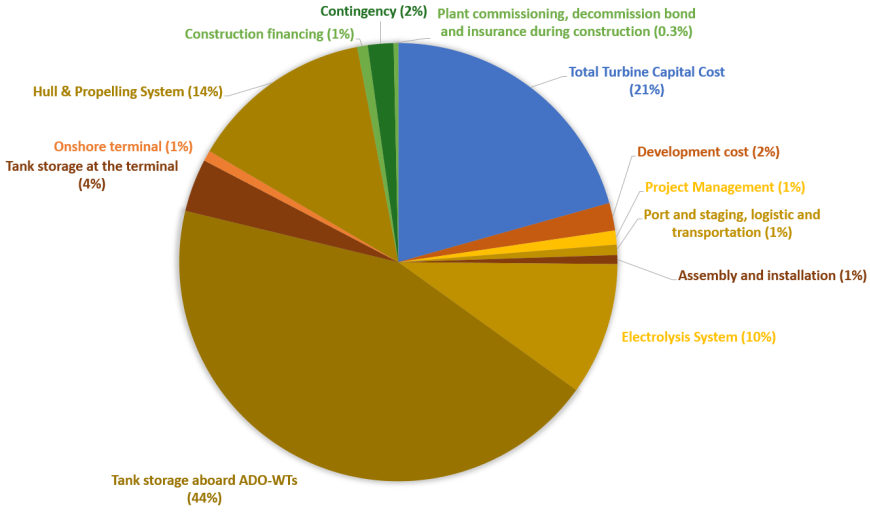

Figure 6.3: CAPEX case 3.1: LH2 ADO-WTs with onshore terminal.

(91%), see Figure D.6 in Appendix D.

6.4.3 Costs - Discussion

LCOE results are compared with LCOE found in prestigious publications: "2017 Cost of Wind Energy Review" from the National Renewable Energy Laboratory (NREL) [51] –which was used to estimate most of the costs–, "Renewable Power Generation Costs in 2017" from the International Renewable Energy Agency (Irena) [59] and "Unleashing Europe's offshore wind potential" from the BVG Associates Limited [8].

The LCOE obtained for case 1, \$88.34/MWh is lower than the LCOEs found in [51] for both BFOW (\$124/MWh) and FOW (\$146/MWh). Costs items for case 1 were taken directly from [51] with no modification, which led to having the same CAPEX in case 1 as in BFOW from [51]. However, the reason of having a lower LCOE is that the capacity factor obtained form WEYA model is much higher than the one used in NREL [51]: 42.7% for BFOW and 42.6% for FOW; whereas it is 61.45% for case 1 obtained from the Conventional model form WEYA. This means that for the same costs, case 1 would produce more energy, lowering the LCOE. It is believed that costs estimated for case 1 in this research are too low, because the location of the wind farm would require greater expenditures on export cable, among others. Notice that it was decided to use values from BFOW since it is the technology consolidated in the market and it represents a more solid reference, to date. Moreover, the capacity factor for FOW might be too conservative in [51], since during the first month, the only commercial floating offshore wind farm in the world achieved a capacity factor of 65% (please read 2.2).

Regarding cases 2.1 and 3.1, both of them also present lower LCOE values (104.81% and 99.37%, respectively) than the ones from [51], even though CAPEX are M\$16.24 and M\$14.23 greater than in [51], respectively. The reason of this difference is, on the one hand, the decrease in OPEX estimated for LH2 ADO-WTs, which is \$100,000/year and \$140,000/year lower, respectively, comparing with OPEX from case 1; and, on the other hand, and especially, the greater AEP from cases 2.1 and 3.1: both having a capacity factor of 74.35%, which leads to 14,398 MWh more every year (almost 80% more energy every year). Deeper research should be carried out to calculate the Levelised Cost of Hydrogen generation and compare it with current results, such as the ones presented in [5, 60].

LCOE for cases 2.2 and 3.2 are completely out of any comparison. LCOE is specially affected by the storage costs of the batteries, which account for almost 96% of the whole CAPEX for both cases 2.2 and 3.2; also, the hull design for ADO-WT carrying Li-ion is much bigger than for LH2 ADO-WTs due to the huge weight of the batteries. To conclude, the low energy density of Li-ion batteries represents the biggest disadvantage of this technology against LH2. Moreover, regarding OPEX, hull & propelling system accounts for approximately 90% of the total OPEX for both cases 2.2 and 3.2. The reason is that such a huge ship requires more O&M, since it is estimated as 5% of the CAPEX for the hull & propelling system, which is much

higher for ADO-WT carrying batteries than LH2 ADO-WTs. However, notice that the source of this extra cost is the much lower energy density from the Li-ion batteries compared with LH2.

Most of the LCOE values presented in [59] are above $100/MWh, from 2020 several LCOE for proposed auctions are between $50/MWh and $100/MWh for wind farms of 400MW or greater. Moreover, [8] projects LCOE values until 2030, foreseeing LCOE values around $60/MWh by 2030. They also publish LCOE estimated for current projects, 3 of which are between $60-$80/MWh, two are between $80-$100/MWh and two more are between $120-$140/MWh. LCOE values obtained in this analysis for ADO-WTs with LH2 are around $100/MWh. ADO-WT would be a expensive technology able to compete with current technologies but would be within the most expensive projects presented in [59] and more expensive than projections seen in [8] for 2030.

Finally, it is observed a certain tendency to reduce the share of the WT cost component among the overall CAPEX while moving further offshore. The wind turbine represents 68% of the total CAPEX in onshore wind, whereas it represents 34% of the BFOW and 27% of the FOW [51]. WTs wind turbine makes up 21% of the total CAPEX for LH2 ADO-WTs —in both cases studies– and less than 0.5% for ADO-WTs carrying Li-ion batteries, which is totally inadmissible. Bear in mind that the source of revenues of this whole system is nothing but the wind turbine. A compromise can be found between having more costs due to components surrounding the WT and the extra energy yielded do to such improvement; however, these extra costs must be compensated by the revenues coming from an increase in the AEP. In an ideal world where ADO-WTs could move around all the seas around the world, this might be very profitable, since the possibility of hunting best wind resources in real time may maximize the AEP.

As a final conclusion regarding the cost analysis, these results should only bring hope and quantitative reasons to keep exploring the proposed technology. More R&D should be carried out to both mature the concept and find more precise results.

6.4.4 Targets for making ADO-WTs competitive

Two main targets are established for Captial Expenditures of both hull & propelling system and the Energy Storage System (ESS). Table 6.2 shows these targets in order to make ADO-WT competitive against Bottom-Fixed Offshore Wind (BFOW) and Floating Offshore Wind (FOW). These targets constitute an initial approach to estimate cost reductions the current state of art should aim at. More accurate data and detailed calculations should be carried out in future works to define definitive goals.

Targets for the hull & propelling system are set as the cost of offshore foundations and substructure from [51] for BFOW ($613/kW) and FOW ($1653/kW). Notice that the cost could be greater and still be competitive, since AEP is greater for ADO-WT due to the moving system; however, as an initial approach this simple reasoning helps to illustrate future research.

Targets for ESS are estimated assuming that they substitute the array cables and export cable from current offshore wind. Notice that if the terminal is set offshore, they would need a pipeline –although it would be cheaper than current export table–; also the substation might be cheaper if it is sized as a fraction of the total capacity available with the whole fleet of ADO-WTs (since they would not discharge at the same time); also inefficiencies should be taken into account in a more accurate calculation. As a first approximation, it is set as the 47% of the Electrical Infrastructure cost item assuming that it represents costs of both export and intra-array cables (the rest is due to the substation costs, please refer to 6.2.2.2 for more information). ESS target is referred to the sum of the Power Conversion System (electrolyser for hydrogen, e.g.) and Storage aboard ADO-WTs; storage at the terminal is not computed here.

Bear in mind that by achieving these targets, ADO-WT may be more competitive that BFOW or FOW, since for a same CAPEX, LCOE would be lower for ADO-WTs due to the greater energy production. A study more in depth must be carried out to confirm this; the study should take into account OPEX and CAPEX for other components, such as the terminal and storage on land, among others.

Tables 6.3 and 6.4 show current costs of hull & propelling system and ESS and the cost reduction required to be competitive, for both LH2 and Li-ion solutions, respectively. All costs are referred to nominal power of the WT (dividing by 5,000kW); cost reduction are also shown as the relative decrease current technology should perform (in percentage). Negative cost reduction means that ADO-WTs do better for such item. The ESS storage costs were calculated assuming a capacity of 2,400MWh.

Results show that LH2 ADO-WTs require a reduction of almost 40% of the current hull and propelling system in order to compete with BFOW current foundations but are 65% cheaper than current floating foundations. Regarding the ESS, LH2 ADO-WTs still have a huge challenge, since costs should be reduced approximately by 86% to compete with either of the technologies.

	BFOW	FOW
Hull & Propelling System	613	1653
Energy Storage System	520.4706	552.9412

Table 6.2: Targets for Hull & Propelling System and ESS to make ADO-WTs competitive against BFOW and FOW.

	ADO-WT LH2	ADO-WT vs BFOW	ADO-WT vs FOW
Hull & Propelling System ($/kW)	996.4	383.4 (38.5%)	-656.6 (-65.9%)
Energy Storage System ($/kW)	3,949.2	3,428.7 (86.8%)	3,396.3 (86.0%)

Table 6.3: Current performance and potential improvement for ADO-WTs storing energy as LH2.

	ADO-WT Li-ion	ADO-WT vs BFOW	ADO-WT vs FOW
Hull & Propelling System (M$/kW)	59.964	59.964 (100.0%)	59.963 (100.0%)
Energy Storage System (M$/kW)	0.327	0.326 (99.8%)	0.326 (99.8%)

Table 6.4: Current performance and potential improvement for ADO-WTs storing energy in Li-ion batteries.

Li-ion would require almost a 100% of cost reduction in both items to be competitive with either of the technologies. Li-ion are clearly much more expensive and this is the reason why this technology does not seem likely to perform well for ADO-WTs. Other concerns related with this technology are the self-discharging performance, which may limit the time ADO-WTs would store the energy, which is believed that should be around 20-40 days in order to reach the far offshore an capitalize the ability to freely move without the need to go to discharge energy with higher frequency.

Hull & Propelling System should be lower than –$/kW in order to compete with bottom-fixed offshore wind power and – $/kW in order to compete with floating offshore wind power.

The whole energy storage system should be lower than –$/kW in order to compete with bottom-fixed offshore wind power and – $/kW in order to compete with floating offshore wind power.

Regarding O&M costs, Hull & Propelling System should not cost more than –$/kW/year in order to compete with bottom-fixed offshore wind power and – $/kW/year in order to compete with floating offshore wind power. Whereas O&M costs of the whole energy storage system should not be greater than –$/kW/year in order to compete with bottom-fixed offshore wind power and – $/kW/year in order to compete with floating offshore wind power.

CHAPTER 7

Conclusions

7.1 Conclusions

This research proposes a *new* R&D branch of offshore wind power. It suppress the constraint of keeping offshore WTs fixed to the sea floor and studies potential benefits this leads to, with an attempt of clarifying whether it is worth it to allocate more time, efforts and resources on this new research area. Certainly, this ADO-WTs have a huge potential that worth it a study more in depth. Moreover, along the way, new questions and potential improvements that could be applied to current WTs are found; perhaps this could be used itself as a methodology of finding new solution to the current state of art.

Three models are developed to quantify the extra energy that one could get from moving WTs; two models describe the proposed technology whereas the third models current *immobile* WTs (either BFOWT or FOWT). These three models are referred to as one called Wind Energy Yield Assessment model (WEYA). Results from simulations implemented in the Southern region of the North Sea shown that a single ADO-WT could have no more than 45% extra AEP than a conventional WT (leading to a capacity factor of 89.24% for the Upper Bound model). A model accounting for the time it takes the ADO-WT to move at 10 knots shown that it could yield 21% more AEP than a conventional WT (a capacity factor of 74.34% for Reachable Area model). Moreover, it is observed that simulating with greater numbers of wind turbines these values increase.

The State of Art of current Energy Storage Systems is reviewed and three technologies are pre-selected as potential technologies suitable to be aboard ADO-WTs: Li-ion batteries, Zinc-air batteries and hydrogen –obtained from electrolysis from water and liquefied and stored aboard–.

WEYA model does not account for the energy it takes to move the whole ADO-WTs. A Power Losses model was implemented for that purpose. Results show that sailing at optimal boat speeds, the wind itself would push the whole system at no energy cost in most of the cases. Moreover, optimal boat speeds for LH2 ADO-WTs do not exceed 9 m/s with the wind and 3 m/s against the wind. A huge potential is found by changing the relative wind speed the wind turbine rotor *perceives*. By targetting the rated wind speed –giving rated power–, more power than current wind turbines could be extracted for the same wind speed. In addition, ADO-WTs would not be shut down until 31m/s, if storing energy in form of hydrogen, without increasing the

loads the WT perceives, because of this principle.

A cost analysis is presented for five cases. First case accounts for current BFOWTs costs, which is used as a reference. Second and third quantify costs from ADO-WTs discharging the energy to an offshore terminal which transports the energy to an onshore terminal for both ADO-WTs storing energy in Li-ion batteries and in form of hydrogen. Forth and fifth quantify costs from ADO-WTs moving to shore to discharge the energy, for both LH2 ADO-WTs and for ADO-WTs carrying Li-ion batteries. Li-ion batteries would not be a cost-effective solution in any case. LH2 ADO-WTs (storing liquefied hydrogen) present the best alternative, offloading LH2 both in an offshore terminal as well as onshore. Conventional offshore wind turbines present an LCOE of \$88.34/MWh, ADO-WTs storing hydrogen an LCOE of \$99.37/MWh if the terminal is onshore and \$104.81/MWh if it is offshore; whereas ADO-WTs storing energy in Li-ion batteries present an LCOE of \$3,767.10/MWh if the discharging substation is onshore and \$3,774.08/MWh if it is offshore.

To conclude, ADO-WTs storing LH2 present certainly good results that worth it a deeper research. A list with future works is presented and a road map is drawn for further R&D.

7.2 Future work proposed

This section lists future research commented along the report; each item is linked to the section where it is introduced, perhaps reading the context helps understanding why this future work is proposed. Future works are focused on ADO-WTs; however, a couple of comments are proposed to the current industry which were found along the way. Finally, a road map summarizes what is believed to be the most important next steps to develop ADO-WTs further. New R&D could try to clarify:

- The Concept
  - Water turbines to slow down the whole ADO-WTs system by extracting energy from the water and keeping ADO-WTs relative wind speed right above rated wind speed (section: 5.2.4).
  - Legislation, permits and market regulations for ADO-WTs (section: 6.1).
- Whole integrated model
  - Integrate WEYA and Power Losses in a whole model accounting for the ESS (losses, when to discharge according to best energy prices and the State of Charge, etc.) (sections: 3.2.6, 3.1.4 and 3.3.4).
  - In the integrated model, study the compromise between sailing at the optimal boat speed –both in module and direction– and the need to move to a certain location (section: 5.2.3). Also, how losses increase when not moving at optimal boat speeds.

  - Wind Energy Yield Assessment model
    - Increase wind turbine size (power) 3.3.2
    - Implement a decision-making algorithm by formulating the optimization problem, finding genetic algorithms, using machine learning techniques, etc. (section: 3.1.4).
    - Find the best configuration of $P\&Q$ parameters for every boat speed (section: 3.2.6).
    - Explore longer time horizons up to 30 years (section: 3.3).
    - Find wind speed areas complementing each other which would not be interesting for current offshore wind but for ADO-WTs (section: 3.3.2).
    - Explore other regions such as the Northern North Sea (section: 3.3.2).
  - Power Losses model
    - A huge concern is the stability of ADO-WTs (sections: 5.1.1, 5.2.1, 5.1.2 and 6.1.2).
    - Future works could focus on modelling more accurately the whole system mass (section: 5.1.1).
    - Implement a more realistic Power Loss model, accounting for wake making losses, propeller performance, etc. (section: 5.2.4).
    - Include wind directions in the Power Losses model (section: 5.1.3).
    - Dynamics of ADO-WTs: transient while changing boat speed, movement traversed (sections: 5.1.3 and VII).
    - Minimizing the whole ADO-WT system mass (section: 5.2.4).
  - Energy Storage
    - ADO-WTs storing energy in form of hydrogen –liquefied– seem to be the better solution, deeper research should be carried out on how to integrate this technology aboard moving ADO-WTs.
    - Model the State of Charge which would determine the need to go to the substations to discharge the energy (section: 4.3.1).
    - Study Zn-Air and Li-ion in more detail to fully discard them (section: 6).

- Cost analysis
  - Have more accurate data and perform feasibility studies using revenues for each energy carrier (section: 6).
  - future works should explore how costs may evolve, specially for the ESS (section: 4.3.2).
  - Define more accurate targets for ADO-WTs components (section: 6.4.4).

  - Optimal design of the number of piers and storage capacity at the terminals (section: 6.1.1.2).

Whereas, regarding the current industry, future research could explore:

- Find a relationship between WT wear –extra O&M– and the capacity factor –extra revenues– (section: 6).
- New type of WTG delivering DC power for offshore wind farms with DC link (section: 6.2.1).

The lean philosophy seems to be the most appropriate approach to research and develop this concept further, the following road map is proposed:

1. **Lean Research** This means, engineering hours of simulation and developing the model further on this stage. No prototype should be built on this stage. Finding collaborations with DTU and companies as well as other universities such as Central Nantes, willing to invest on a very few researchers. At this stage, WEYA should be upgraded including losses and modelling the energy storage system as well as finding the way of utilizing the kinetic energy at speeds higher than the rated wind speed, perhaps with a water turbine. Moreover, both the region and the time horizon should be broaden. After computing losses and operations of charge/discharge from ADO-WTs within the WEYA model, a study of how forecast could affect the energy output should be studied.
2. **Prototype:** If results are good, a first prototype could be build, developing a business model which could capitalize services from having a portable mast which could go ”anywhere in the sea” to collect data which could be used by current offshore wind developers. A solid network should be built within the industry before, during and after this stage.
3. **Further R&D:** some incomes would have come from the previous phase, a lot of new inputs would be assimilated and a more realistic ADO-WTs could be designed. Collaborating with a company a bigger prototype might be built.

Bibliography

[1] IEA, "Co2 emissions statistics," 2018.

[2] etipwind.eu, "Strategic research and innovation agenda 2018," 2018.

[3] CarbonTrust, "Key findings from electrical systems mooring systems, and infrastructure and logistics studies," 2018.

[4] J. Jonkman, S. Butterfield, W. Musial, and G. Scott, "Definition of a 5-mw reference wind turbine for offshore system development," National Renewable Energy Lab.(NREL), Golden, CO (United States), Tech. Rep., 2009.

[5] A. Babarit, J.-C. Gilloteaux, G. Clodic, M. Duchet, A. Simoneau, and M. F. Platzer, "Techno-economic feasibility of fleets of far offshore hydrogen-producing wind energy converters," *International Journal of Hydrogen Energy*, volume 43, number 15, pages 7266–7289, 2018.

[6] W. Europe, "Wind energy in europe in 2018: Trends and statistics," 2019.

[7] ——, "Offshore wind in europe: Key trends and statistics 2018," 2019.

[8] B. Associates Limited, "Unleashing europe's offshore wind potential. a new resource assessment," 2017.

[9] A. Myhr, C. Bjerkseter, A. Ågotnes, and T. A. Nygaard, "Levelised cost of energy for offshore floating wind turbines in a life cycle perspective," *Renewable Energy*, volume 66, pages 714–728, 2014.

[10] D. Energinet, "Technology data for energy plants for electricity and district heating generation," 2016.

[11] H. Stiesdal, "Tetraspar and tetrabase - industrialized offshore wind turbine foundations," 2019.

[12] M. T. Andersen, "Floating foundations for offshore wind turbines," PhD thesis, Ph. D. Thesis, Aalborg University, 2016.

[13] W. Europe, "Floating offshore wind vision statement," 2017.

[14] C. Abi, A. Parry, R. Wakefield, and A. West, "Construction method statement. kinkardine offshore wind farm project," Tech. Rep., 2018.

[15] W. Europe, "Offshore wind in europe: Key trends and statistics 2017," 2018.

[16] A. B. Bauer, "The ancient interface–faster than the wind," *Bauer and Associates, Orange, California*, 1969.

[17] ——, "Sailing al points of the compass," *power*, volume 2, number 3, pages 4–5,

[18] J.-P. Vidal, *System for propulsion of boats by means of winds and streams and for recovery of energy*, US Patent 4,371,346, 1983.

[19] H. Barkla, "The vertical-axis turbine/propeller for ship propulsion," *Wind Engineering*, pages 237–252, 1984.

[20] M. Gaunaa, S. Øye, and R. F. Mikkelsen, "Theory and design of flow driven vehicles using rotors for energy conversion," in *2009 European Wind Energy Conference and Exhibition*, EWEC, 2009.

[21] J.-C. Gilloteaux and A. Babarit, "Preliminary design of a wind driven vessel dedicated to hydrogen production," in *ASME 2017 36th International Conference on Ocean, Offshore and Arctic Engineering*, American Society of Mechanical Engineers, 2017, V010T09A065–V010T09A065.

[22] G. Clodic, J.-C. Gilloteaux, and A. Babarit, "Wind propulsion options for energy ships," 2018.

[23] R. A. Jamil, A. Chaigneau, J.-C. Gilloteaux, P. Lelong, and A. Babarit, "Comparison of the capacity factor of stationary wind turbines and weather-routed energy ships in the far-offshore," 2019.

[24] K.-Y. Oh, W. Nam, M. S. Ryu, J.-Y. Kim, and B. I. Epureanu, "A review of foundations of offshore wind energy convertors: Current status and future perspectives," *Renewable and Sustainable Energy Reviews*, volume 88, pages 16–36, 2018.

[25] B. Zakeri and S. Syri, "Electrical energy storage systems: A comparative life cycle cost analysis," *Renewable and sustainable energy reviews*, volume 42, pages 569–596, 2015.

[26] A. Dewan and M. Asgarpour, *Reference O & M Concepts for Near and Far Offshore Wind Farms*. 2016.

[27] M. O. Hansen, *Aerodynamics of wind turbines*. Routledge, 2015.

[28] A. Saenz-Aguirre, S. Fernandez-Resines, I. Aramendia, U. Fernandez-Gamiz, E. Zulueta, J. M. Lopez-Guede, and J. Sancho, "5 mw wind turbine annual energy production improvement by flow control devices," in *Multidisciplinary Digital Publishing Institute Proceedings*, volume 2, 2018, page 1452.

[29] A. Statoil, "Environmental statement," 2015.

[30] D. Morris, J. Pinnegar, D. Maxwell, S. Dye, L. Fernand, S. Flatman, O. Williams, and S. Rogers, "Over 10 million seawater temperature records for the united kingdom continental shelf between 1880 and 2014 from 17 cefas (united kingdom government) marine data systems," *Earth System Science Data*, volume 10, pages 27–51, 2018.

[31] M. Aneke and M. Wang, "Energy storage technologies and real life applications–a state of the art review," *Applied Energy*, volume 179, pages 350–377, 2016.

[32] "Energy storage systems—characteristics and comparisons," *Renewable and Sustainable Energy Reviews*, volume 12, number 5, pages 1221 –1250, 2008.

[33] T Kousksou, P Bruel, A Jamil, T El Rhaf iki, and Y Zeraouli, "Energy storage: Applications and challenges," *Solar Energy Materials and Solar Cells*, volume 120, pages 59–80, 2013.

[34] F. Díaz-González, A. Sumper, O. Gomis-Bellmunt, and R. Villafáfila-Robles, "A review of energy storage technologies for wind power applications," *Renewable and sustainable energy reviews*, volume 16, number 4, pages 2154–2171, 2012.

[35] A. Basile and A. Iulianelli, *Advances in hydrogen production, storage and distribution*. Elsevier, 2014.

[36] Eurostat, "Greenhouse gas emission statistics - emission inventories 2019," 2019.

[37] K. Divya and J. Østergaard, "Battery energy storage technology for power systems—an overview," *Electric power systems research*, volume 79, number 4, pages 511–520, 2009.

[38] A. A. Akhil, G. Huff, A. B. Currier, B. C. Kaun, D. M. Rastler, S. B. Chen, A. L. Cotter, D. T. Bradshaw, and W. D. Gauntlett, "Doe/epri electricity storage handbook in collaboration with nreca," *Sandia national laboratories*, 2015.

[39] T. Mahlia, T. Saktisahdan, A Jannifar, M. Hasan, and H. Matseelar, "A review of available methods and development on energy storage; technology update," *Renewable and Sustainable Energy Reviews*, volume 33, pages 532–545, 2014.

[40] T. Kousksou, P. Bruel, A. Jamil, T El Rhafiki, and Y. Zeraouli, "Energy storage: Applications and challenges," *Solar Energy Materials and Solar Cells*, volume 120, pages 59–80, 2014.

[41] A. Khaligh and Z. Li, "Battery, ultracapacitor, fuel cell, and hybrid energy storage systems for electric, hybrid electric, fuel cell, and plug-in hybrid electric vehicles: State of the art," *IEEE transactions on Vehicular Technology*, volume 59, number 6, pages 2806–2814, 2010.

[42] Z. Zhou, M. Benbouzid, J. F. Charpentier, F. Scuiller, and T. Tang, "A review of energy storage technologies for marine current energy systems," *Renewable and Sustainable Energy Reviews*, volume 18, pages 390–400, 2013.

[43] K. E. Nielsen and M. Molinas, "Superconducting magnetic energy storage (smes) in power systems with renewable energy sources," in *2010 IEEE International Symposium on Industrial Electronics*, IEEE, 2010, pages 2487–2492.

[44] H. Europe, "Hydrogen europe vision on the role of hydrogen and gas infrastructure on the road toward a climate neutral economy," 2019.

[45] AEP, "American electric power, transmission facts," 2011.

[46] D. Haeseldonckx and W. D'haeseleer, "The use of the natural-gas pipeline infrastructure for hydrogen transport in a changing market structure," *International Journal of Hydrogen Energy*, volume 32, number 10-11, pages 1381–1386, 2007.

[47] B. Barrass, *Ship design and performance for masters and mates*. Elsevier, 2004.

[48] J. P. Comstock, "Principles of naval architecture," 1967.

[49] F. Zouridakis, "A preliminary design tool for resistance and powering prediction of catamaran vessels," PhD thesis, Massachusetts Institute of Technology, 2005.

[50] I. T. T. Conference, "Uncertainty analysis, example for resistance test," *Via Internet (16.07. 2019)< https://ittc.info/media/1818/75-02-02-02.pdf*, 2002.

[51] T. J. Stehly, P. C. Beiter, D. M. Heimiller, and G. N. Scott, "2017 cost of wind energy review," National Renewable Energy Lab.(NREL), Golden, CO (United States), Tech. Rep., 2018.

[52] M. Stopford, *Maritime economics 2e*. Routledge, 2003.

[53] W. Short, D. J. Packey, and T. Holt, "A manual for the economic evaluation of energy efficiency and renewable energy technologies," National Renewable Energy Lab., Golden, CO (United States), Tech. Rep., 1995.

[54] C. Moné, A Smith, B. Maples, and M. Hand, "2013 cost of wind energy review," National Renewable Energy Lab.(NREL), Golden, CO (United States), Tech. Rep., 2013.

[55] S. B. Briefing, "World steel review," *SBB's weekly*, 2008.

[56] I. Staffell, D. Scamman, A. V. Abad, P. Balcombe, P. E. Dodds, P. Ekins, N. Shah, and K. R. Ward, "The role of hydrogen and fuel cells in the global energy system," *Energy & Environmental Science*, volume 12, number 2, pages 463–491, 2019.

[57] B. Zakeri and S. Syri, "Corrigendum to "electrical energy storage systems: A comparative life cycle cost analysis"[renew. sustain. energy rev. 42 (2015) 569–596]," *Renewable and Sustainable Energy Reviews*, volume 100, number 53, pages 1634–1635, 2016.

[58] G Parks, R Boyd, J Cornish, and R Remick, "Hydrogen station compression, storage, and dispensing technical status and costs: Systems integration," National Renewable Energy Lab.(NREL), Golden, CO (United States), Tech. Rep., 2014.

[59] Irena, "Renewable power generation costs in 2017," 2018.

[60] ——, "Hydrogen from renewable power. technology outlook for the energy transition," 2018.

APPENDIX A

Appendices Wind Energy Yield Assessment -Code

A.1 General Parameters

```
function ado = case1
%% Data input ERA-5: hourly data!
%% Number of Wind Turbines
ado.numWT=1; %numWT

%% Some parameters of the wind turbine
ado.cp=16/27; % Bentz Limit
ado.ro=1.2250; % (kg/m-3 at 15C) air density
ado.Diameter=128; % (m) wind turbine blades-span (diameter) from NREL 5MW;
ado.Area=pi/4*ado.Diameter^2; % (m2) Wind Turbine span area
ado.root='C:\Users\xavmi\Desktop\MSc Thesis\model\data\';

%% Define North Sea Geometry in coordinates
% Note: initial approach, geometry and vertex could be imporoved
ado.lat0=54; % Initial latitude in degrees
ado.latf=57; % Final latitude in degrees
ado.lon0=0; % Initial longitud in degrees
ado.lonf=7; % Final longitud in degrees


%% Time-related Paramenters
ado.Time=3600; % (in seconds) Time between two samples from ERA5

%% Time costs of travelling
ado.TimeTravel=24; %(P) in hours
ado.TimeForecast=24; %(Q) in hours
ado.speed=18.5200/3600; %km/s % Temporal limitation
% (platform moves at constant speed of 10 knots)

%% Wake model
ado.WakeDCoeff=10;
```

.

A.2 main

```
function main(varargin)
%% Newest version by Xavier Martinez Beseler
% Started on February ended on June 19
% Several ADO-WTs can move around the North Sea, only to the areas they can
% reach time-wise, while moving, they produce while moving and they do not
% consume energy to do so. Power Curve is included in Vo2E from version v16.
% The brand-new algorithm implemented & designed by Xavier in end March
% 2019 is used for choosing Z target and move to B point.
% The model choses the best spot the WT will move the next hour taking into
% account "the wind forecast" within the area they can reach in the next P
% hours, the forecast goes from P to P+Q hours.
% No energy travelling costs are associated
clc
%% I Paramenters
ado=case1;
speed=ado.speed; %km/s
AggHours=ado.AggHours; % Aggregation of time in hours
numWT=ado.numWT; % Number of WTs
% Time parameters
P=ado.TimeTravel; %in hours
Q=ado.TimeForecast; %in hours

%% II Data
root='';
DataInfo.DataBase='ERA5';
DataInfo.month='Dec';
DataInfo.version=input('Introduce the version that is being...
 running now (e.g. v17): ','s');
ERA5=load([root 'NS_' DataInfo.DataBase DataInfo.month '.mat']);
u=ERA5.NS_u_pt;
v=ERA5.NS_v_pt;
[lat,lon,A,B]=getLonLat_interp;
E_site_total=zeros(A,B);
ws=sqrt(u.^2+v.^2);
TimeL=size(u,3)-P-Q+1;
AggTimeL=ceil(TimeL/AggHours);

%% III Initialize variables
if nargin
temporary=varargin{1};
[E_ADO,E_conv,E_extra_ADO,E_extra_upper,k_t0,shift,SiteADO,SiteConv,...
SiteUpper,E_upper,E_sites,t0]=updateVar(temporary);
else
[E_ADO,E_conv,E_extra_ADO,E_extra_upper,k_t0,shift,SiteADO,SiteConv,...
SiteUpper,E_upper,E_sites,t0]=updateVar(TimeL,numWT,AggTimeL,Q,ws);
end
```

```
47
48 tic
49 %% IV Conventional Model - Initialize variables for the Conv. Model
50 AEP_conv_wt=zeros(numWT,1);
51
52 %% 2 ENERGY HARVESTED
53 for k_t=k_t0+1:TimeL
54   SpotsTaken=NaN(numWT,2,2); % Third dimension is 2,
55   %one for utopic point (Z) and the other for the next hour point (B)
56
57   %% 2.3 Upper Bound Model
58   %% 2.3.1 Upper Bound Model- Sort from max to min values of Energy
59   X=E_sites(:,:,k_t);
60   [X,I]=sort(X(:),'descend');
61   %% 2.3.2 Upper Bound Model- Get Energy Yield for best positions
62   E_upper(k_t,1:numWT) = X(1:numWT); % Gives the max Energy (in J)
63   %% 2.3.3 Upper Bound Model- Get the Index for each site
64   [SiteUpper.ind(1:numWT,2*k_t-1),SiteUpper.ind(1:numWT,2*k_t)] =...
65    ind2sub(size(E_sites(:,:,k_t)),I(1:numWT)); % Get the index position
66   %% 2.3.4 Upper Bound Model- Get the coordinates for
67   %such positions (for each "upper-bound-WT")
68   SiteUpper.coor(1:numWT,2*k_t-1)=lon(SiteUpper.ind(1:numWT,2*k_t-1));
69   % Get the site in coordenates
70   SiteUpper.coor(1:numWT,2*k_t)= lat(SiteUpper.ind(1:numWT,2*k_t));
71   %% 2.3.5 Get total energy harvested by Upper bound so far
72   AEP_Upper=sum(E_upper);
73
74   %% 2.2 Conventional Model
75   %% 2.2.2 Conventional Model - Get total energy per
76   % site (from first hour to the current one)
77   for i=1:length(lon)
78     for j=1:length(lat)
79       E_site_total(i,j)=sum(E_sites(i,j,1:k_t));
80     end
81   end
82
83   %% 2.2.3 Conventional Model - Get the maximum value
84   % and save the location and the total energy
85   [X,I] = sort(E_site_total(:),'descend');
86   AEP_conv_wt(1:numWT)=X(1:numWT);% get the total energy
87   [SiteConv.ind(1:numWT,1),SiteConv.ind(1:numWT,2)] =...
88   ind2sub(size(E_site_total),I(1:numWT)); % Get the site
89   SiteConv.coor(1:numWT,1)=lon(SiteConv.ind(1:numWT,1));
90   SiteConv.coor(1:numWT,2)=lat(SiteConv.ind(1:numWT,2));
91   %% 2.2.4 Conventional Model - Calculate the total Energy supplied
92   AEP_conv=sum(AEP_conv_wt);
93
94   %% 2.1.1 ADO Model - Interpolate Wind Speed geographically
95   ForecastTime=k_t:k_t+P+Q-1; % Trom the current time,
96   %until P+Q hours ahead (-1 bs of discretization)
97   WS=interpWS(ws(:,:,ForecastTime),A,B);
98   for k_wt=1:numWT
99     %% 2.2.5 Save the E_conventional for the position
100    %chosen so far
101    for k_t_aux=k_t0:k_t
```

```
      E_conv(k_t_aux,k_wt)=...
      E_sites(SiteConv.ind(k_wt,1),...
      SiteConv.ind(k_wt,2),k_t_aux);
    end
    %% 2.1.2 ADO Model - Update PointA (current point =previous)
    PointA.ind=SiteADO.ind(k_wt,2*(k_t-1)-1:2*(k_t-1));
    PointA.coor=SiteADO.coor(k_wt,2*(k_t-1)-1:2*(k_t-1));
    %% 2.1.3 ADO Model - Get the next point where the
    %ADO.WT will go within the next hour
    [PointB,SpotsTaken]=getB(PointA,lon,lat,WS,SpotsTaken,k_wt);
    %% 2.1.4 ADO Model - Uptate the position vector
    SiteADO.ind(k_wt,2*k_t-1)=PointB.ind(1);
    SiteADO.ind(k_wt,2*k_t)=PointB.ind(2);
    SiteADO.coor(k_wt,2*k_t-1)=PointB.coor(1);
    SiteADO.coor(k_wt,2*k_t)= PointB.coor(2);

    %% 2.1.5 ADO Model - Save the Energy harvested
    E_ADO(k_t,k_wt)=PointB.Energy;

    %% 2.1.6 ADO Model - Calculate the distance for
    %Autonomously Driven Offshore WT (ADO-WT)in km
    shift.dist(k_wt,k_t-1)= haversine([SiteADO.coor(k_wt...
    ,2*k_t-2),SiteADO.coor(k_wt,2*k_t-3)],[SiteADO.coor...
    (k_wt,2*k_t),SiteADO.coor(k_wt,2*k_t-1)]);
    shift.time(k_wt,k_t-1)=shift.dist(k_wt,k_t-1)/speed/3600; %in h
  end

  %% 2.1.7 ADO Model - Calculate the total Energy supplied
  AEP_ADO=sum(E_ADO(:));

  %% 3 Comparing models
  E_extra_ADO(k_t)=(AEP_ADO-AEP_conv)/AEP_conv;
  E_extra_upper(k_t)=(AEP_Upper-AEP_conv)/AEP_conv;

  %% Save temporary results
  TimeToc=toc+t0; %#ok<NASGU>
  save([DataInfo.version '_Q' num2str(Q) '_P'...
  num2str(P) '_T' num2str(TimeL) '_WT' num2str(numWT)...
  '_temporaryResults'],'E_ADO','E_conv','E_extra_ADO',...
  'E_extra_upper','P','Q','numWT','TimeL','SiteConv',...
  'SiteADO','shift','TimeToc','speed','DataInfo','k_t',...
  'SiteUpper','E_sites','E_upper')
end

shiftUpper.dist=zeros(numWT,TimeL-1);
shiftUpper.time=zeros(numWT,TimeL-1);
shiftADO.dist=zeros(numWT,TimeL-1);
shiftADO.time=zeros(numWT,TimeL-1);

for k_t=k_t0+1:TimeL
  for k_wt=1:numWT
    shiftADO.dist(k_wt,k_t-1)=haversine([SiteADO.coor(k_wt,...
    2*k_t-2),SiteADO.coor(k_wt,2*k_t-3)],[SiteADO.coor(k_wt,...
    2*k_t), SiteADO.coor(k_wt,2*k_t-1)]);
    shiftADO.time(k_wt,k_t-1)=...
```

```
    shift.dist(k_wt,k_t-1)/speed/3600; %in hours
    shiftUpper.dist(k_wt,k_t-1)=haversine([...
    SiteUpper.coor(k_wt,2*k_t-2),SiteUpper.coor(k_wt,2*k_t-3)],...
    [SiteUpper.coor(k_wt,2*k_t), SiteUpper.coor(k_wt,2*k_t-1)]);
    shiftUpper.time(k_wt,k_t-1)=shiftUpper.dist(k_wt,...
    k_t-1)/speed/3600; %time in hours
  end
end

TimeToc=toc+t0;
save([DataInfo.version '_Q' num2str(Q) '_P' num2str(P)...
 '_T' num2str(TimeL) '_WT' num2str(numWT)...
  '_Results'],'E_ADO','E_conv','E_extra_ADO','E_extra_upper',...
  'P','Q','numWT','TimeL','SiteConv','SiteADO','shift','TimeToc',...
  'speed','DataInfo','SiteUpper','E_sites')

end
```

.

A.3 updateVar

```
function [E_ADO,E_conv,E_extra_ADO,E_extra_upper,k_t0,shift,...
SiteADO,SiteConv,SiteUpper,E_upper,E_sites,t0]=updateVar(varargin)


if nargin==1
  temporary=varargin{1};
  if isfile(temporary)
    temp=load(temporary);
    E_ADO=temp.E_ADO;
    E_conv=temp.E_conv;
    E_extra_ADO=temp.E_extra_ADO;
    E_extra_upper=temp.E_extra_upper;
    k_t0=temp.k_t;
    shift=temp.shift;
    SiteADO=temp.SiteADO;
    SiteConv=temp.SiteConv;
    E_sites=temp.E_sites;
    E_upper=temp.E_upper;
    SiteUpper=temp.SiteUpper;
    t0=temp.TimeToc;
  else
    disp('No file found')
  end
else
  tic
  TimeL=varargin{1};
  numWT=varargin{2};
  AggTimeL=varargin{3};
  [lat,lon,A,B]=getLonLat_interp;
  E_sites=zeros(A,B,AggTimeL);
```

```
Q=varargin{4};
ws=varargin{5};
%% III ADO MODEL - Initialize variables
% travelling_time=zeros(TimeL,1);
E_ADO=zeros(TimeL,numWT);
SiteADO.ind=zeros(numWT,2*TimeL);
SiteADO.coor=zeros(numWT,2*TimeL); % real coordinate
shift.dist=zeros(numWT,TimeL-1);
shift.time=zeros(numWT,TimeL-1);
E_extra_ADO=zeros(TimeL,1);
E_extra_upper=zeros(TimeL,1);
E_upper=zeros(TimeL,numWT);
%% IV Conventional Model - Initialize variables
SiteConv.ind=zeros(numWT,2*TimeL);
SiteConv.coor=zeros(numWT,2*TimeL);
% lat_ind_conv=zeros(numWT,1);
E_conv=zeros(TimeL,numWT);
k_t0=1;

%% V Upper.bound Model - Initialize variables
SiteUpper.ind=zeros(numWT,2*TimeL);
SiteUpper.coor=zeros(numWT,2*TimeL);

%% 1 INITIAL POSITION
%% 1.1 ADO Model - Get Initial position for ADO-WTs
%% 1.1.1 ADO Model - Get the Wind Speed
% geographically interpolated for the first Q hours
k_t=1;
NS_ws=interpWS(ws(:,:,k_t:Q),A,B);
%% 1.1.2 ADO Model - Get the Wind Energy for every
%site for the following Q hours
E_provisional=Vo2E(NS_ws);
%% 1.1.3 ADO Model - Aggregate (sum up)
%the following 1:Q hours
X=zeros(size(E_provisional,1),size(E_provisional,2));
for i=1:size(E_provisional,1)
  for j=1:size(E_provisional,2)
    X(i,j)=sum(E_provisional(i,j,:));
  end
end
%% 1.1.4 ADO Model - Get the Maximum best spots for the 1:Q hours
[~,I]=sort(X(:),'descend'); % ADO Model - Sort Energy from max2min
% ADO Model - Get the Index where the WTs are sited
[SiteADO.ind(1:numWT,2*k_t-1),SiteADO.ind(1:numWT,2*k_t)] = ...
ind2sub(size(E_sites(:,:,k_t)),I(1:numWT));
%% 1.1.5 ADO Model - Save the coordinates for best
% position positions for each WT
SiteADO.coor(1:numWT,2*k_t-1)=  lon(SiteADO.ind(1:numWT,2*k_t-1));
% Get the site in coordenates
SiteADO.coor(1:numWT,2*k_t)= lat(SiteADO.ind(1:numWT,2*k_t));
%% 1.1.6 ADO Model - Save the Energy harvested for
%the first hour at the location, for each WTs
for k_wt=1:numWT
  i=SiteADO.ind(k_wt,2*k_t-1);
  j=SiteADO.ind(k_wt,2*k_t);
```

```
    E_ADO(k_t,k_wt) = Vo2E(NS_ws(i,j,k_t)); % Energy (in J)
  end

  %% 1.2 Conventional & Upper-Bound Models
  %% 2.2.1 Conventional & Upper-Bound Models -
  %Get Energy Potential for every site and time
  E_sites(:,:,1)=E_provisional(:,:,1);
  for k_t=k_t0+1:TimeL
    E_sites(:,:,k_t)=Vo2E(interpWS(ws(:,:,k_t),A,B));
  end

  %% 1.3 Upper-Bound Model - Get Initial Position for "upper-bound-WTs"
  %% 1.3.1 Upper Bound Model- Sort from max to min values of Energy
  X=E_sites(:,:,k_t0);
  [X,I]=sort(X(:),'descend');
  %% 2.3.2 Upper Bound Model- Get the Gross Energy
  % harvested for the top positions (the first numWT ones)
  E_upper(k_t0,1:numWT) = X(1:numWT); % Emax (in Joules)
  %% 2.3.3 Upper Bound Model- Get Index where WTs are located
  [SiteUpper.Ind(1:numWT,2*k_t-1),SiteUpper.Ind(1:numWT,2*k_t)] =...
   ind2sub(size(E_sites(:,:,k_t)),I(1:numWT)); % Get the index
  %% 2.3.4 Upper Bound Model- Get the coordinates for
  %such positions (for each "upper-bound-WT")
  SiteUpper.Coor(1:numWT,2*k_t-1)=lon(SiteUpper.Ind(1:numWT,2*k_t-1));
  SiteUpper.Coor(1:numWT,2*k_t)=...
  lat(SiteUpper.Ind(1:numWT,2*k_t)); % Get the site in coordenates
  t0=toc;
end


end
```

.

A.4 Vo2E

```
function E=Vo2E(varargin)
%% This function transformes a given wind speed (and WT span area) into
    energy
% Developped by Xavier Martinez Beseler 20th Feb 2019 updated in June 2019
% main input: V wind speed (m/s) up to three variables
% extra input: t sample time (s) time at which wind is blowing at V
% If no extra input is given, the ado.Time set in case1 is taken.
% outputs: Energy in J harvested from the wind during t time
ado = case1;
if nargin ==1
V=varargin{1};
t=ado.Time;
elseif nargin ==2
V=varargin{1};
t=varargin{2};
end
```

```

%% Wind speed and force on the NREL 5MW turbine
WS_p=[3,4,5,5.5,6,6.5,7.5,8,9,9.5,10.5,11.5,12]; % in m/s
Pg=[0,.2,.4,.5,.75,1,1.5,1.75,2.5,3,4,5,5]*1e6; % in W
% WS_t=[3,4,5,5.5,6,6.5,7,8.5,9,10,11,11.3,12,13,15,25]; % in m/s
% T=[.2,.25,.3,.325,.35,.375,.4,.5,.55,.67,.75,.76,.67,.6,.5,.4]*1e6;

P=zeros(size(V));
%% Energy extracted from the wind
for i=1:size(V,1)
for j=1:size(V,2)
for k=1:size(V,3)
if V(i,j,k)<3 || V(i,j,k)>25
P(i,j,k)=0;
elseif V(i,j,k)>12
P(i,j,k)=5e6;
else
P(i,j,k)=interp1(WS_p,Pg,V(i,j,k));
end
end
end
end
%% Old version
% %% Parameters
% cp=ado.cp; % Bentz Limit.
% rho=ado.ro;%  air density
% A=ado.Area; % (m2) Wind Turbine span area
% %% Power
% P=1/2*rho*cp*A*V.^3;
E=P*t; % Energy extracted from the wind in J
end
```

.

A.5 getArea

```
function Area=getArea(PointA,lon,lat,SpotsTaken,varargin)
% This function calculates the reachible area for an ADO-WT to move between
% P hours
% Based on NearbyPoints function from v5, this function was created on
% April 4th 2019 by Xavier and finalized April 5th 2019
% lon and lat must be vectors in absolute values for all the coordenates of
% the North Sea

ado=case1;

%% In case it is willing to be used another travelling time which is not P
if isempty(varargin)
  P=ado.TimeTravel;
else
  P=varargin{1};
end
```

```
17
18 %% Define initial points
19 west=PointA.ind(1);
20 east=PointA.ind(1);
21 south=PointA.ind(2);
22 north=PointA.ind(2);
23
24 %% Define the speed
25 speed=ado.speed*3600; % in km/h
26
27 %% 1 move WEST (backwards in lon, keeping lat fixed)
28 while west-1>=1 && haversine([PointA.coor(2),PointA.coor(1)],...
29 [PointA.coor(2),lon(west-1)])<=P*speed
30   west=west-1;
31 end
32
33
34 %% 2 move EAST (forwards in lon, keeping lat fixed)
35 while east+1<=length(lon) && haversine([PointA.coor(2),PointA.coor(1)],...
36 [PointA.coor(2),
37 lon(east+1)])<=P*speed
38   east=east+1;
39 end
40
41
42 %% 3 move SOUTH (backwards in lat, keeping lon fixed)
43 while south-1>=1 && haversine([PointA.coor(2),PointA.coor(1)],...
44 [lat(south-1),PointA.coor(1)])<=P*speed
45   south=south-1;
46 end
47
48
49 %% 4 move NORTH (forwards in lat, keeping lon fixed)
50 while north+1<=length(lat) && haversine([PointA.coor(2),PointA.coor(1)],...
51 [lat(north+1),PointA.coor(1)])<=P*speed
52   north=north+1;
53 end
54
55 Area.north=north;
56 Area.south=south;
57 Area.east=east;
58 Area.west=west;
59 Area.lon=lon(west:east);
60 Area.lat=lat(south:north);
61
62 Area.state=zeros(length(Area.lon),length(Area.lat));
63 %% 5 -Having the borders defined,
64 %check which points are within the travelling time
65 for i=1:length(Area.lon)
66   for j=1:length(Area.lat)
67     if haversine([PointA.coor(2),PointA.coor(1)],...
68     [Area.lat(j),Area.lon(i)])<=P*speed
69       Area.state(i,j)=1;
70     end
71   end
```

```
end


%% 6 Check if there are any site already taken by the other WTs
numWT=size(SpotsTaken,1);
% 0 if it's not taken and 1 if it's taken
Area.taken=zeros(length(Area.lon),length(Area.lat));

for i=1:length(Area.lon)
  for j=1:length(Area.lat)
    for k_wt=1:numWT
      if isequal(SpotsTaken(k_wt,:),...
      [Area.lon(i), Area.lat(j)])
        Area.taken(i,j)=1;
      end
    end
  end
end

end
```

.

A.6 getB

```
function [PointB,SpotsTaken]=getB(PointA,lon,lat,WS,SpotsTaken,k_wt)

% This function gets as inputs
% - A a vector (lon,lat) with the info of the current point
% - k the index of the current hour
% The function gives a vector (lon,lat) with the position of the next hour
% destination point
% The logic behind is as follows:
% First the Area reacheable after P hours of travelling is calculated.
% Then, the potential wind resources within that area for Q hours after the
% travelling time (P) is obtained. The maximum of this resources
% constitutes the "utopic" target Z for P-hours ahead from the current time
% (k). This target Z will lead to the next hour target, B. By getting the
% maximum wind potentential within the area resulting of the interesection
% between a 1h reacheble area from A and an area (P-1) hours from Z.
% Spots taken is a 2 x numWT x P matrix with the pair of coordinates of the
% points that are taken for every wind turbine at every travelling hour
% within the forecasted time.
% Created/Modified by Xavier March 5th  2019
% SpotsTaken(:,:,1) refers to the taken points SpotsTaken(i,j,1)=1 by a WT
% for such (i,j) spot at the next hour (B), whereas SpotsTaken(:,:,2) does
% it at P hours ahead (Z). If SpotsTaken(i,j,k)=0 it means that at the
% location (i,j) at the next hour (if k=1) or P hours ahead (if k=2) is not
% taken by any WT so far

ado=case1;
%% Paramenters
```

```
28 P=ado.TimeTravel; %in hours
29 Q=ado.TimeForecast; %in hours
30
31 %% 1 Get the area that a single ADO-WT can reach in P hours or less
32 % instead of allowing going P hours far by restricting to  95% of P
33 % the intersection of areas is guaranteed (empirically)
34 AreaP=getArea(PointA,lon,lat,SpotsTaken(:,:,2),0.95*P);
35 south=AreaP.south;
36 north=AreaP.north;
37 west=AreaP.west;
38 east=AreaP.east;
39
40 %% Select the wind data only for that area within [P,P+Q]
41 % hours from the current time
42 ws=WS(west:east,south:north,P:P+Q).*AreaP.state.*~AreaP.taken;
43 % State is a matrix whose values are 1 if the site is available, 0
44 % otherwise. ~Taken is 0 1 if the spot is taken
45
46 %% Get the utopic target Z
47 PointZ=getZ(ws,AreaP); % Z is the main target
48
49 % Get absolute coordenates for Z site
50 PointZ.coor(1)=lon(PointZ.ind(1));
51 PointZ.coor(2)=lat(PointZ.ind(2));
52
53 %% Update the SpotsTaken vector that target Z cannot be used by another ADO-
       WT
54 SpotsTaken(k_wt,1,2)=PointZ.coor(1);
55 SpotsTaken(k_wt,2,2)=PointZ.coor(2);
56
57 %% Get intersected area
58 Area=getIntersection(PointA,PointZ,P-1,lon,lat,SpotsTaken(:,:,1));
59
60 %% We select only Wind Speed data from the Intersected Area
61 % at the forecasted time P-k hours
62 ws=WS(Area.west:Area.east,Area.south:Area.north,1).*Area.state.*~Area.taken;
63 PointB=getZ(ws,Area);
64
65 %% Get absolute coordenates for Z site
66 PointB.coor(1)=lon(PointB.ind(1));
67 PointB.coor(2)=lat(PointB.ind(2));
68
69 %% Update the SpotsTaken vector
70 SpotsTaken(k_wt,1,1)=PointB.coor(1);
71 SpotsTaken(k_wt,2,1)=PointB.coor(2);
72
73 end
```

.

A.7 getZ

```
function Z=getZ(ws,Area)
% This function gets as inputs:
% - Area: a structure with Area.lon as a vector with the longitud
% coordinates taken, Area.lat for latituted and Area.state, a 0/1 matrix
% with info of whether the Area at lon,lat position is within the area or
% not. E.g., if Area.state(i,j)=1 it means that lon(i),lat(j) is a
% coordenate to consider. Area.north, and then .south, .east and .west are
% the absolute index defining the Area at the North Sea.
% ado=case1;


a=size(ws,1);
b=size(ws,2);

E=Vo2E(ws);

E_tot=zeros(a,b);

for i=1:a
  for j=1:b
    E_tot(i,j)=sum(E(i,j,:));
  end
end

[Z.Energy,I]=max(E_tot(:));
[Z.ind(1),Z.ind(2)]=ind2sub(size(E_tot),I);

%% Transfore relative to absolute indexis
%Since ws is not the whole NS region but a certain area, the indecis are
%relative by adding the reference points (south and west) they are
%converted into absolute values
Z.ind(1)=Z.ind(1)+Area.west-1;
Z.ind(2)=Z.ind(2)+Area.south-1;
end
```

.

A.8 getIntersection

```
% This function was created April 5th 2019 by Xavier

%% Get the area which is 1 hour far from A and k hours (P-1) far from Z
Area_A=getArea(A,lon,lat,SpotsTaken,1);
Area_Z=getArea(Z,lon,lat,SpotsTaken,k);


%% Get the maximum number of rows to avoid problems with subindexes
east=max([Area_A.east,Area_Z.east]);
west=min([Area_A.west,Area_Z.west]);

%% Get the maximum number of colums to avoid problems with subindexes
```

```
north=max([Area_A.north,Area_Z.north]);
south=min([Area_A.south,Area_Z.south]);

%% In order to get the area where there is a real (squared) interection
Area.east=min([Area_A.east,Area_Z.east]);
Area.west=max([Area_A.west,Area_Z.west]);
Area.north=min([Area_A.north,Area_Z.north]);
Area.south=max([Area_A.south,Area_Z.south]);

%% create an initial state matrix with absolute coordinates
Area.taken=zeros(length(Area.west:Area.east),length(Area.south:Area.north));
Area.state=zeros(length(Area.west:Area.east),length(Area.south:Area.north));

%% Uptate the coordinates vectors
Area.lon=lon(Area.west:Area.east);
Area.lat=lat(Area.south:Area.north);

for i=1:east % west:east
  for j=1:north
    if i>=Area_A.west && i<=Area_A.east && j>=Area_A.south...
    && j<=Area_A.north && i>=Area_Z.west && i<=Area_Z.east...
    && j>=Area_Z.south && j<=Area_Z.north &&...
    Area_A.state(1+i-Area_A.west,1+j-Area_A.south) &&...
    Area_Z.state(1+i-Area_Z.west,1+j-Area_Z.south)
      m=i-Area.west+1;
      n=j-Area.south+1;
      Area.state(m,n)=1;
    end
    if i>=Area_A.west && i<=Area_A.east && j>=Area_A.south...
    && j<=Area_A.north && i>=Area_Z.west && i<=Area_Z.east...
    && j>=Area_Z.south && j<=Area_Z.north &&...
    (Area_A.taken(1+i-Area_A.west,1+j-Area_A.south) ||...
    Area_Z.taken(1+i-Area_Z.west,1+j-Area_Z.south))
      Area.taken(i-Area.west+1,j-Area.south+1)=1;
    end
  end
end
```

.

Where lon and lat (not Area.lon and Area.lat) are the absolute longitude and latitude coordinate vectors of the whole North Sea (they would cover the whole big rectangle labelled as North Sea).

A.9 getLonLatInterp

```
function [NS_lat,NS_lon,A,B]=getLonLat_interp

ado=case1;
D=ado.Diameter;
WakeDCoeff=ado.WakeDCoeff;
```

```
D_margin=WakeDCoeff*D*1e-3;

root='';
ERA5=load([root 'NS_ERA5Dec.mat']);
NS_lon_raw=ERA5.NS_lon_pt;
NS_lat_raw=ERA5.NS_lat_pt;

%% Get the disances between each raw-latitude coordinate
distance_h=zeros(length(NS_lat_raw),1);
for j=1:length(NS_lat_raw)
  distance_h(j)=haversine([NS_lat_raw(j),NS_lon_raw(1)],...
  [NS_lat_raw(j),NS_lon_raw(2)]);
end

%% Get the disances between each raw-longitude coordinate
distance_v=zeros(length(NS_lon_raw),1);
for i=1:length(NS_lon_raw)
  distance_v(i)=haversine([NS_lat_raw(1),NS_lon_raw(i)],...
  [NS_lat_raw(2),NS_lon_raw(i)]);
end

%% Number of divisions to make in order to have a yD x yD grid
[a,b,~]=size(ERA5.NS_u_pt); % raw geographic dimensions
A=a+(a-1)*floor(max(distance_v)/D_margin);
B=b+(b-1)*floor(max(distance_h)/D_margin);


NS_lon=zeros(A,1);
for i=1:a-1
  for I=1:A
    fx2=NS_lon_raw(i+1);
    fx1=NS_lon_raw(i);
    dx=((A-a)/(a-1)+1);
    x=I;
    x1=(((A-a)/(a-1)+1)*(i-1)+1);
    NS_lon(I)=(fx2-fx1)/(dx)*(x-x1)+fx1;
  end
end

NS_lat=zeros(B,1);
for j=1:b-1
  for J=1:B
    fx2=NS_lat_raw(j+1);
    fx1=NS_lat_raw(j);
    dx=((B-b)/(b-1)+1);
    x=J;
    x1=(((B-b)/(b-1)+1)*(j-1)+1);
    NS_lat(J)=(fx2-fx1)/dx*(x-x1)+fx1;
  end
end

end
```

.

A.10 interpWS

```
function WS=interpWS(WS_raw,A,B)

[a,b,c]=size(WS_raw);

WS=NaN(A,B,c);
%% Fill in the interpolated matrix with the raw data
for k=1:c
  for i=1:a
    for j=1:b
      I=(((A-a)/(a-1)+1)*(i-1)+1);
      J=(((B-b)/(b-1)+1)*(j-1)+1);
      WS(I,J,k)=WS_raw(i,j,k);
    end
  end
end

%% Interpolate in between
for k=1:c
  for i=1:A
    WS(i,:,k)= fillmissing(WS(i,:,k),'linear');
  end
  for j=1:B
    WS(:,j,k)= fillmissing(WS(:,j,k),'linear');
  end
end

end
```

.

A.11 getLonLanInterp

```
function [NS_lat,NS_lon,A,B]=getLonLat_interp

ado=case1;
D=ado.Diameter;
WakeDCoeff=ado.WakeDCoeff;
D_margin=WakeDCoeff*D*1e-3;


root='';
ERA5=load([root 'NS_ERA5Dec.mat']);
NS_lon_raw=ERA5.NS_lon_pt;
NS_lat_raw=ERA5.NS_lat_pt;
NS_ws_raw=sqrt(ERA5.NS_u_pt.^2+ERA5.NS_v_pt.^2);

distance_h=zeros(length(NS_lat_raw),1);
for j=1:length(NS_lat_raw)
  distance_h(j)=haversine([NS_lat_raw(j),NS_lon_raw(1)],...
```

```
  [NS_lat_raw(j),NS_lon_raw(2)]);
end

distance_v=zeros(length(NS_lon_raw),1);
for i=1:length(NS_lon_raw)
  distance_v(i)=haversine([NS_lat_raw(1),NS_lon_raw(i)],...
  [NS_lat_raw(2),NS_lon_raw(i)]);
end

%% Number of divisions to make in order to have a yD x yD grid
[a,b,~]=size(NS_ws_raw);
A=a+(a-1)*floor(max(distance_v)/D_margin);
B=b+(b-1)*floor(max(distance_h)/D_margin);


NS_lon=zeros(A,1);
for i=1:a-1
  for I=1:A
    fx2=NS_lon_raw(i+1);
    fx1=NS_lon_raw(i);
    dx=((A-a)/(a-1)+1);
    x=I;
    x1=(((A-a)/(a-1)+1)*(i-1)+1);
    NS_lon(I)=(fx2-fx1)/(dx)*(x-x1)+fx1;
  end
end

NS_lat=zeros(B,1);
for j=1:b-1
  for J=1:B
    fx2=NS_lat_raw(j+1);
    fx1=NS_lat_raw(j);
    dx=((B-b)/(b-1)+1);
    x=J;
    x1=(((B-b)/(b-1)+1)*(j-1)+1);
    NS_lat(J)=(fx2-fx1)/dx*(x-x1)+fx1;
  end
end

% save('2point5DInterpLonLat','NS_lat','NS_lon','A','B')

end
```

.

APPENDIX B

Appendices Wind Energy Yield Assessment -Results

B.1 Interpolation vs No Interpolation Graphs

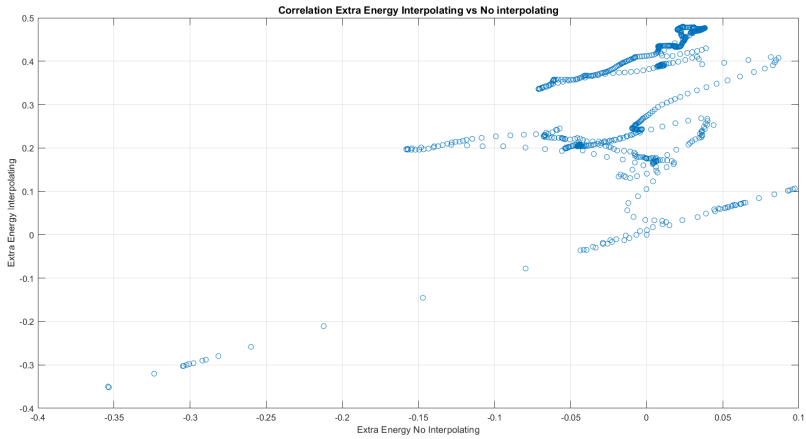

Figure B.1: Correlation Extra Wind Energy interpolating or not interpolating for 1 WT Dec18.

B.2 Vo2E. Extra Results Sensitivity analysis

This section presents extra results of the same research presented in section 3.2.5, that is, keeping the interpolation module, for a grid 10D x 10D –the one presenting

better results as explained in 3.2.1–.
Correlation for the Extra Energy outcome from the Upper-Bound model with and without Power Curve is shown in Figure B.2. That is, comparing outcomes from Upper-Bound model with NREL power curve (represented in Figure 3.1.1.4) and with the Aerodynamic approximation, Eq. (3.1). More information can be found in 3.1.1.4 (for methodology), A.4 (for code) and 3.2.5 for results. The same correlation for outcomes from Reachable-Area model is shown in B.2

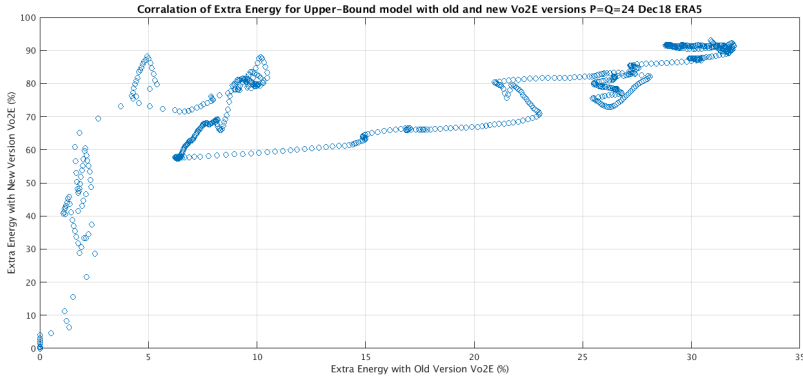

Figure B.2: Correlation of Extra Wind Energy for Upper Bound model old vs new Vo2E versions.

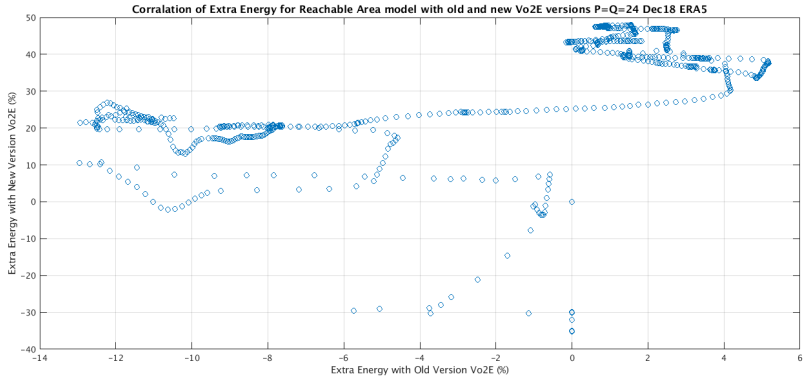

Figure B.3: Correlation of Extra Wind Energy for Reachable Area model old vs new Vo2E versions.

B.3 P&Q Configurations. Extra Results

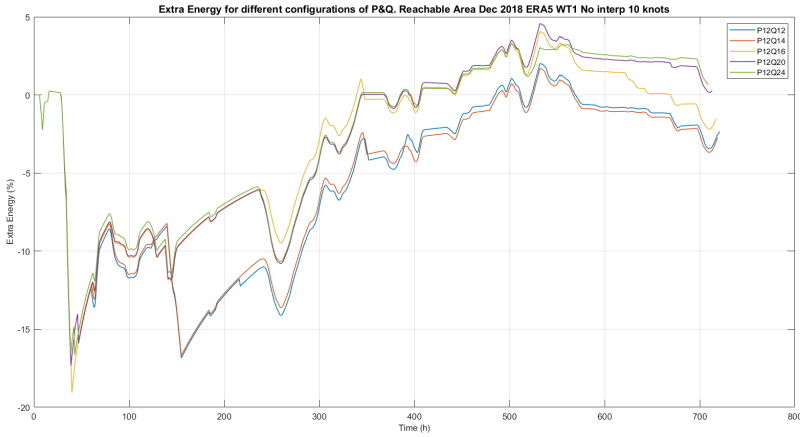

Figure B.4: Extra Wind Energy for different configurations of Q with $P = 12$. ERA5 Dec18.

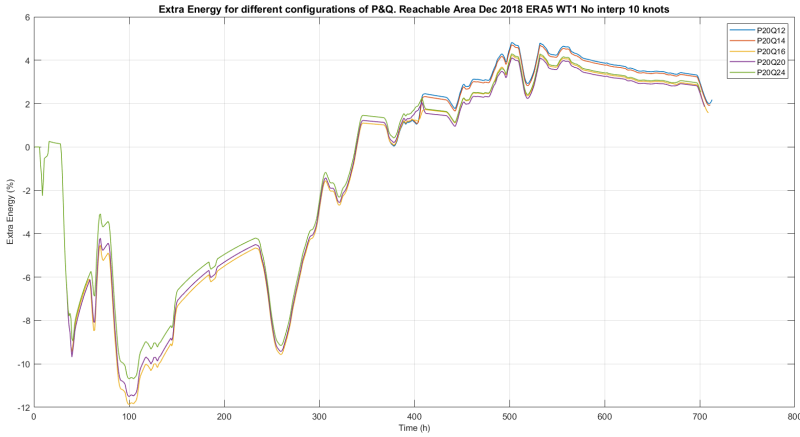

Figure B.5: Extra Wind Energy for different configurations of Q with $P = 20$. ERA5 Dec18.

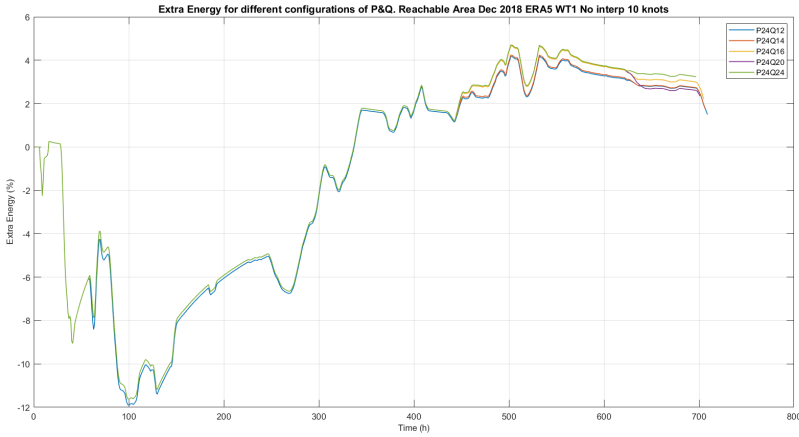

Figure B.6: Extra Wind Energy for different configurations of Q with $P = 24$. ERA5 Dec18.

B.4 ADO-WTs extra energy time series 2018

A graph represented in Figure B.4 shows the evolution of Extra Energy over the simulated time (2018), even though the most important value is the last value. The reason of showing the time series is to see the evolution of the Extra Energy, to check if there is a certain tendency while broaden the time horizon. Note that the first range (approximately 0 to 700) does not correspond to the usual range seen in other sections, since that corresponded to data for December 2018. In fact, December of 2018 corresponds to the last range of the presented results in Figure B.4, however, because the Extra Energy is calculated with the accumulated energy production, results do not match either.

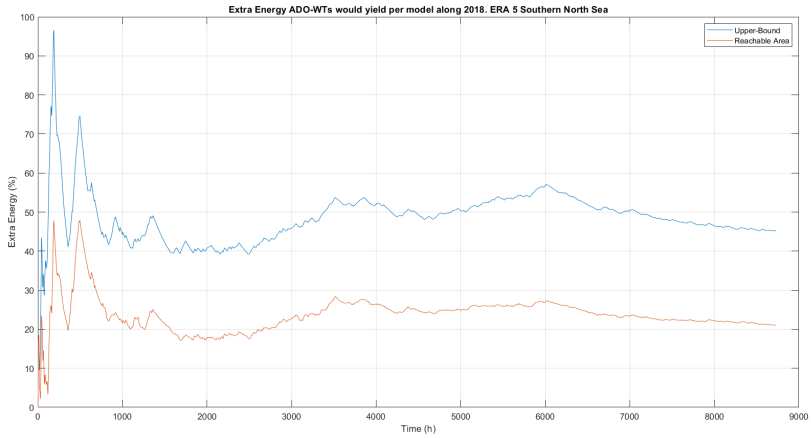

Figure B.7: Evolution of Extra Wind Energy for the whole 2018 with a 5-MW ADO-WT. ERA5 Souther North Sea.

B.5 ADO-WTs Sites per month

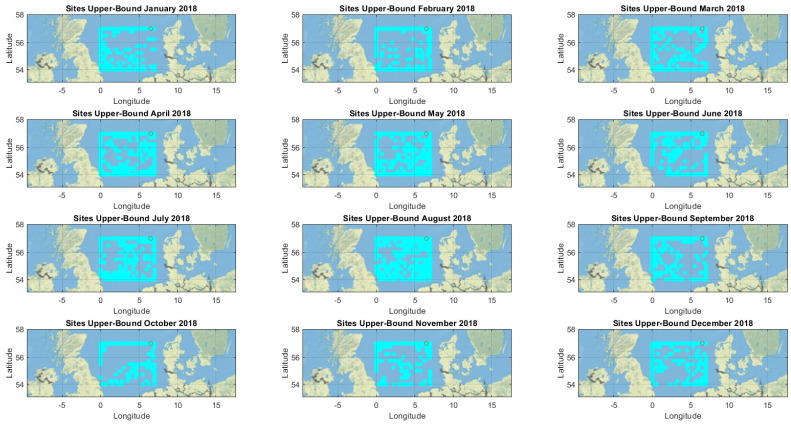

Figure B.8: Sites where a single ADO-WT would move per month according to Upper-Bound model. ERA5 2018.

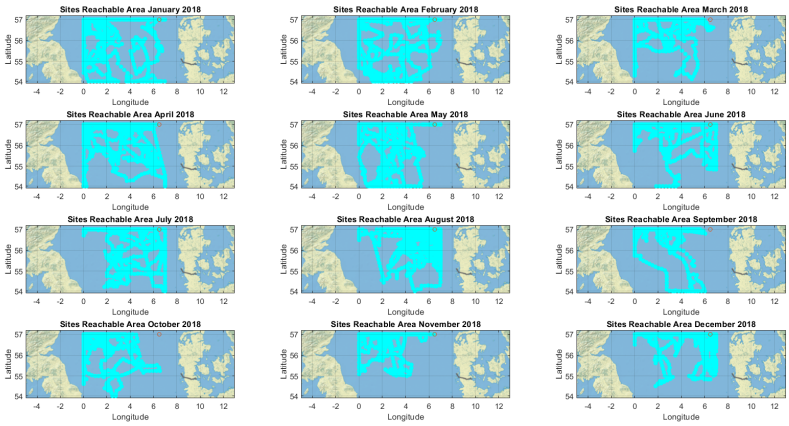

Figure B.9: Sites where a single ADO-WT would go per month –at 10knots– with $P = 14$ & $Q = 16$ according to Reachable Area model. ERA5 2018.

APPENDIX C

Appendices Power Losses -Code

C.1 Lpp design

```
%% Chose the Case, Tech and Bound
EnergyTech=char('Hydrgn','Li-ion','Zn-Air');
% It can be 'H2', 'Li-ion' or 'Zn-Air'
CaseM=1; %It can be 1, 2 or 3

%% Constants
rho_water=1024; % The water density

%% Define Free wind speed
Vo=0:0.1:35; Volength=length(Vo);
%% Define the boat speed
Vb=-15:0.1:5; Vblength=length(Vb);
Fw=zeros(1,Vblength);
Pw_losses=zeros(6,Vblength);

if size(Vb,2)==1
  Pextra=zeros(6,Volength);
end

lpp=[100,150,200];
for l=1:length(lpp)
  for bnd=1:2
    for ESS=1:3
      %% Calculate displacement
      ADOWT=charactADOWT(CaseM,ESS,bnd);
      Cd=.3; % tipical for Ro-Ro Vessel
      DWT=sum(ADOWT.Mass);
      Disp=DWT/Cd; % (kg)
      LW=Disp-DWT; % (kg)
      %% Design the hull dimensions
      % Volume to be displaced
      Vol=Disp/rho_water; % The displaced volume (m3)
      % Take the ship length to be between 100m and 200m
      Lpp=lpp(l); % (m)
      % Assuming a Catamaran as two semi-cylinders
```

```
      R=sqrt(Vol/(Lpp*pi)); % R (m)
      %% Calculate the wetted surface area of the ship
      Aw=2*(Lpp*pi*R+pi*R^2); % (m2)

      if bnd==1
        ind=ESS;
      else
        ind=ESS+3;
      end
      %% Go through the loop
      for j=1:Vblength

        %% Get water frictional losses
        % Reynolds number (for every Vb and Lpp)
        Re=abs(Vb(j))*Lpp/1.e-6;
        % Water frictional coeff. ITTC recommendation
        Cf=0.075/(log10(Re)-2);
        % Water Frictional Resistance
        Fw(j)=1/2*rho_water*Aw*Vb(j)^2*Cf; % (N)

        Pw_losses(ind,j)=abs(Vb(j))*Fw(j); % ideal Case

      end
    end
    if bnd==2
      Bound='Up';
    else
      Bound='Down';
    end
    switch ESS
      case 1
        Tech='Hydrogen ES';
        techID='H2';
      case 2
        Tech='Li-ion battery';
        techID='LiIon';
      case 3
        Tech='Zn-Air battery';
        techID='ZnAir';
    end
  end
end
```

.

C.2 Power Losses

```
EnergyTech=char('Hydrgn','Li-ion','Zn-Air');
% It can be 'H2', 'Li-ion' or 'Zn-Air'
CaseM=1; %It can be 1, 2 or 3

%% Constants
```

```
rho_water=1024; % The water density


%% WIND TURBINE Let's consider the NREL 5MW turbine.
% Wind speed and force on the NREL 5MW turbine
WS_p=[3,4,5,5.5,6,6.5,7.5,8,9,9.5,10.5,11.5,12]; % in m/s
Pg=[0,.2,.4,.5,.75,1,1.5,1.75,2.5,3,4,5,5]*1e6; % in W
WS_t=[0,3,4,5,5.5,6,6.5,7,8.5,9,10,11,11.3,12,13,15,25]; % in m/s
T=[0,.2,.25,.3,.325,.35,.375,.4,.5,.55,.67,.75,.76,.67,.6,.5,.4]*1e6; %in N

%% Define Free wind speed
Vo=0:0.1:35; Volength=length(Vo);
%% Define the boat speed
Vb=-15:0.1:5; Vblength=length(Vb);
Vr_ADO=zeros(Volength,Vblength);
Pgen_ADO=zeros(Volength,Vblength);
Pgen_conv=zeros(Volength,Vblength);
Ft=zeros(Volength,Vblength);
Fw=zeros(1,Vblength);
Plosses=zeros(Volength,Vblength);
Ppropeller=zeros(Volength,Vblength);
Eloss_ratio_opt=zeros(6,Volength);
Vb_LossMin_opt=zeros(6,Volength);
Egen_opt=zeros(6,Volength);
Eloss_opt=zeros(6,Volength);
Fw_opt=zeros(6,Volength);
Ft_opt=zeros(6,Volength);
Pnet_opt=zeros(6,Volength);
Vb_opt=zeros(6,Volength);
Vr_ADO_opt=zeros(6,Volength);
Pgen_ADO_opt=zeros(6,Volength);
Ppropeller_opt=zeros(6,Volength);
I=ones(Volength,1);
if size(Vb,2)==1
  Pextra=zeros(6,Volength);
end

for bnd=1:2
  for ESS=1:3
    %% Calculate displacement
    ADOWT=charactADOWT(CaseM,ESS,bnd);
    Cd=.3; % tipical for Ro-Ro Vessel
    DWT=sum(ADOWT.Mass);
    Disp=DWT/Cd; % (kg)
    LW=Disp-DWT; % (kg)
    %% Design the hull dimensions
    % Volume to be displaced
    Vol=Disp/rho_water; % The displaced volume
    % Take the ship length to be between 100m and 200m
    Lpp=100;
    % Assuming a Catamaran as two semi-cylinders
    R=sqrt(Vol/(Lpp*pi)); %R (m)

    %% Calculate the wetted surface area of the ship in
    Aw=2*(Lpp*pi*R+pi*R^2); % (m2)
```

```
61
62      %% Go through the loop
63      for i=1:Volength
64        for j=1:Vblength
65          %% Get a relative wind speed the rotor sees
66          Vr_ADO(i,j)=abs(Vo(i)+Vb(j));
67          %% WT yaws to always face Vo perpendicular
68
69          %% Get the power generated by ADO-WTs
70          if Vr_ADO(i,j)<3 || Vr_ADO(i,j)>25
71            Pgen_ADO(i,j)=0;
72          elseif Vr_ADO(i,j)>12
73            Pgen_ADO(i,j)=5e6;
74          else
75            Pgen_ADO(i,j)=...
76            interp1(WS_p,Pg,Vr_ADO(i,j));
77          end
78          %% Get the power generated by BFWT
79          if Vo(i)<3 || Vo(i)>25
80            Pgen_conv(i,j)=0;
81          elseif Vo(i)>12
82            Pgen_conv(i,j)=5e6;
83          else
84            Pgen_conv(i,j)=...
85            interp1(WS_p,Pg,Vo(i));
86          end
87
88          %% Get the trhust force (N)
89          if Vr_ADO(i,j)>25
90            Ft(i,j)=0;
91          else
92            Ft(i,j)=...
93            interp1(WS_t,T,Vr_ADO(i,j));
94          end
95
96          %% Get water frictional losses
97          % Reynolds number (for every Vb and Lpp)
98          Re=abs(Vb(j))*Lpp/1.e-6;
99          % H2O frict. coef. by ITTC recommendation
100         Cf=0.075/(log10(Re)-2);
101         % Water Frictional Resistance
102         Fw(j)=1/2*rho_water*Aw*Vb(j)^2*Cf; % (N)
103
104         % If WT goes with the wind but the sum
105         %Vo+Vb is still positive, the thrust
106         %pushes the ADO-WT towards its movement
107         if Vo(i)+Vb(j)>0 && Vb(j)<0
108           sgn=-1;
109         else % Thrust opposes the movement
110           sgn=1;
111         end
112         Ft(i,j)=Ft(i,j)*sgn;
113         Plosses(i,j)=...
114         abs(Vb(j))*(Ft(i,j)+Fw(j)); % ideal Case
115         Ppropeller(i,j)=Plosses(i,j);
```

```
        if Plosses(i,j)<0
          Plosses(i,j)=0;
        end
      end
    end

    if bnd==1
      ind=ESS;
    else
      ind=ESS+3;
    end

    %% Calculate the Net Power
    Pnet_ADO=Pgen_ADO-Plosses;

    %% Get the Optimal Vb* at which Pnet is max
    for Vo_ind=1:Volength
      [Pnet_opt(ind,Vo_ind),I(Vo_ind)]=...
      max(Pnet_ADO(Vo_ind,:)); % in W
      Vb_opt(ind,Vo_ind)=Vb(I(Vo_ind));
      Vr_ADO_opt(ind,Vo_ind)=...
      Vr_ADO(Vo_ind,I(Vo_ind));
      Eloss_ratio_opt(ind,Vo_ind)=...
      100*Plosses(Vo_ind,I(Vo_ind))/...
      Pgen_ADO(Vo_ind,I(Vo_ind));
      Pgen_ADO_opt(ind,Vo_ind)=...
      Pgen_ADO(Vo_ind,I(Vo_ind));
      Ppropeller_opt(ind,Vo_ind)=...
      Plosses(Vo_ind,I(Vo_ind));
      Ft_opt(ind,Vo_ind)=Ft(Vo_ind,I(Vo_ind));
      Fw_opt(ind,Vo_ind)=Fw(I(Vo_ind));
    end
    if bnd==2
      Bound='Up';
    else
      Bound='Down';
    end
    switch ESS
      case 1
        Tech='Hydrogen ES';
        techID='H2';
      case 2
        Tech='Li-ion battery';
        techID='LiIon';
      case 3
        Tech='Zn-Air battery';
        techID='ZnAir';
    end


    eval(['Pnet_' techID '_' Bound '=Pnet_ADO;'])

    if size(Pnet_ADO,2)==1
      Pextra(ind,:)=...
      100*((Pnet_ADO-Pgen_conv)./Pgen_conv)';
```

```
      eval(['Pextra_' techID '_' Bound '=Pextra;'])
    else
      Pextra=100*((Pnet_ADO-Pgen_conv)./Pgen_conv)';
      eval(['Pextra_' techID '_' Bound '=Pextra;'])
    end
  end
end
```

.

C.3 Mass characteristics of NREL Wind turbine

```
function ADOWT=charactADOWT(varargin)
% This function gives the mass characteristics of the ADO-WTs
% Given three values (e.g. charactADOWT(1,2,1) the Case1 is selected where
% the 2 ESS (Li-ion) is selected to get the Mass of the first Bound
% (upper-bound). Only Case 1 is available

%% Wind turbine Characteristics
% NREL 5MW turbine

ADOWT.Power=5e6; %Rated Electric Power in W

%% case1
%       Weight (tonnes) Weight (tonnes) Time (Days) Time (Days
M1=[240e3 24000e3 40  100;
  12000e3 32000e3 22.22222222 25.64102564;
  800e3 16000e3 36.36363636 40];

caseM=varargin{1};
ESS=varargin{2};
Bound=varargin{3};
ESS_Mass=eval(['M' num2str(caseM) '(' num2str(ESS) ',' num2str(Bound) ')']);
ADOWT.days=eval(['M1(' num2str(ESS) ',' num2str(Bound+2) ')']);
Capacity=2400e6;

%Rotor Nacelle  Tower  Storage
ADOWT.Mass=[110e3 240e3 347460  ESS_Mass];     % Weight of turbine in kg
ADOWT.Storage=Capacity;
```

.

APPENDIX D

Appendices Costs Results

D.1 Cost Breakdown

This section shows results not included in results section.

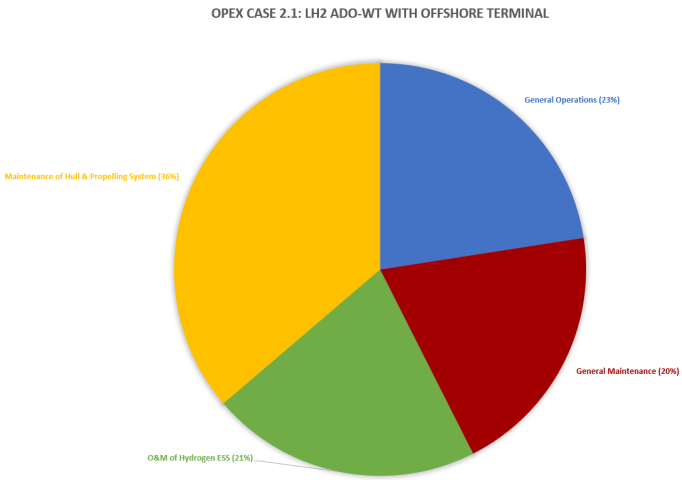

Figure D.1: OPEX case 2.1.

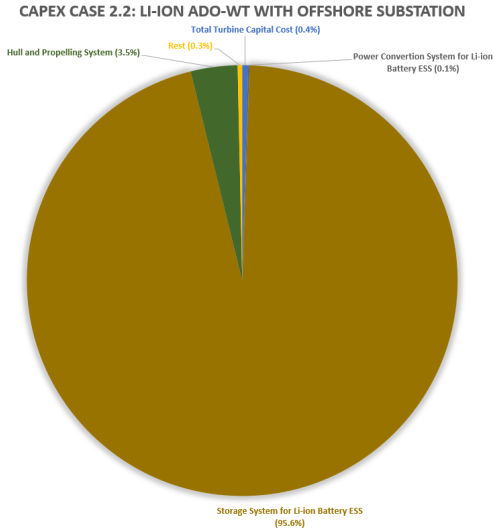

Figure D.2: CAPEX case 2.2.

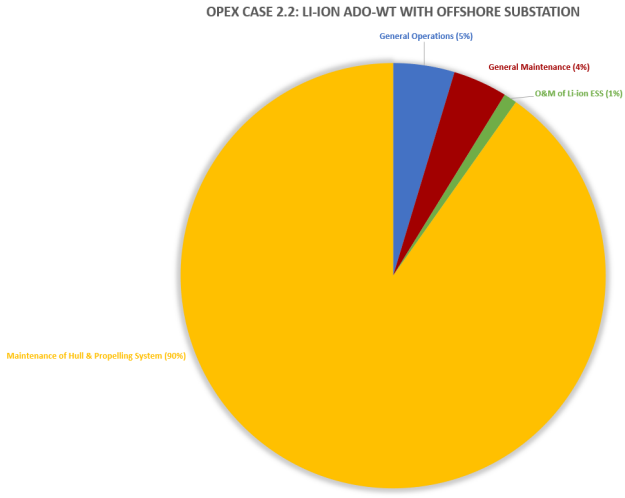

Figure D.3: OPEX case 2.2.

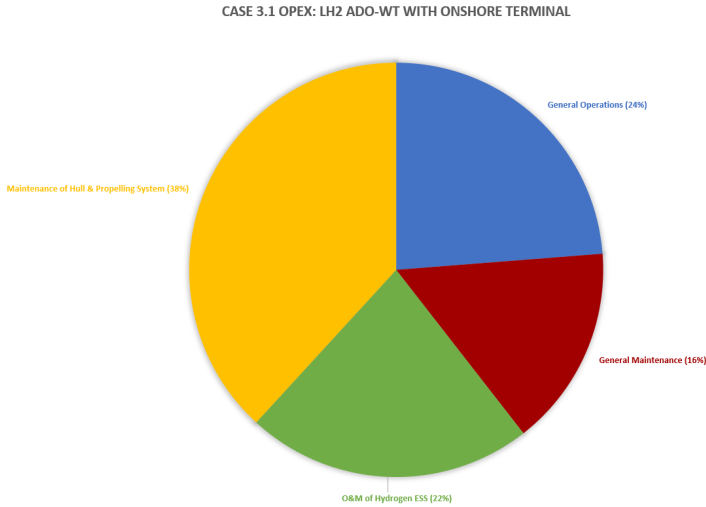

Figure D.4: OPEX case 3.1.

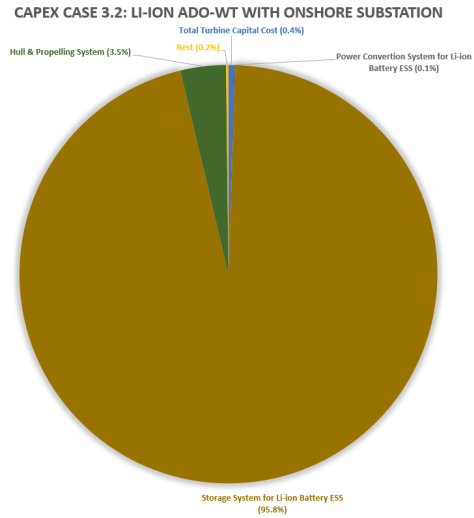

Figure D.5: CAPEX case 3.2.

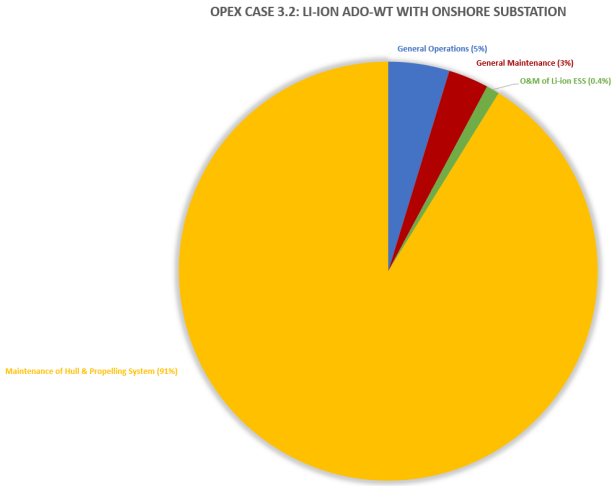

Figure D.6: OPEX case 3.2.

{2.7182818284}ϑφερτυθιοπσδφγηξκλ